GKSS
FORSCHUNGSZENTRUM
in der HELMHOLTZ-GEMEINSCHAFT

Analysis of a high-resolution regional climate simulation for Alpine temperature: Validation and influence of the NAO

(Vom Department Geowissenschaften der Universität Hamburg als Dissertation angenommene Arbeit)

Authoress:

K. Prömmel

ISSN 0344-9629

HELMHOLTZ
| GEMEINSCHAFT

wissen
schafft
nutzen

GKSS 2008/3

GKSS 2008/3

Analysis of a high-resolution regional climate simulation for Alpine temperature: Validation and influence of the NAO

(Vom Department Geowissenschaften der Universität Hamburg als Dissertation angenommene Arbeit)

Authoress:

K. Prömmel

(Institute for Coastal Research)

GKSS-Forschungszentrum Geesthacht GmbH · Geesthacht · 2008

Die Berichte der GKSS werden kostenlos abgegeben.
The delivery of the GKSS reports is free of charge.

Anforderungen/Requests:

GKSS-Forschungszentrum Geesthacht GmbH
Bibliothek/Library
Postfach 11 60
D-21494 Geesthacht
Germany
Fax.: (49) 04152/871717

Als Manuskript vervielfältigt.

ISSN 0344-9629

GKSS-Forschungszentrum Geesthacht GmbH · Telefon (04152) 87-0
Max-Planck-Straße 1 · D-21502 Geesthacht / Postfach 11 60 · D-21494 Geesthacht

GKSS 2008/3

Analysis of a high-resolution regional climate simulation for Alpine temperature: Validation and influence of the NAO

(Vom Department Geowissenschaften der Universität Hamburg als Dissertation angenommene Arbeit)

Kerstin Prömmel

105 pages with 34 figures

Abstract

To determine whether the increase in resolution of climate models improves the representation of climate is a crucial topic in regional climate modelling. An improvement over coarser-scale models is expected especially in areas with complex orography or along coastlines. However, some studies have shown no clear added value for regional climate models. In this study a high-resolution regional climate model simulation performed with REMO over the period 1958–1998 is analysed for 2 m temperature over the orographically complex European Alps and their surroundings called the Greater Alpine Region (GAR). The model setup is in hindcast mode meaning that the simulation is driven with perfect boundary conditions by the ERA40 reanalysis through prescribing the values at the lateral boundaries and spectral nudging of the large-scale wind field inside the model domain. The added value is analysed between the regional climate simulation with a resolution of 1/6° and the driving reanalysis with a resolution of 1.125°.

Before analysing the added value both the REMO simulation and the ERA40 reanalysis are validated against different station datasets of monthly and daily mean 2m temperature. The largest dataset is the dense, homogenised and quality controlled HISTALP dataset covering the whole GAR, which gave the opportunity for the validation undertaken in this study. The temporal variability of temperature, as quantified by correlation, is well represented by both REMO and ERA40. However, both show considerable biases. The REMO bias reaches 3 K in summer in regions known to experience a problem with summer drying in a number of regional models. In winter the bias is strongly influenced by the choice of the temperature lapse rate, which is applied to compare grid box and station data at different altitudes, and has the strongest influence on inner Alpine subregions where the altitude differences are largest. By applying a constant lapse rate the REMO bias in winter in the high elevations reaches –3.5 K, whereas by applying a monthly varying lapse rate based on the station data it reaches only about –1 K.

The comparison of the REMO simulation and ERA40 reanalysis shows that the added value of the former varies between seasons and regions. In some regions it also depends on the selection of stations used for the validation. Robust features include a better performance of REMO in the inner Alpine subregions, where the orography is most complex. The lack of consistent value added by REMO in this hindcast setup may be partly explicable by the fact that meteorological measurements are assimilated in the ERA40 reanalysis but not in the REMO simulation.

As the higher resolution leads to an added value in the simulation of temperature, at least in the most complex areas, the question is addressed whether it also leads to more detailed structures in the temperature response to circulation variability. In this study the temperature response to the North Atlantic Oscillation (NAO) with its strong influence on European winter climate is analysed over the GAR by using a very dense homogenised station dataset (HISTALP and stations from Austrian and Swiss weather services), the high-resolution simulation (for information in areas, where no station data are available) and the reanalysis. In earlier studies only a few individual stations or gridded data not higher resolved than 1° were used. The temperature signals based on the station data and based on the model data have very similar patterns and are in agreement with the European-wide pattern. The highly resolved model data show an additional clear small-scale pattern with a strong signal south of the main Alpine ridge potentially caused by the föhn effect. This small-scale structure is not visible in the reanalysis due to the coarser resolution and was also not found in previous studies based on both station and model data for the same reason.

Analyse einer hoch aufgelösten regionalen Klimasimulation für die Temperatur in den Alpen: Validierung und Einfluss der NAO

Zusammenfassung

Ein wichtiges Thema in der regionalen Klimamodellierung ist die Untersuchung, ob durch die Erhöhung der Auflösung in Klimamodellen das Klima besser dargestellt wird. Eine Verbesserung im Vergleich zu gröber aufgelösten Modellen wird besonders in Gebieten mit komplexer Orographie oder entlang von Küstenlinien erwartet, wobei es Untersuchungen gibt, die keinen eindeutigen Mehrwert der regionalen Klimamodelle zeigen. In dieser Arbeit wird eine hoch aufgelöste regionale Klimasimulation mit REMO für die 2 m Temperatur für den Zeitraum 1958–1998 über den orographisch komplexen Alpen und deren Umgebung (GAR) analysiert. Die Simulation wurde als Hindcast durchgeführt, d.h. sie wurde mit perfekten Randbedingungen der ERA40 Reanalyse durch Vorschreiben der äußeren Randwerte und spektralem Nudging des großskaligen Windfeldes innerhalb des Modellgebietes angetrieben. Der Mehrwert der regionalen Klimasimulation mit einer Auflösung von 1/6° wird im Vergleich zur antreibenden Reanalyse mit einer Auflösung von 1,125° untersucht.

Sowohl die REMO Simulation als auch die ERA40-Reanalyse werden vor der Untersuchung des Mehrwerts gegen verschiedene Stationsdatensätze der Tages- und Monatsmittel der 2 m Temperatur validiert. Der größte Datensatz ist der dichte, homogenisierte und qualitätskontrollierte HISTALP-Datensatz, der die gesamte GAR abdeckt und die Validierung auf Stationsbasis erst möglich macht. Die zeitliche Variabilität der Temperatur, die durch die Korrelation angegeben wird, wird sowohl von REMO als auch ERA40 gut wiedergegeben, jedoch zeigen beide erhebliche systematische Fehler. In REMO erreicht dieser 3 K im Sommer in Regionen, die bekannt dafür sind, dass viele regionale Klimamodelle dort ein Problem mit der sommerlichen Austrocknung haben. Im Winter hängt der systematische Fehler stark davon ab, welche Höhenkorrektur angewandt wird. Diese ist nötig, da die Gitterboxen und die Stationen, deren Temperatur verglichen wird, unterschiedliche Höhen haben. Sie hat in den inneralpinen Regionen den stärksten Einfluss, da dort die Höhendifferenz am größten ist. Die Anwendung einer konstanten Höhenkorrektur führt dazu, dass REMO im Winter in den hoch gelegenen Regionen mit einem Fehler von –3,5 K deutlich zu kalt ist, wohingegen eine monatlich variierende Höhenkorrektur basierend auf den Stationsdaten dazu führt, dass sich der Fehler auf etwa –1 K verringert.

Der Vergleich zwischen REMO und ERA40 mit der unterschiedlichen Auflösung zeigt, dass der Mehrwert von REMO zwischen den Jahreszeiten und den Regionen variiert. In einigen Regionen hängt er auch von der Auswahl der Stationen ab, die für die Validierung genutzt werden. Ein eindeutiges Muster ist allerdings die realitätsnähere Wiedergabe der Temperatur durch REMO innerhalb der Alpen, wo die Orography am komplexesten ist. Das Fehlen eines einheitlichen Mehrwerts dieses Hindcasts über dem gesamten Gebiet ist zum Teil dadurch zu erklären, dass meteorologische Messungen nur in der ERA40-Reanalyse assimiliert sind und nicht in REMO.

Die höhere Auflösung führt also zumindest in den orographisch komplexesten Gebieten zu einer realitätsnäheren Simulation der Temperatur. Desweiteren wird untersucht, ob sie auch zu detaillierteren Strukturen in der Reaktion der Temperatur auf Zirkulationsvariabilität führt. Hier wird die Reaktion der Temperatur in den Alpen auf die Nordatlantische Oszillation (NAO) mit ihrem starken Einfluss auf das europäische Klima untersucht. Dazu werden ein sehr dichter homogenisierter Datensatz (HISTALP und Stationen vom österreichischen und schweizer Wetterdienst), die hoch aufgelöste Simulation (für Informationen in Gebieten, in denen keine Stationen vorhanden sind) und die Reanalyse genutzt. In früheren Untersuchungen wurden entweder nur ein paar einzelne Stationen oder gegitterte Daten mit einer groben Auflösung von höchstens 1° genutzt. Das Temperatursignal zeigt basierend auf den Stationsdaten und den Modelldaten sehr ähnliche Muster, die sich auch in das bekannte Bild über Europa mit einem Süd-Nord-Gradienten einfügen. In dem lückenlosen Muster aus den Modelldaten zeigt sich ein sehr starkes Signal südlich und ein sehr schwaches Signal nördlich des Alpenhauptkamms, was dem großskaligen Signal entgegengesetzt ist und mit dem Föhneffekt erklärt werden kann. Diese kleinskalige Struktur ist in der Reanalyse durch die gröbere Auflösung nicht zu erkennen und wurde deshalb auch in früheren Untersuchungen nicht entdeckt.

Manuscript received / Manuskripteingang in TKP: 3. März 2008

Contents

Chapter 1

Introduction

1.1 The Alps and Alpine climate

The Alps are a curved mountain range in Western Europe ranging from the north-western coast of the Gulf of Genoa to Vienna with a length of about 1200 km and a width of 150 to 200 km in the West and about 300 km in the East (Fig. 1.1.1). In the North the transition to the Alpine foreland is quite smooth whereas in the south the transition to the Po Plain is much steeper. The Western and Eastern Alps are divided by a line from Lake Constance along the Rhine and over Pass Splügen to Lake Como. Located in the curved Western Alps are the highest peaks of the whole Alps, namely Mont Blanc (4808 m), Mont Blanc de Courmayeur (4748 m) and Dufourspitze (4634 m) in the Monte Rosa Massif. The Western Alps are stretched across Italy, France and Switzerland. The Eastern Alps are hardly curved, lower than the Western Alps and fan out into single mountain ranges. They are stretched across Switzerland, Liechtenstein, Germany, Austria, Italy and Slovenia.

The Alps are located at a latitude between 44° and 48° North on the southern side of the extratropical westerlies. They serve as a watershed and a climatic border between the Mediterranean in the South and Central Europe in the North with a division between maritime climate in the West and continental climate in the East. On this natural barrier larger-scale weather systems can be deflected, modified or newly built like the Genoa cyclone developing in the lee of the Alps in the vicinity of the Gulf of Genoa (Barry 1992). Therefore, the Alps have a large influence on the climate of the surroundings. In the lowest parts of the Swiss Midland bounded by the Jura Mountains in the West and the Alps in the East

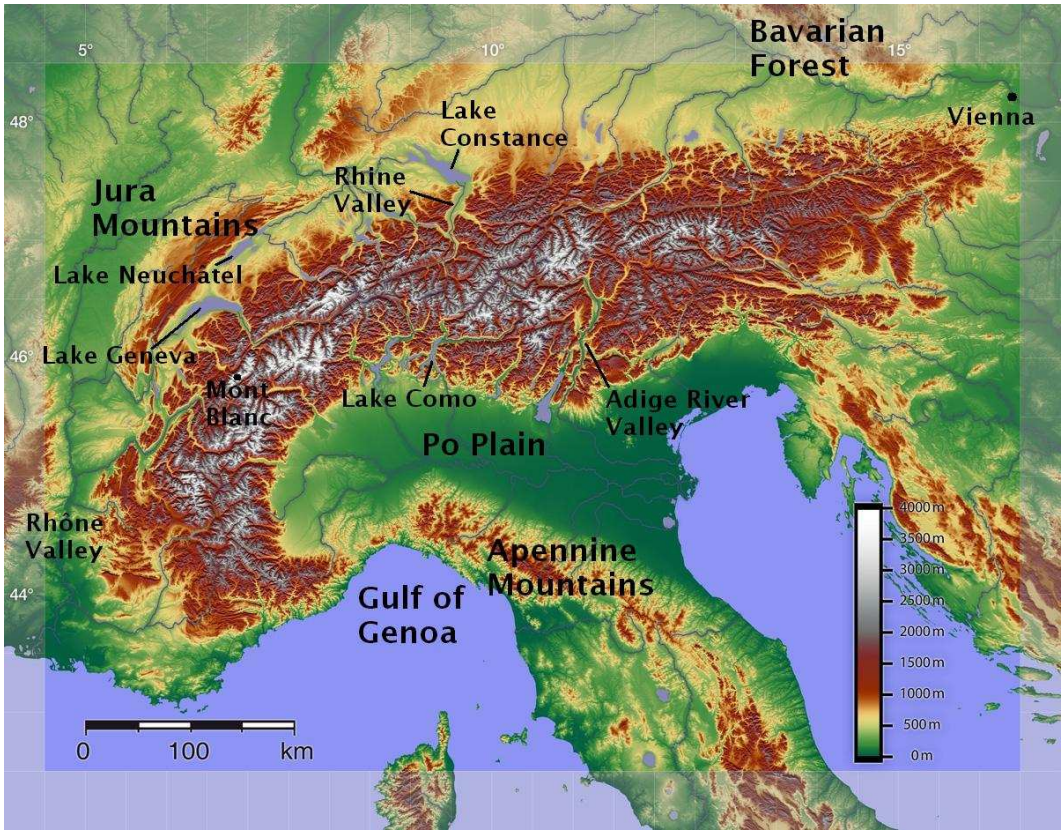

Figure 1.1.1: Digital relief of the Alps showing altitudes, based on Shuttle Radar Topography Mission Data. Based on Wikipedia (2007).

cold air flowing down the Alpine valleys at night is captured leading to ground fog and low stratus in late autumn and winter (Schüepp and Schirmer 1977). The same happens in the Po Plain a wide basin surrounded by the Alps in the North and West and the Apennine Mountains in the South (Cantú 1977). In the German and Austrian Alpine foreland temperatures are quite low in winter due to the high altitude and the increasing continental influence from the East. In summer the extension of the Azores high leads to dominantly anticyclonic weather over the whole region, however, frequent instability phenomena occur causing heavy showers and thunderstorms (Schüepp and Schirmer 1977). In the Po Plain these instabilities are supported by the weak thermal depression forming during daytime (Cantú 1977).

As the Alps do not consist of only a north slope and a south slope, the inner Alps with their countless valleys have their own climatic features (Schüepp and Schirmer 1977). Valleys with a west-east orientation are located in the rain shadow from both north and south leading to a quite dry climate. In winter very

strong temperature inversions with minimum temperatures of less than −30°C occur in the snow-covered valleys. In summer, when the Azores high extends to the Alps and the mountain slopes are warmed faster than the surrounding air during daytime, anabatic winds appear leading to towering cumulus clouds over the peaks and crests.

Mountain meteorology and climatology started developing at the end of the 18th century in the Alps (Barry 1978). In general, mountain climates are most strongly influenced by four geographical factors, namely latitude, continentality, altitude and topography (Barry 1992). Besides the mean temperature affecting the elevations of the treeline and snowline, latitude influences the amplitude of the annual and diurnal cycle of temperature. In low latitudes the annual range is small compared to the diurnal range, whereas in middle und high latitudes it is the other way around. Continentality also has an influence on the temperature range, which is smaller in a maritime climate nearer to the ocean and larger in a continental climate due to the different heat capacites of water and land. The ocean as a large source of moisture favours precipitation in a maritime climate. Altitude undoubtedly is the most fundamental characteristic of mountain climate as numerous atmospheric variables change with altitude, e.g. pressure, density and temperature generally decrease with altitude. Topography affects weather and climate on different spatial scales. For large-scale processes like planetary and gravity waves the dimension and the orientation of mountain ranges play a decisive role. On regional scales the relief modifying the wind field is more important. On local scales temperature and radiation are affected by slope angle and orientation towards the sun.

1.2 EU project ALP-IMP

This work has been realised within the EU framework 5 project "Multi-centennial climate variability in the Alps based on Instrumental data, Model simulations and Proxy Data" (ALP-IMP, `http://www.zamg.ac.at/ALP-IMP/`), which was carried out from March 2003 to August 2006. The aim of the whole project was to define the range of natural climate variability in the Greater Alpine Region (GAR) for the last 50, the last 150 to 250 and the last 1000 years.

The Alps are in meteorological terms the best-known mountain range in the world due to their long and spatially dense climate data such as instrumental

data and mountain-specific proxies like tree-rings and ice cores (Barry 1992). These data are distributed over elevations from 0 to 4500 m above mean sea level providing climate information from the surface and also the lower troposphere. The Alps are also highly sensitive to climate change and its impacts (Jungo and Beniston 2001). Therefore, the Alps as a unique region help broadening the knowledge of the regional features of past climate variability.

However, the Alps are stretched across different countries leading to a lack of uniform research activities over the whole region. Therefore, in ALP-IMP the existing unique climate data potential was used to reduce this deficit and to produce a consistent picture of regional climate variability in the whole GAR through three worktasks. In the Data Worktask climate datasets for the past millenium were collected and completed to create instrumental, tree-ring, isotope ice core and glacier records (e.g. Auer et al. 2007, Büntgen et al. 2005, Zemp et al. 2007). The instrumental record is the HISTALP database described in section 2.2. The Consistency Worktask aimed at the evaluation of the records. To do so the instrumental dataset consisting of seven climate parameters was tested for internal consistency by inter-parameter comparison with respect to their physical correctness (e.g. Auer et al. 2007). The external consistency was tested by comparing the dataset to exiting continental to global scale datasets (e.g. Efthymiadis et al. 2007). Additionally, in this worktask a regional climate simulation was performed and validated against the instrumental dataset and other datasets (e.g. Scheifinger 2006). The quality-controlled and validated records were used in the Synthesis Worktask for a 4-dimensional climate variability analysis within the GAR and of the GAR in the greater context of continental to hemispheric scale for the past millenium (e.g. Brunetti et al. 2006, Efthymiadis et al. 2007).

The part of ALP-IMP described in this work involves the analysis of the temperature performance of a high-resolution regional climate simulation in hindcast mode over the GAR for the last 50 years and a consistency analysis between this simulation and the instrumental dataset created in ALP-IMP. Further, the link between temperature variability in the GAR and large-scale circulation variability is analysed.

1.3 Background and motivation

1.3.1 Hindcasts and added value analysis

Regional Climate Models (RCMs) are an important tool for the regionalisation of global reanalyses or global simulations performed with General Circulation Models (GCMs). The horizontal resolution of reanalyses and GCMs is usually not finer than about 100 km, while the RCMs that are driven by the reanalyses or GCMs typically have resolutions between 10 km and 60 km (Giorgi et al. 2001 and references herein, Wang et al. 2004). Global reanalyses like the National Centers for Environmental Prediction/National Center for Atmospheric Research (NCEP/NCAR) reanalysis (Kalnay et al. 1996) or the European Centre for Medium-Range Weather Forecasts (ECMWF) reanalyses ERA15 (Gibson et al. 1997) and ERA40 (Uppala et al. 2005) or analyses of observations provide perfect boundary conditions. RCMs driven by such perfect boundary conditions provide so called hindcasts covering about the last 50 years. These hindcasts are used as reconstructions of regional climate, which are needed in areas where no high-resolution data exist or in complex terrain where the observations are unrepresentatively distributed (Bromwich et al. 2005). In these areas high-resolution regional reanalyses using state-of-the-art data assimilation would be another approach leading to a best estimate of the state and evolution of the climate. Examples for such regional reanaylses are the North American Regional Reanalysis (NARR, Mesinger et al. 2006) and the ongoing projects "Mesoscale meteorological reanalysis over the Iberian Peninsula" (ECMWF 2007) and "High-resolution data assimilation, modelling and reanalysis for the Arctic" (IPY 2007). Such reanalyses are complicated and computationally demanding and are therefore in many regional climate applications replaced by hindcasts driven by global reanalyses.

In addition to the performance of hindcasts another main application of RCMs is dynamical downscaling of simulations of future climate change scenarios using GCMs. However, before analysing the regional simulation of future climate a validation of the RCM is necessary, performed as a comparison between observations and a simulation of the same RCM of present climate, to determine the trustworthiness of the model for future climate change applications (Giorgi et al. 2001). A validation against observations is possible for past and present climate but not for future climate and has also been done for GCMs for years. To detect system-

atic biases of the RCM, that are caused by internal model dynamics and physics, perfect boundary conditions are required, as the boundary conditions for present climate derived from the GCM would already induce errors in the large-scale fields due to the fact, that GCMs have limited ability to simulate present climate (Christensen et al. 1997, Giorgi et al. 2001). Therefore, hindcasts are not only used as reconstructions of climate but also for the validation of RCMs for mean climate and variabilty. By contrast, the validation of RCMs driven by GCMs for present climate is only possible for climatologies (Giorgi et al. 2001). Hindcasts covering the second half of the 20th century have been analysed in many studies for pure validation (e.g. Hagemann et al. 2002, Vidale et al. 2003, Feser 2006, Sotillo et al. 2006, Bergant et al. 2007), additionally as input for hydrological applications (e.g. Sotillo et al. 2005, Kotlarski et al. 2005) or additionally as high-resolution datasets to analyse local or regional climate (e.g. Bromwich et al. 2005, Sotillo et al. 2006). References earlier than 2002 can be found in appendix 10.1 in Giorgi et al. (2001).

In both applications, regionalisation of present and future climate, it is expected that RCMs do not only yield results with just a higher resolution but that the explicit simulation of smaller-scale processes and the more detailed representation of the orography makes the RCM simulations more realistic than the GCM results (Denis et al. 2002, Wang et al. 2004).

Thus although as explained previously the skill of RCMs has been assessed in a number of validation studies, these studies do not explicitly address the crucial question of whether the skill of the RCM is actually better than the skill of the driving global model, in other words whether the RCM adds value to the global model. An added value is only desired on regional scales as the large scales are already well resolved by the global model (Feser 2005). With respect to the usage as a reconstruction of climate, the added value analysis of hindcasts compared to the driving reanalysis shows, whether the higher resolution leads to a more realistic reconstruction of present climate or whether the reanalysis, which includes assimilated observations as described in section 2.1, represents present climate more realistic despite the coarser resolution. As many variables are spatially quite homogenous, a higher resolution does not necessarily have to lead to a better representation.

1.3.2 Previous studies of added value of RCMs

The value added by an RCM appears to have been analysed in only a few studies, which were all published recently despite many years of use of RCMs. These studies fall into two groups. In the first group the RCM skill is compared to standard GCM simulations (Duffy et al. 2006, Seth et al. 2007), while in the second group the skill of reanalysis-driven RCM hindcasts is compared to the driving reanalyses (Roads et al. 2003, Sotillo et al. 2005, Sotillo et al. 2006, Feser 2006). These studies show that a general added value of the RCM in comparison to the driving model or reanalysis can not be found. Duffy et al. (2006) analysed present and future climates in the Western United States with different RCMs with resolutions from 36 to 60 km and compared them to gridded observational data for means and interannual variability. For precipitation they found added value for some, but not all RCMs, whereas for temperature they found an improvement for all RCMs in comparison to the driving GCM. Seth et al. (2007) concentrated on low latitudes by comparing a regional and a global simulation with gridded observational data over the whole of South America for means and interannual variability of precipitation. For the analysis they concentrated on four subregions, which are not located over the complexest areas but show interesting precipitation features. They concluded that the RCM with a resolution of 80 km did not add value to the driving GCM simulation. They suggest advancement of the physical parameterisations in both GCMs and RCMs to improve the simulations especially of tropical climate.

A comparison of four different RCMs with a resolution of 50 km and the driving NCEP/NCAR reanalysis with a gridded climatology for precipitation was performed by Roads et al. (2003) over the whole of South America north of 40° South for means and variability. Their analysis domain contains the Andes with a complex orography, where precipitation is overestimated by all models. They showed that no single RCM but the ensemble mean of all RCMs performed better than the reanalysis for some months. They see a reason for this worse performance in the parameterisations used in RCMs which are derived from GCMs and are not optimized for the regional scales. Sotillo et al. (2005) analysed the improvement of REMO with a resolution of 50 km compared to the NCEP/NCAR reanalysis at 15 offshore stations in the Mediterranean and Atlantic for means, variability and distributions of 2 m temperature, mean sea level pressure and 10 m wind field. For 2 m temperature they found added value introduced by REMO mainly for

extreme values. The validation and added value analysis of Sotillo et al. (2006) concentrated on a winter precipitation hindcast performed with REMO with a resolution of 50 km over the Iberian Peninsula. They found added value not only for total amount values but also for the spatial distribution by a comparison to a high-resolution station database. Feser (2006) applied a spatial two-dimensional filter (Feser and von Storch 2005) to separate the temperature and air pressure fields into large (larger than 700 km) and medium (250-550 km) spatial scales. The comparison of REMO simulations over the whole of Europe with a resolution of 50 km driven by the NCEP/NCAR reanalysis, as well as of the reanalysis, to gridded observations yielded added value for temperature over Europe mainly on medium scales, which has already been suggested by Laprise (2003). This improvement compared to the reanalysis was even larger if the large-scale wind field was nudged to the RCM. The positive influence of spectral nudging was already shown by Weisse and Feser (2003) for wind fields and wave heights.

1.3.3 Aims and objectives

The aim of this study is to validate and analyse a reanalysis-driven regional climate simulation for both means and variability of temperature over the GAR for the period 1958-1998. The simulation with a high resolution of 1/6° has been performed over the whole of Europe. It is the first study with such a high resolution in the GAR with its very complex orography. In previous studies RCMs had resolutions not finer than 0.44° and were analysed over larger areas. The validation performed in the present study is very detailed due to the high resolution. As explained in section 1.3.1 validation of RCMs is very important for the interpretation of downscaled future climate change simulations, which are of great interest (Christensen et al. 2007).

For the validation of RCMs comprehensive instrumental datasets are needed because global datasets and reanalyses have resolutions between 0.5° and 2.5°, which is too low to properly represent the real situation (Bergant et al. 2007). This is especially the case in regions with complex orography, where observations are sparse or not readily available (Giorgi et al. 2001). Such instrumental datasets are still missing in most regions. For the GAR with its very complex orography gridded precipitation datasets exist with a resolution of 25 km for the period from 1971 to 1999 (Frei and Schär 1998) and for most of the 20th century (Schmidli et al. 2002) and with a resolution of 10 min for the period 1800-2003 (Efthymiadis

et al. 2006). These gridded datasets have been used for many validation studies of precipitation over the GAR (e.g. Frei et al. 2003, Scheifinger 2006, Kotlarski 2007). With respect to multi-variable station data the lack of comprehensive instrumental datasets was recently closed by the availability of the homogenised and dense high-quality station dataset HISTALP covering the whole GAR (Auer et al. 2007). This dataset offers the possibility to perform a detailed validation of RCMs over the GAR not only for precipitation but also for temperature, which is less spatially homogenous in the GAR than in areas with a less complex orography. In the present study the REMO simulation with the very high resolution of 1/6° is therefore validated against this temperature station dataset over the Alps. The focus on the GAR, which was chosen as the analysis domain in the ALP-IMP project, is due to the complex orography a particular challenge for numerical simulations and one may expect considerable differences between the RCM and the reanalysis.

The HISTALP dataset enables the analysis of the added value of the RCM in comparison to the driving global reanalysis. Previously, added value analyses of RCMs were performed over larger regions with less complex orography and a coarser resolution of about 0.5°. Therefore, a very detailed added value analysis over different subregions of a limited area is possible for the first time.

In a hindcast the added value is measured relative to a field that is close to reality, because the driving reanalysis includes assimilated observations of the field variable. As no observations are directly assimilated in the regional simulation, the reanalysis has an advantage over the regional simulation with respect to simulating this variable. Therefore, the added value analysis performed with the reanalysis-driven hindcast is tougher than that performed with a GCM-driven regional simulation for present climate, which delivers an added value, that can be expected for a downscaled future climate change simulation. However, the added value from the reanalysis-driven hindcast might serve as a lower limit of the added value of the same RCM driven by a GCM simulation for future climate.

In addition to the validation of the regional simulation, this hindcast is used as a high-resolution gridded dataset. This gridded dataset together with the high-quality station dataset gives insight into small-scale temperature responses to large-scale circulation variability. Previously, such analyses were limited to individual stations or too coarse grids to resolve spatial details which play an important role in mountainous regions such as the GAR. This analysis is also

important for future climate change studies because the North Atlantic Oscillation (NAO), which is analysed in this study as a phenomenon representing the large-scale circulation variability, is supposed to change in future (e.g. Cubasch et al. 2001, Gillett et al. 2003, Meehl et al. 2007). Therefore, the temperature response to the NAO, which might also change in future, should be analysed and validated in detail for present climate.

Chapter 2

Model and station data used in this study

2.1 Model data

The high-resolution simulation analysed in this study has been performed with the regional climate model REMO version 5.0 (REgional MOdel, Jacob and Podzun 1997) by Beate Geyer from the GKSS Research Centre. The dynamical core of REMO is based on the numerical weather prediction model EM (Europa Modell) of the German Weather Service (DWD) (Majewski and Schrodin 1994) and was further developed at the Max Planck Institute for Meteorology (MPI) and at the GKSS Research Centre. The parameterisations are taken from the ECHAM4 climate model (Roeckner et al. 1996) of the MPI. REMO is based on the primitive equations, which include the hydrostatic approximation, in a terrain-following hybrid coordinate system. The prognostic variables are surface pressure, horizontal wind components, temperature, specific humidity and cloud liquid water. The variable relevant for the present study is 2 m temperature which is not a prognostic variable but is rather determined from the prognostic values at the surface and the lowermost model layer taken into account the Monin-Obukhov similarity theory (e.g. Jacobson 2005).

This study covers the period 1958 to 1998. The integration area has a very high horizontal spherical resolution of $1/6^\circ \times 1/6^\circ$ (in rotated coordinates approximately 17 km) on 20 vertical levels in the troposphere and lower stratosphere. The grid is rotated so that the equator is located above the centre of the integration area of 201×217 grid points to achieve a minimum distortion of the grid boxes.

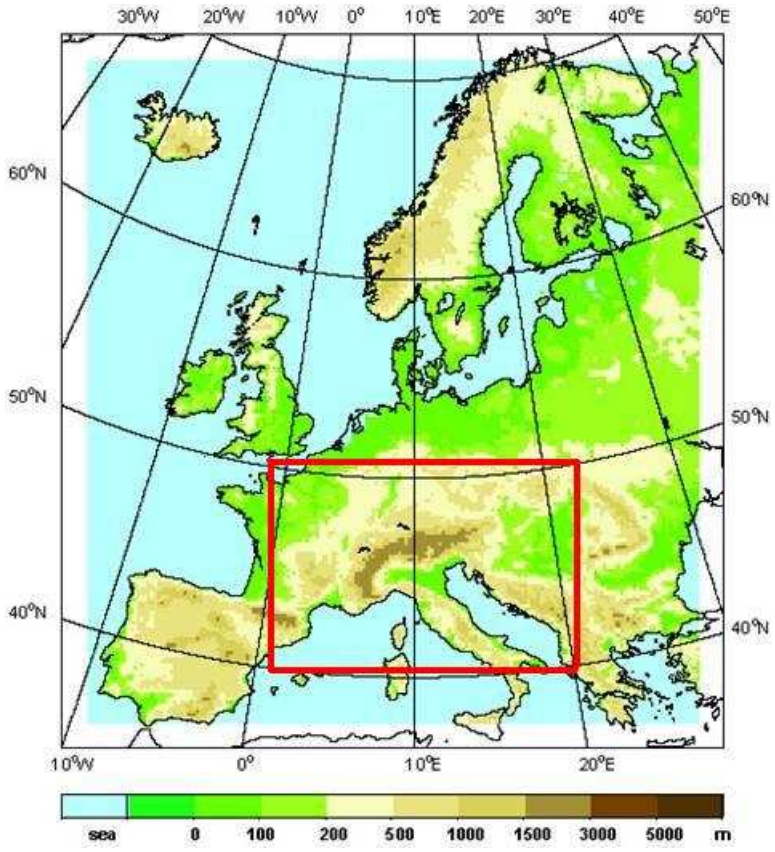

Figure 2.1.1: Whole simulation area with model orography in m. Red rectangle: study area.

The rotated north pole is located at 170° West and 32.5° North. The resulting integration area covers the whole of Europe including Iceland, Spain, Greece and Scandinavia and is presented in Fig. 2.1.1. The area of interest analysed in this study, the Greater Alpine Region (GAR, 0° to 20° East and 40° to 50° North), is marked by the red rectangle and consists of 66×90 grid points.

The high-resolution simulation is driven by the global ERA40 reanalysis (hereafter ERA, Uppala et al. 2005) through prescribing the values of the prognostic and many other variables at the lateral boundaries and through forcing solely the large-scale horizontal wind field within the model domain by spectral nudging (von Storch et al. 2000) at every time step on levels above 850 hPa. By spectrally nudging the large-scale horizontal wind field, the regional model is restrained from deviating from the driving field on large spatial scales.

A reanalysis is a recalculated analysis for the past with a state-of-the-art forecast model undertaken by assimilation of observations, including among others surface data, radiosondes, satellite data and radar. This gives the best estimate

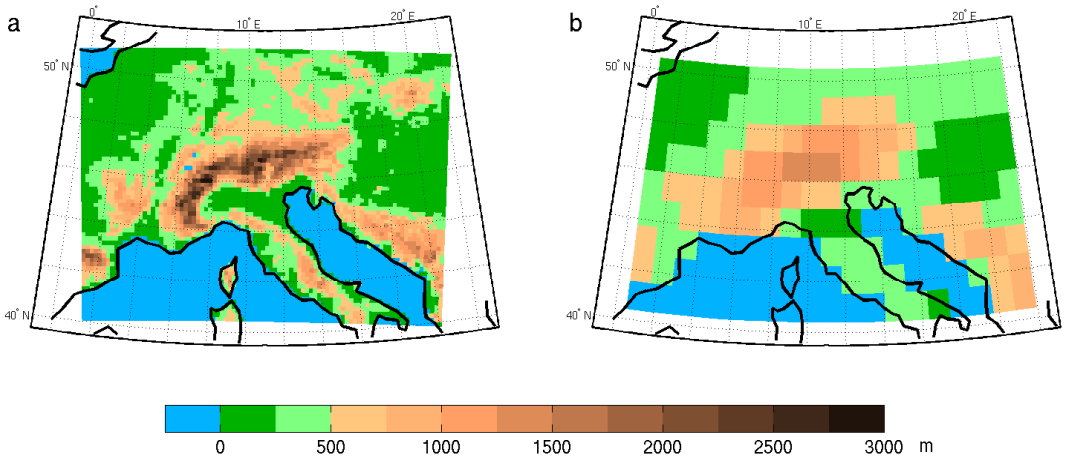

Figure 2.1.2: Orography in m of REMO (a) and ERA (b) in the study area.

of the state of the environment on a regular grid also for variables difficult to observe. ERA covers the period from September 1957 to August 2002 and has a horizontal resolution of $1.125° \times 1.125°$ (in Central Europe this corresponds to approx. $80\,\text{km} \times 125\,\text{km}$).

In ERA 2 m temperature is not directly assimilated. Instead, a separate analysis of dry-bulb temperature and dew point at a height of 2 m is performed by applying optimal interpolation (Simmons et al 2004, Uppala et al. 2005). For this analysis only those stations located within a radius of 1000 km around the model grid point in question were used. Additionally, those stations with a height difference to the model orography of more than 300 m were rejected. More detailed information about the temperature assimilation can be found in Simmons et al. (2004).

REMO and ERA have very different resolutions leading to a very different representation of the Alpine orography. Both REMO and ERA orography are presented in Fig. 2.1.2 for the GAR. In REMO the highest grid box is located at 2870 m above mean sea level. This grid box is located in the Monte Rosa Massif containing the second highest peak in the Alps with a height of 4663 m. In ERA the highest grid box reaches 1434 m and is located over the Swiss-Austrian border where the Alps are widest.

Due to the high resolution, the orography of REMO shows much more detail than the ERA orography. First of all, the shape of the Alpine ridge is much more realistic. The Bavarian Forest, the Po Plain and the Apennine Mountains, the Jura Mountains and the Swiss plateau with Lake Geneva and Lake Neuchâtel, and the Rhône Valley are also well resolved. In the inner Alps the resolution of

REMO is too coarse to identify single valleys except the Adige River valley and the Rhine Valley. However, single peak grid boxes can be found, which are located near real summits. In ERA the Alps are represented as a single low mountain.

2.2 Station data

In this study the high-resolution REMO simulation and the ERA40 reanalysis are compared to different instrumental temperature datasets over the GAR. The largest station dataset is the HISTALP dataset covering the whole GAR and is described in detail in Auer et al. (2007). It consists of monthly homogenised, outlier-corrected and gap-filled records of temperature, precipitation, pressure, sunshine, cloudiness, relative humidity and vapour pressure. The acquisition of data was challenging as the stations are located in different countries and some changed their nationality, language and even their names over time. HISTALP is therefore the only multi-variable climate database for the whole GAR with such a quality and station density. For temperature up to 131 stations are included, for precipitation up to 192, for pressure up to 72, for sunshine up to 55 and for cloudiness up to 66 depending on the time period. Another advantage of the HISTALP dataset is its length. For temperature and pressure the longest series extends back to 1760, for precipitation to 1800, for sunshine to the 1880s and for cloudiness to the 1840s. However, until now this dataset exists only as monthly means. In this study temperature, precipitation and cloudiness of the HISTALP dataset are used. For temperature the stations are displayed in Fig. 3.1.1a in section 3.1. For precipitation and cloudiness the stations are presented in Fig. 2.2.1. The precipitation dataset is described in more detail in Auer et al. (2005).

As the HISTALP dataset does not contain daily data, a second temperature dataset is used in this study. This dataset consists of daily data from 59 stations from Austria and Switzerland and is named ZMdaily. The Austrian data were provided by the ZAMG (Central Institute for Meteorology and Geodynamics) and are described in Schöner et al. (2003). The Swiss data were provided by Meteoswiss (`http://www.meteoschweiz.ch`). 23 of the 59 stations also belong to the HISTALP temperature dataset. The daily mean temperature station dataset is also converted in this study to a monthly mean station dataset (ZMmonthly). One main difference to HISTALP is that the Austrian and Swiss stations are quality-controlled to a smaller extent and only homogenised at a national level.

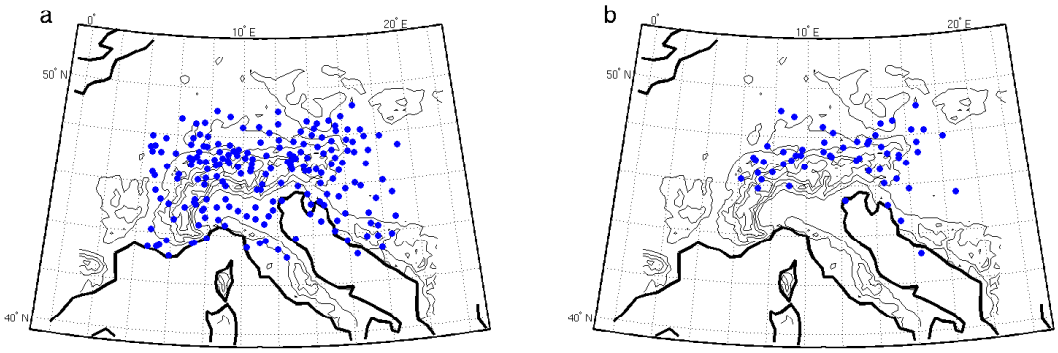

Figure 2.2.1: HISTALP stations for precipitation (a) and cloudiness (b). Contour lines in the background represent orography used in REMO with an interval of 500 m.

The comparison between the results based on ZMmonthly and those based on HISTALP are used to analyse whether the selection of the stations has an influence on the results. The effect of the temporal resolution can be analysed by comparing the results based on ZMmonthly to those based on ZMdaily. The ZMdaily/ZMmonthly stations are presented in Fig. 3.1.1b in section 3.1.

A further dataset used in this study is the CRU TS 2.0 dataset of the Climatic Research Unit (CRU), which is described in Mitchell et al. (2004). The updated and extended version CRU TS 2.1 is described in Mitchell and Jones (2005). CRU TS 2.0 extends over the global land surface und covers the period 1901 to 2000. It is a gridded dataset with a resolution of $0.5° \times 0.5°$ and includes the variables temperature, precipitation, diurnal temperature range, vapour pressure and cloud cover. In this study only temperature is used. The station data included in this dataset are mainly derived from national meteorological agencies, the WMO and CRU global datasets of station timeseries. The monthly absolute values are a combination of the 1961-90 mean monthly climatology (New et al. 1999) and the anomaly fields for each month for the whole century (New et al. 2000). For the mean monthly climatology thin-plate splines were used for interpolation with elevation as an independent predictor variable. Therefore, the interpolation generates spatially varying temperature lapse rates (New et al. 1999). For the anomaly fields an angular distance-weighted interpolation ignoring the influence of the elevation was used, which is suggested to be adequate (New et al. 2000).

Chapter 3

Evaluation of the skill and added value of a reanalysis-driven regional simulation for Alpine temperature

In this chapter the skill and added value of a high-resolution RCM hindcast for temperature over the GAR is assessed. As outlined in section 2.1 the RCM has been run with a spatial resolution of about 17 km and has been driven by, and compared against, the ERA40 reanalysis for the period 1958-1998. The validation is performed against station temperatures because of the practical relevance of the local skill, and because in the Alps a relatively dense network of homogenised temperature datasets exists. This high quality network in combination with the RCM simulation of 41 years allows for a robust estimation of the simulation skill.

This chapter is organised as follows: In section 3.1 the use of station data and gridded observations for validation is discussed and the validation method is described. The results are presented in section 3.2 separated for skill, added value and the comparison to daily data. Additionally, the potential problems with height differences as outlined by Moberg and Jones (2004) and explained later in this chapter are investigated. Section 3.3 concludes the chapter.

3.1 Method

3.1.1 The use of station data in comparison to gridded observations

The validation of RCM simulations can be performed either against gridded data or against station data. Obviously, the advantage of using gridded data is that grid box values in GCMs and RCMs represent area means. However, gridded climatologies can include errors that have been introduced through the interpolation method. This may be of particular concern over mountainous areas or along coastlines where the estimation of area means from station networks with standard station density may be difficult due to the relatively low correlations between values at different locations (this effect is quantitatively discussed for rainday frequency in Osborne and Hulme (1997)). The estimation of absolute area means rather than anomalies is further complicated over complex orography by the strong height dependence of many meteorological variables combined with the usually non-representative height distribution of the station network. Furthermore, it should be noted that area means simulated in a regional model, even in a model with "perfect" physics, differ from the real-world area means due to the differences between real and model orography (compare Fig. 1.1.1 and Fig. 2.1.2a). In other words, the model simulates a system that is different to the real one, and thus a comparison of simulated and real-world area means over complex orography is not a comparison of conceptually identical variables.

The choice between gridded or station data for validation may also depend on what the RCM simulation will be used for. If area means are of interest, they are the natural choice as a validation variable. If the estimation of local values from the RCMs without further postprocessing (statistical downscaling or Model Output Statistics) is of interest, which may often be the case, assessing the model skill by comparing the simulated area means against point observations will yield the practically relevant information. The orography-related differences between the model and the real world, as well as the height dependence of many variables are as much an issue for station-based validation as they are for the comparison of area means and should be taken into account in any analysis.

Most GCM or RCM validation studies compare simulations to gridded climatologies and reanalyses (e.g. Noguer et al. 1998, Giorgi et al. 2003, Vidale et al. 2003, Bergant et al. 2007, Jacob et al. 2007). Less work has been done on

the validation against station temperature data (Kyselý 2002, Moberg and Jones 2004, Bromwich et al. 2005), which is partly attributable to the limited availability of good quality, high-resolution observations (Giorgi et al. 2001, Wang et al. 2004, Bergant et al. 2007). Kyselý (2002) focusses on the extreme values of annual minimum and maximum temperatures over central Europe and compares raw and statistically downscaled GCM output from two GCMs with observations at four sites, finding improvements through the downscaling. Moberg and Jones (2004) compare RCM maximum and minimum temperatures with station data over Europe. The RCM has a resolution of 50 km. They note problems when directly comparing simulations and observations along the coastlines where sometimes sea grid boxes are compared to land stations. For complex areas like the Alps with large height differences between the grid boxes and the stations, they advise against a detailed comparison as the height differences lead to a different beginning of snow melting which has a large effect on temperature variability. However, as pointed out above, the different orography in the model and the real world would also affect the comparison with area means, as systematic differences between the simulated and the real world do not get reduced through the spatial averaging. The work by Bromwich et al. (2005) concentrates on a regional climate simulation over Iceland with a resolution of 8 km. They compared among other variables monthly mean 2 m temperature simulated by the RCM with data from 70 stations. In regions with most complex orography large negative biases were found, which were explained by the too coarse resolution of the RCM which they suggest led to poor mixing in the lower atmosphere.

3.1.2 Skill measures

In this study 2 m temperature is analysed, which largely depends on altitude and therefore the altitude dependency needs to be considered in this study, which focusses on the Alps. As the complex orography of the Alps can not be fully captured by the reanalysis and not even by the high-resolution REMO simulation, large differences in altitude may occur between the stations of the instrumental datasets and the corresponding grid boxes of REMO and ERA, respectively. To avoid a bias due to altitude differences, altitude corrections are applied to the temperature of REMO and ERA. First, a mean altitude correction of 0.65 K/100 m is applied. This constant value was also chosen in earlier studies (Christensen et al. 1997, Moberg and Jones 2004, Kotlarski 2007, Jacob et al. 2007). Second, a

monthly varying lapse rate based on the station data is applied and the differences to the constant lapse rate are discussed.

For validation of the simulations different measures of skill are available. For the present analysis correlation and bias are used in order to investigate the representation of variability and the systematic error of the simulation, respectively. A further possible measure of skill is the hitrate, which includes the uncertainty of the observations (Schlünzen and Katzfey 2003). The hitrate is the amount of cases in percent, when the simulations agree within a given accuracy with the observations. For temperature an accuracy of 2°C has been used established by the United States Air Force and Defense Special Weapons Agency (Cox et al. 1998). As the calculation of hitrates leads to similar results as the calculation of biases (not shown), this study concentrates on bias.

To determine the reduction of error for the analysis of the added value, the root mean squared error (rmse), combining correlation and bias, is also calculated. Correlation, bias and reduction of error (defined in section 3.2.3) are calculated between the observed temperature at the stations and the altitude corrected temperature at the corresponding grid boxes of REMO and ERA, respectively, over the whole simulation period of 41 years for each month separately. It should be noted that the station data which we compare with REMO and ERA are partly assimilated in ERA as explained in section 2.1.

To summarise the information at the 131 HISTALP stations and the 59 ZMmonthly/ZMdaily stations, respectively, the resulting values are averaged over six subregions defined by Böhm et al. (2001) based on rotated principal component analysis. The subregions are named West, East, South, Po Plain, Central Alpine Low Level (CALL) and High Level (HL) and are shown for HISTALP in Fig. 3.1.1a. Subregion HL is defined as stations with heights above 1500 m above mean sea level. As ZMdaily and ZMmonthly contain only Austrian and Swiss stations these datasets are limited to subregions West, East, CALL and HL and are presented in Fig. 3.1.1b.

3.2 Results

In this section the skill of REMO and ERA is evaluated by considering correlation and bias separately. Additionally, the performance of REMO and ERA is briefly compared in these subsections. An investigation concerning the grid box/station

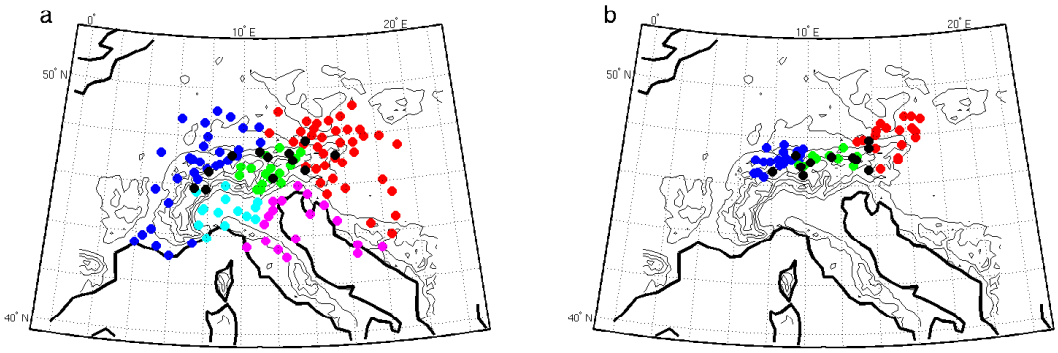

Figure 3.1.1: HISTALP stations (a) and ZMmonthly/ZMdaily stations (b) divided into subregions West (blue), East (red), South (magenta), Po Plain (cyan), Central Alpine Low Level (green) and High Level (black). Contour lines in the background represent orography used in REMO with an interval of 500 m.

problem, which was already oulined in section 3.1.1, follows. Thereafter, the added value of REMO compared to ERA is analysed in detail. Finally, the skill from daily data is calculated and compared to the monthly results.

3.2.1 The skill of REMO and ERA compared to monthly mean observed station data

3.2.1.1 Correlation

In Fig. 3.2.1a annual cycles of correlation between the monthly mean temperature of HISTALP station data and REMO and ERA, respectively, are presented for the six subregions. The generally very high correlations for both REMO and ERA indicate that the temporal variability of temperature in the GAR is represented quite well. For REMO, lowest correlations are observed in November and December and highest values in March and September for all subregions. Subregions with generally very high correlations are West and East which are situated to the north of the Alps where orography is less complex and atmospheric circulation is less influenced by the mountains than south of the Alps in the lee of the mountains with regard to the prevailing wind direction (Barry 1992). Here, lowest correlations are found for the subregion Po Plain during nearly the whole year, especially from April to August. The inner Alpine subregions CALL and HL have the most pronounced annual cycle with lowest correlations in winter. These low correlations are probably due to the differences in altitude between the grid box and the station which lead to differences in snow fall due to differ-

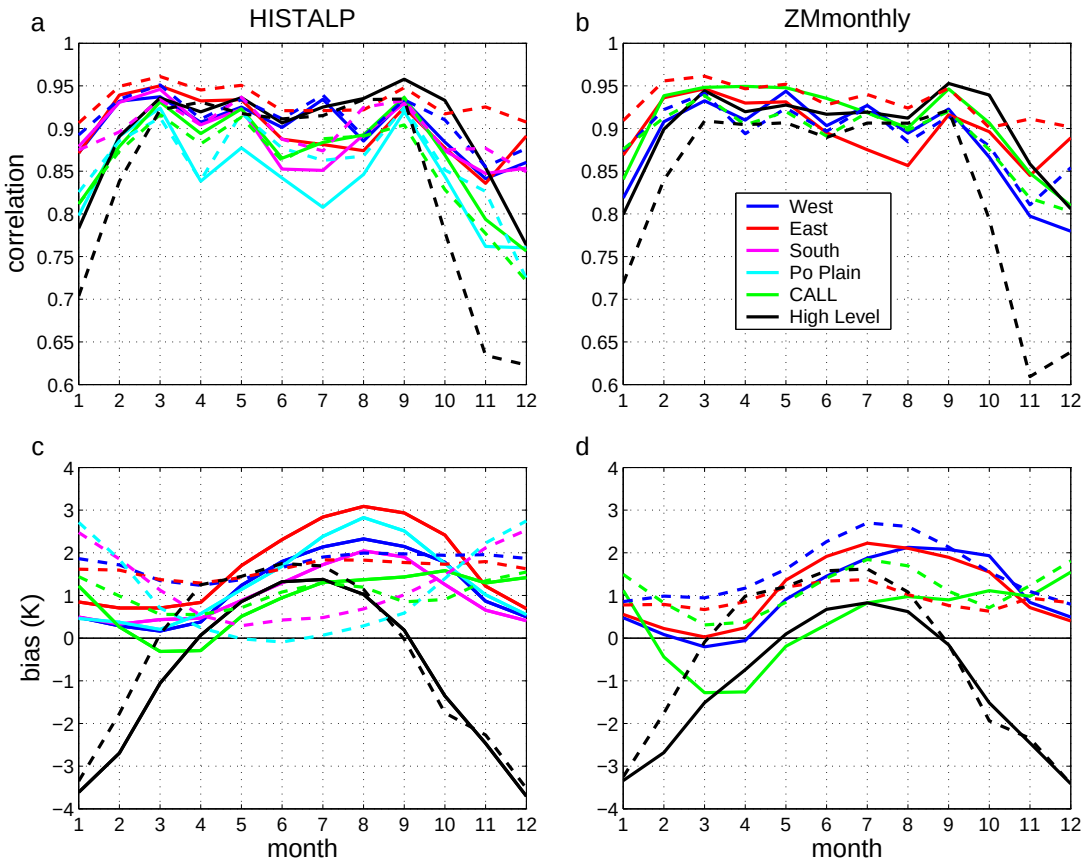

Figure 3.2.1: The annual cycles of the performance of REMO (solid) and ERA (dashed) are shown for the temperature correlation between the models and HISTALP (a) and ZMmonthly (b) and the temperature bias between the models and HISTALP (c) and ZMmonthly (d) averaged over the subregions.

ent temperatures. This would cause different snow cover and therefore different temperature variability between the model and observed data (Moberg and Jones 2004) as mentioned in section 3.1.1. However, validation against observations of snow cover is difficult (Christensen et al. 1997) and beyond the scope of this thesis.

The ERA correlations have a generally similar annual cycle to REMO, but slightly higher values in all subregions except the inner Alpine subregions CALL and HL with the most complex orography where REMO has higher correlations. As for REMO, ERA has highest correlations north of the Alps in subregions West and East and lower correlations south of the Alps, especially in the Po Plain. As the annual cycles are very similar for REMO and ERA, the low correlations in winter in the inner Alpine subregions do not necessarily identify limitations

specific to the regional model. The low correlations could be caused by both REMO and ERA or can be caused by ERA and be inherited by REMO. The reason is probably the aforementioned difference between the grid box and the station altitudes.

The correlations between REMO and ERA, respectively, and the second monthly mean station dataset ZMmonthly, which is limited to subregions West, East, CALL and HL, show similar annual cycles to the correlations with HISTALP (Fig. 3.2.1b). The only difference is that for REMO in subregions West and CALL correlations are slightly higher than for ERA and not lower as with HISTALP. These differences are however very small and can probably be attributed to the selection of stations.

3.2.1.2 Bias based on standard lapse rate

The bias of REMO and ERA for the six subregions based on the monthly mean dataset HISTALP calculated with the constant lapse rate of 0.65 K/100 m is presented in Fig. 3.2.1c. Both REMO and ERA indicate a warm bias for all subregions except HL in the winter half year. For REMO this positive bias is more pronounced in summer than in winter in subregions West, East, South and Po Plain. The largest positive bias with a value of about +3 K occurs in subregions East and Po Plain in August.

The ERA bias has a different annual cycle for subregions West, East, South and Po Plain than the REMO bias (Fig. 3.2.1c). In subregions West and East the bias is almost constant at about +1.8 K during the whole year whereas for subregions South and Po Plain the bias is largest in winter and smallest in summer, contrary to the REMO bias in these regions. The differences in the annual cycles of the biases of REMO and ERA in subregions West, East, South and Po Plain lead to the conclusion that the strongly positive bias of REMO in summer is a clear feature of the regional model and identifies problematic regions. However, ERA also has large biases. In subregions South and Po Plain in winter the bias reaches nearly 3 K indicating problematic regions or processes in ERA. However, this must be caused by reasons different to those in REMO as the bias is in the opposite direction.

The biases of REMO and ERA in the inner Alpine subregions (Fig. 3.2.1c) have very similar annual cycles and are therefore probably not a problem of REMO. Here biases are probably due to the comparison between grid box and

station data. However, it is possible that both REMO and ERA have problems that cause similar biases. The biases of each single station have also very similar annual cycles (not shown). Therefore, the annual cycle of the bias averaged over all stations belonging to the same subregion is only slightly influenced by the averaging.

In subregion HL the biases of REMO and ERA are largely negative in winter and positive in summer, which can be explained to a large extent by the altitude correction. As all stations are higher than the corresponding grid box (for REMO 260-1620 m and for ERA 650-2800 m higher), the temperature of REMO and ERA is reduced with the mean lapse rate of 0.65 K/100 m. The real lapse rate depends on atmospheric layering, which is more stable (instable) in winter (summer), and is therefore in most cases smaller (larger) in winter (summer). Thus, in winter (summer) the corrected temperature is reduced too much (little). An investigation of the influence of the lapse rate on bias is presented in the following section.

In subregion CALL the biases of REMO and ERA are relatively small during the whole year with a minimum and negative values (for REMO) in spring. However, the bias is influenced by the applied altitude correction as for HL. Therefore, a more detailed investigation of the bias in subregion CALL is presented in the following section.

The biases of REMO and ERA compared to ZMmonthly (Fig. 3.2.1d) show very similar annual cycles for the different subregions in comparison to the results based on HISTALP (Fig. 3.2.1c). The dependency of the geographical selection of stations is visible through the differences for REMO in subregion CALL from February to May, where the bias is more negative, and for ERA in subregion West in summer (winter), where the bias is larger (smaller). The largest difference between ZMmonthly and HISTALP can be found in CALL, where only 20% of the ZMmonthly stations also belong to HISTALP, in East these are 22%, in West 50% and in HL 64%. Therefore, largest differences in bias are expected in CALL. However, the potentially lower quality of ZMmonthly mentioned in section 2.2 also plays a role.

To test to what extent the bias varies within the subregions, the spatial distribution of the bias of REMO compared to HISTALP is analysed. The bias is presented for winter (DJF) and summer (JJA) for each subregion in Fig. 3.2.2. The generally small biases in winter as seen in Fig. 3.2.1c are visible but exceptions for some stations are found in the inner Alpine subregions CALL and HL.

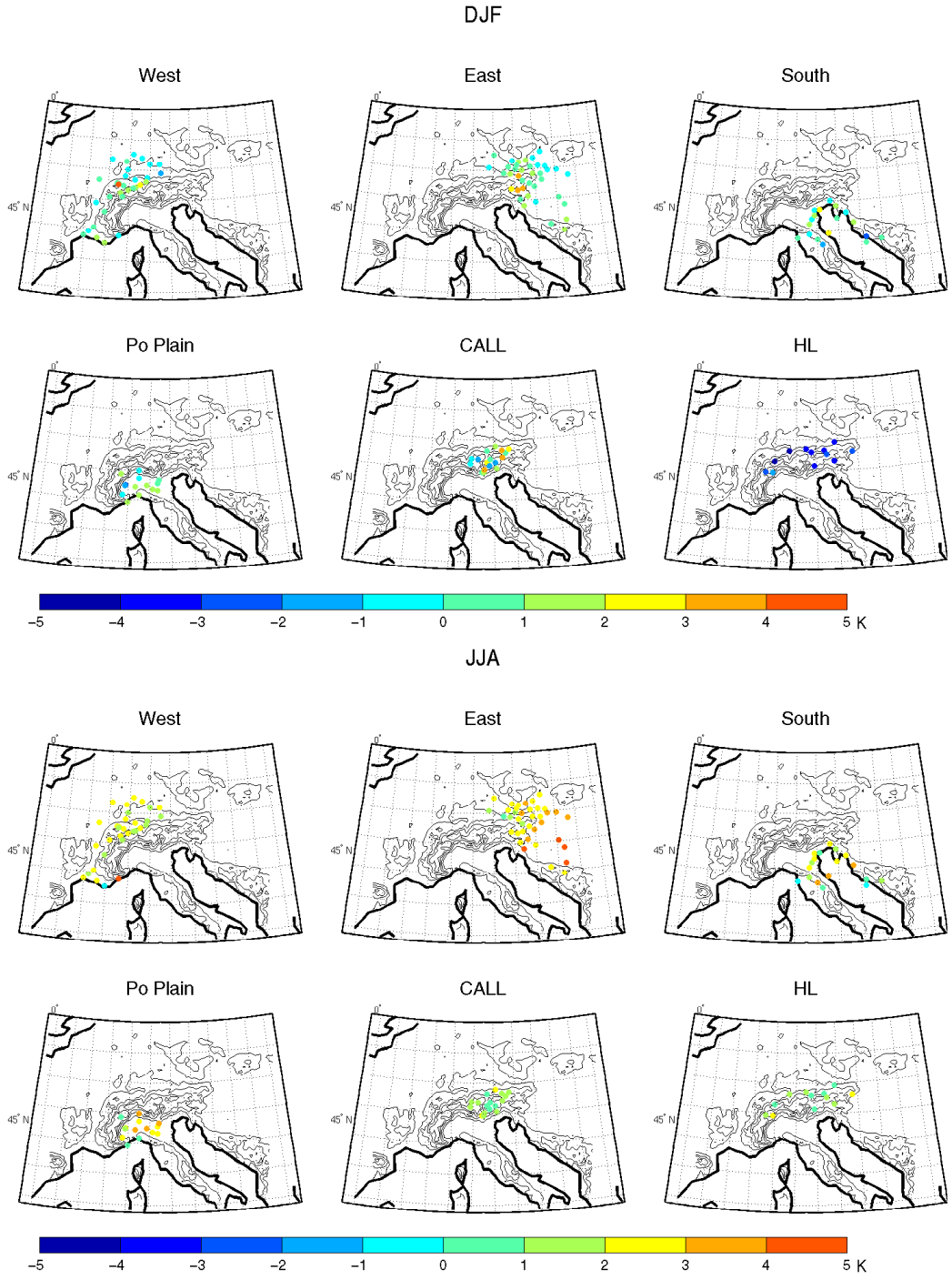

Figure 3.2.2: Spatial distribution of the temperature bias (K) between REMO and HISTALP stations for winter (DJF, top) and summer (JJA, bottom) separated for the six subregions. Contour lines in the background represent orography used in REMO with an interval of 500 m.

Largest spatial inhomogenties in winter are found in CALL. In summer warmer biases can be seen, especially in subregions East and Po Plain. In East largest

spatial inhomogenities occur. However, these figures generally show that the regionalisation of the results does not lose too much information because of the quite homogeneous bias distribution in the different subregions. Additionally, the biases averaged over the subregions were calculated by using only 50, 80 and 90% of the stations in each subregion, which were randomly selcted. Despite the calculation with less stations the annual cycle of the bias does not change much in all subregions meaning that the annual cycles of the averaged biases are robust features with small errors (not shown).

3.2.1.3 Bias based on empirical lapse rate

As mentioned in the previous section, the application of a constant temperature lapse rate might not be realistic and might lead to biases not caused by the model itself. To find monthly varying and therefore potentially more realistic lapse rates, the HISTALP station dataset is used. Seven pairs of low and high elevation stations are selected with a small horizontal distance between pairs and the coverage of most areas of the Alpine chain. The pairs are listed in Table 3.2.1 with their station names, abbreviations, elevation differences, horizontal distances, yearly mean temperature lapse rates and the subregion of the lower station.

station names	abbr.	elev. difference	horiz. distance	yearly mean lapse rate	subregion
Innsbruck/Patscherkofel	INN/PAK	1638 m	9.00 km	0.54 K/100 m	CALL
Zell am See/Schmittenhöhe	ZEL/SCH	1207 m	3.91 km	0.38 K/100 m	CALL
Bad Ischl/Feuerkogel	BIL/FEU	1149 m	13.00 km	0.42 K/100 m	East
Badgastein/Sonnblick	BGA/SON	2005 m	15.71 km	0.55 K/100 m	CALL
Interlaken/Jungfraujoch	ITL/JFJ	2996 m	15.78 km	0.53 K/100 m	West
Aosta/Gr. St. Bernhard	AOS/GSB	1928 m	18.15 km	0.61 K/100 m	Po Plain
Graz/Schöckl	GRA/SCK	1059 m	13.44 km	0.50 K/100 m	East

Table 3.2.1: The seven station pairs used for the calculation of the monthly varying lapse rate with their appreviations, elevation differences, horizontal distances, yearly mean lapse rates and subregion of the lower station.

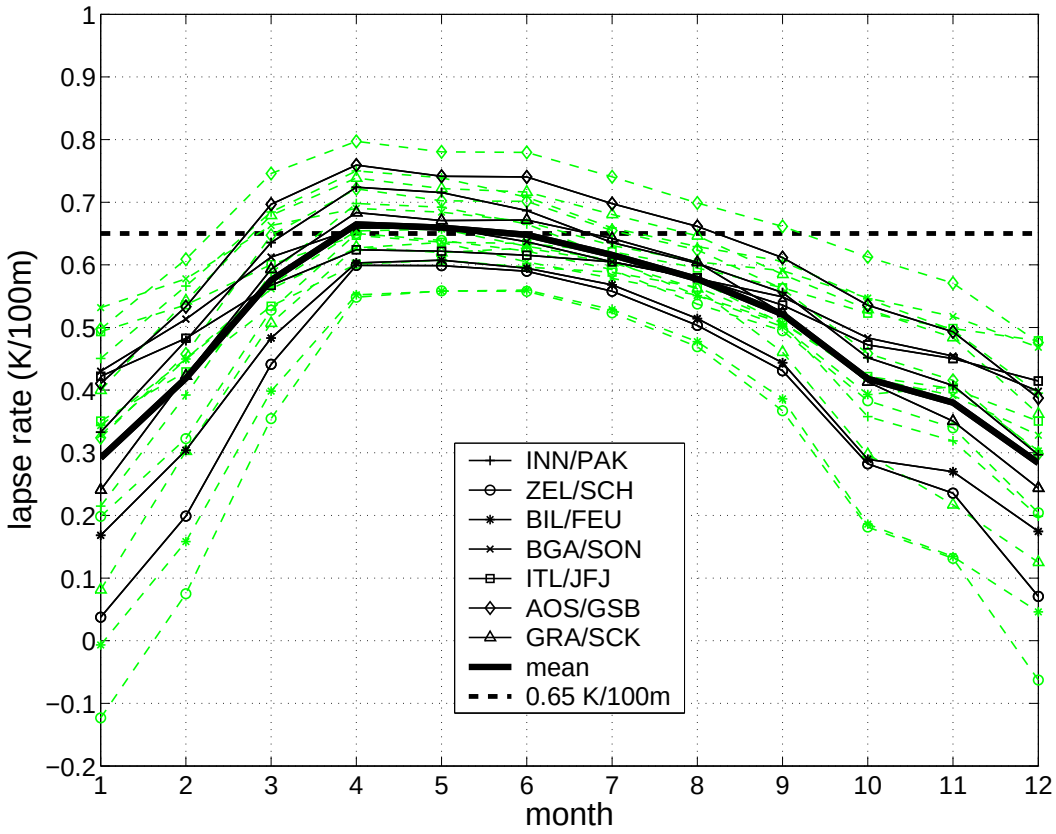

Figure 3.2.3: Annual cycles of lapse rates (K/100 m) based on seven station pairs (thin black lines) with ± 1 standard deviation (green) and the mean of all seven lapse rates (thick black line). The constant lapse rate of 0.65 K/100 m is indicated by the dashed black line.

The monthly mean temperature lapse rates of each pair are calculated from monthly values for the period 1958 to 1998 and are presented in Fig. 3.2.3 with ± 1 standard deviation. All pairs have nearly the same strong annual cycle with largest lapse rates from April to June and smallest vales in December and January, meaning that the atmospheric layering is much more stable in winter than in late spring and early summer. The values of the lapse rates differ between the seven station pairs with largest differences, and also largest variability in winter, probably reflecting the occurance of temperature inversions (Rolland 2003). The shape of the annual cycle is quite in agreement with a study by Rolland (2003), who analysed temperature lapse rates in northern Italy based on four datasets over at least 30 years. In winter his lapse rates averaged over four different regions range between 0.4 and 0.5 K/100 m compared to the area mean lapse rate of around 0.3 K/100 m in the present study. From April to August his mean

temperature lapse rates are constant with values of around 0.65 K/100 m, whereas the lapse rates calculated here are constant from April to June but also with the same mean value of 0.65 K/100 m. These differences might be due to the fact, that Rolland (2003) used a total of more than 600 stations and concentrated on an area around northern Italy. As in the present study the whole GAR is analysed, the monthly varying mean lapse rate calculated here based on stations covering large parts of the Alps are used instead of the lapse rates calculated by Rolland (2003). The monthly varying lapse rate averaged over the seven station pairs and presented by the thick line in Fig. 3.2.3 is used for the next steps.

Before analysing the influence of the new mean monthly varying lapse rate on temperature bias, the new lapse rate is compared to the old constant lapse rate of 0.65 K/100 m, which is presented in Fig. 3.2.3 by the dashed thick line. In late spring and early summer both lapse rates are very similar meaning that the application of the new lapse rate will not change the bias in these months. As mentioned earlier it was expected that in summer the true lapse rate is larger than 0.65 K/100 m due to the more unstable atmospheric layering. The value of 0.65 K/100 m is the mean of the environmental lapse rate varying with time and space. This lapse rate in the free atmosphere can not be expected to be identical to a lapse rate on a mountain slope calculated from station data. In contrast to the surrounding atmosphere, the air over a mountain slope is affected by radiative and turbulent heat exchanges with the surface resulting in warmer air over the slope during daytime and in cooler air during nighttime. This leads to lapse rates differing from the lapse rates in the free atmosphere. However, cloud cover and wind speed also influence the temperature difference between mountains and free air leading to inconclusive results (Barry 1992). These issues might cause the new summer lapse rate not to be larger than the old one. In winter, when atmospheric layering is more stable than denoted by the average environmental lapse rate, the largest differences between the new and the old lapse rates occur. The comparison of the lapse rates leads to the result that from April to June the application of the new lapse rate will not influence the bias whereas from July to March the bias will be influenced, especially in December and January.

However, not only the strength of the difference between the lapse rates affects the influence on the bias but also the elevation difference between the station and the corresponding grid box. The larger this difference is, the stronger is the influence of the application of a different lapse rate on the bias. The elevation

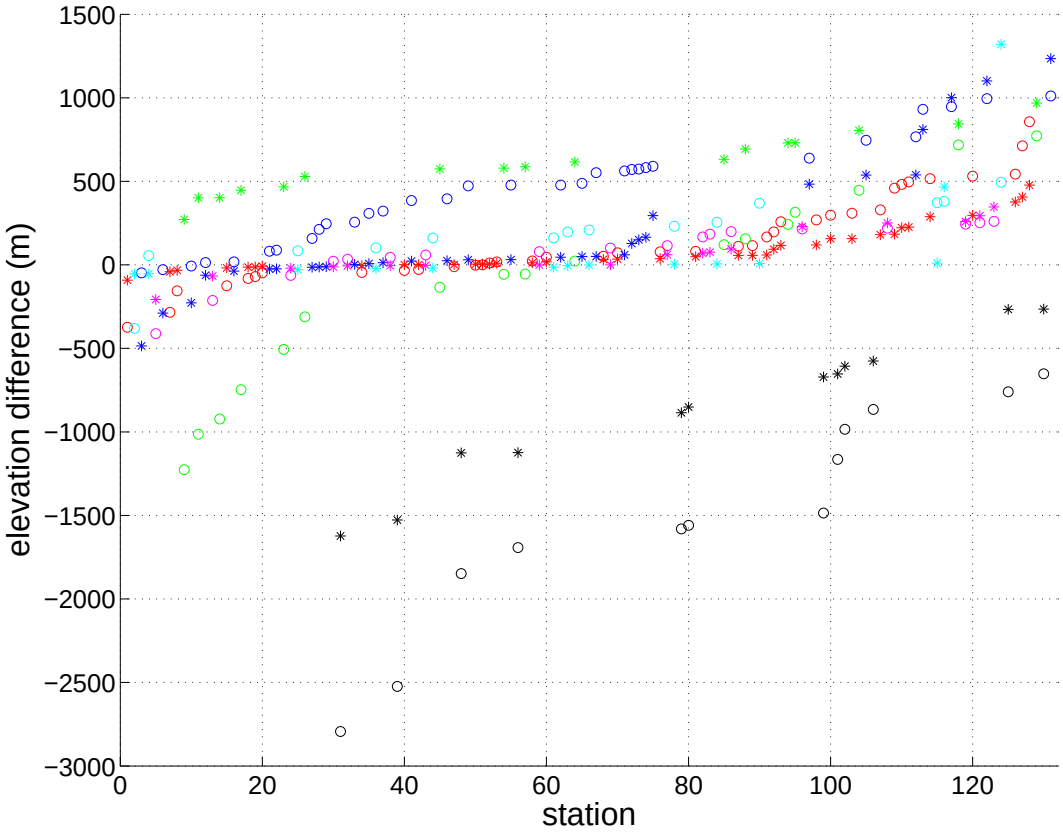

Figure 3.2.4: Elevation differences in m between HISTALP stations and REMO (asterix) and ERA (circle) divided into subregions West (blue), East (red), South (magenta), Po Plain (cyan), CALL (green) and HL (black). Positive (negative) values indicate that the elevation of the grid box of REMO/ERA is larger (smaller) than the elevation of the station.

differences are presented in Fig. 3.2.4 for all HISTALP stations with colour-coded subregions. For both REMO and ERA largest elevation differences between stations and grid boxes occur in subregion HL (black), where the grid boxes are generally too low. This is more pronounced for ERA because in general ERA orography is lower than REMO orography, which is therefore nearer to the high elevation locations. Further large elevation differences are found in subregion CALL (green). All REMO grid boxes are too high indicating that valleys are not well enough resolved, which was already mentioned in section 2.1. For ERA some grid boxes are too low and some too high. It is caused by the generally lower altitude leading in average to a better agreement with the altitude of valleys. Additionally to subregions HL and CALL, ERA has quite large elevation differences in subregion West (blue). As can be seen from the comparison of Fig. 2.1.2b and

1.1.1, ERA is too high mainly over south-eastern France and the Swiss plateau.

The biases between the station datasets (HISTALP and ZMmonthly) and REMO and ERA are recalculated applying the mean monthly varying temperature lapse rate and are averaged over the six subregions. The resulting biases are presented for HISTALP in Fig. 3.2.5a and for ZMmonthly in Fig. 3.2.5b. For both datasets the REMO biases for the different subregions have the same shape of annual cycle. This is also the case for the biases in CALL and HL, which is the largest difference to the biases calculated with the constant lapse rate of 0.65 K/100 m (Fig. 3.2.1c and d). This becomes more clear in Fig. 3.2.5c and d showing the difference between the absolute bias calculated with the constant lapse rate and the absolute bias calculated with the varying lapse rate. Positive values indicate a larger bias by applying the monthly varying lapse rate instead of the constant lapse rate and negative values indicate a smaller bias.

For subregions West, East, South and Po Plain the application of the monthly varying lapse rate only slightly improves the REMO temperature bias, because elevation differences are quite small, except for ZMmonthly in West in February and March where the bias is slightly worsened. The bias in these subregions is small in winter and still largely positive in summer. The positive summer bias is most pronounced in subregions East and Po Plain. In south-eastern Europe the positive summer bias is a common feature not only for REMO (Hagemann et al. 2002, Jacob et al. 2007) but also for other regional models (e.g. Christensen et al. 1997, Machenhauer et al. 1998, Noguer et al. 1998, Hagemann et al. 2001, Vidale et al. 2003, Räisänen et al. 2004, Jacob et al. 2007). It is caused by too dry conditions over this region leading to reduced cloud cover which influences the surface energy fluxes. The abovementioned studies find different reasons for the dry conditions in different models. Christensen et al. (1997) suggest deficiencies in the surface scheme of the different analysed RCMs causing an unrealistic drying-out of the soil, whereas Hagemann et al. (2001) found that improvements in the physical parameterisation of HIRHAM4, which is based on the ECHAM4 parameterisation like REMO, and not in the surface scheme reduce the summer drying problem. These improvements in the physical parameterisation include new land surface parameter fields. Hagemann et al. (2002) showed that problems in the general circulation in REMO and other RCMs lead to too little moisture advection into the region and hence, to the summer drying problem and the consequent influence on surface fluxes. Note that, unlike the REMO simulation

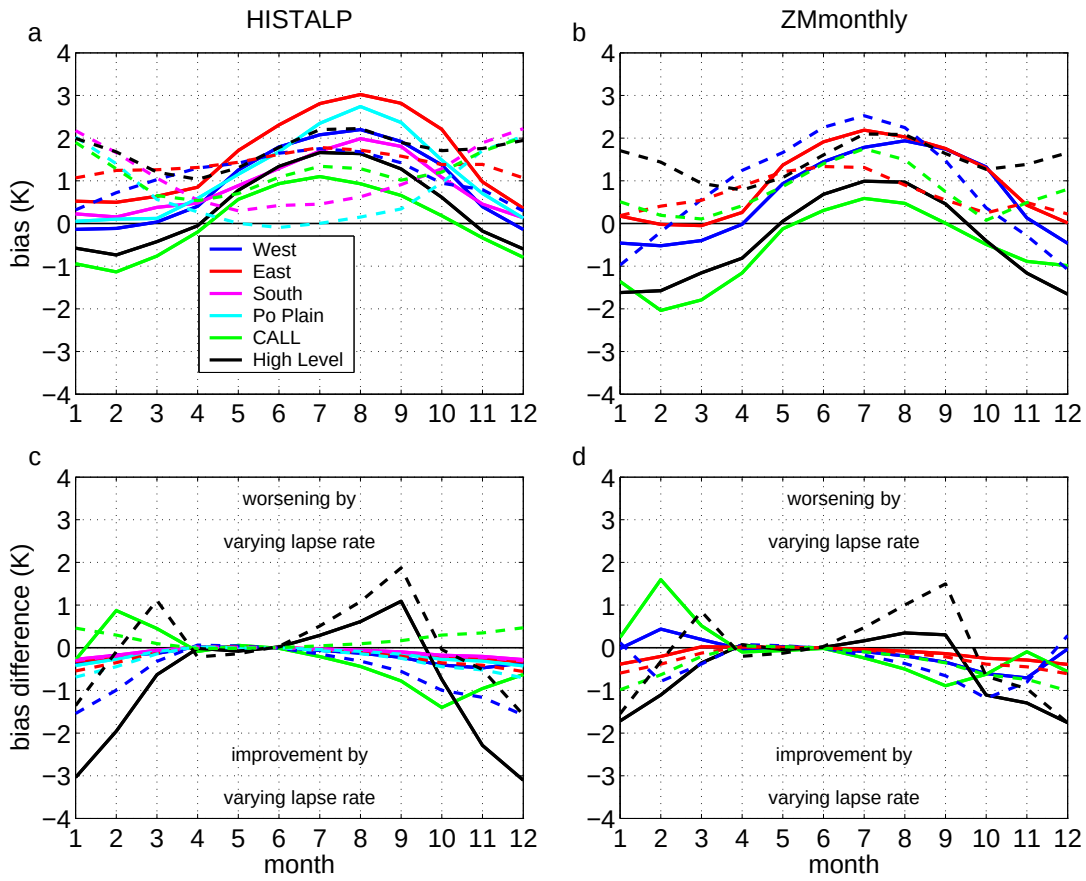

Figure 3.2.5: Annual cycles of biases between both REMO (solid) and ERA (dashed) and both HISTALP (a) and ZMmonthly (b) calculated after applying the monthly varying temperature lapse rate and annual cycles of the differences between absolute biases calculated with the varying lapse rate and the constant lapse rate for HISTALP (c) and ZMmonthly (d) averaged over the subregions.

analysed here, the simulation of Hagemann et al. (2002) was not forced by spectral nudging of the large-scale wind field inside the model domain. Hence, the general circulation in the simulation analysed here should be represented more realistically (Feser 2006). Despite this improvement, the warm bias over south-eastern Europe still exists. This suggests that the main cause of the positive bias may not be a problem in the circulation but rather in the physical parameterisation, mainly of the suface scheme. Van den Hurk et al. (2005) suggest that the too small depth of the hydrological soil reservoir in many RCMs including REMO play an important role.

To investigate the possible causes of the bias in the simulation, simulated cloud cover is compared to observed cloud cover over the period 1958 to 1998

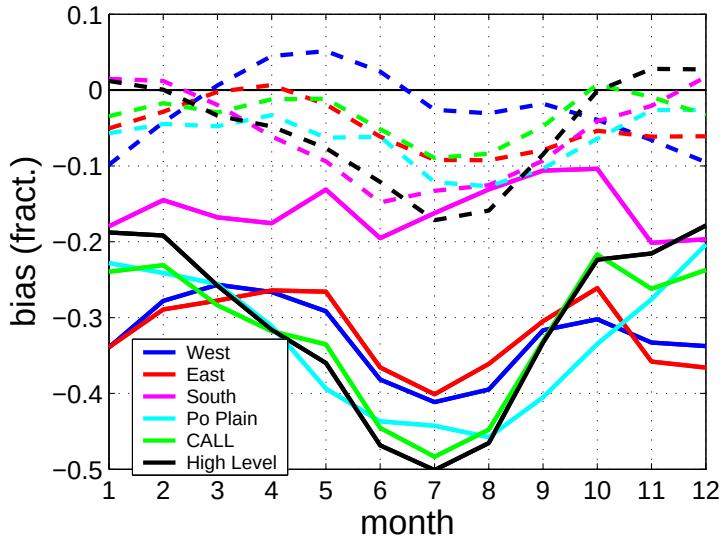

Figure 3.2.6: Annual cycles of cloud cover bias between REMO (solid) and ERA (dashed), respectively, and the HISTALP monthly mean cloud cover station dataset averaged over the six subregions.

for each month separately. The observed values are taken from the HISTALP monthly mean cloud cover station dataset described in section 2.2 consisting of 52 stations, which are also included in the HISTALP temperature dataset. The cloud cover bias shows that the present simulation systematically underestimates observed cloud cover over the whole GAR by 0.1 to 0.5 (Fig. 3.2.6), whereas the ERA bias is very small during the whole year ranging from −0.17 to 0.05. The underestimation of REMO cloud cover is most pronounced in summer, which is consistent with the larger warm bias in this season, indicating a link of the bias to drying.

In addition to the aforementioned widely known positive summer temperature bias in subregion East, the REMO simulation analysed here shows a large positive summer bias in the subregion Po Plain. This is in agreement with Noguer et al. (1998), who analysed different set-ups of an RCM based on the Unified Model by UK Met Office over the whole of Europe. The positive temperature bias in different regions in summer in the simulation analysed in this study might be caused by the bias in cloud cover. Additionally, the REMO simulation has a negative precipitation bias in the Po Plain and south-eastern Europe compared to the gridded precipitation climatology of Frei and Schär (1998) interpolated on the REMO grid (Scheifinger 2006). This may not explain the whole bias, but a more detailed examination of the physical causes of this positive summer bias is

beyond the scope of this thesis.

In the inner Alps quite large differences occur between the bias based on the constant lapse rate and the bias based on the monthly varying lapse rate (Fig. 3.2.5c and d). The newly calculated REMO bias in HL is smaller from October to March and larger from July to September. From May to June the constant lapse rate approximately equals the varying lapse rate so there is little change. The reduction of the cold bias in winter suggests that the constant lapse rate was indeed too large due to the on average more stable atmosphere in winter. The reduced varying lapse rate from July to September slightly increases the existing warm bias. In CALL the new bias for HISTALP (ZMmonthly) is smaller from July to January (December) and larger from February (January) to March leading to an annual cycle similar to HL with positive biases in summer and negative biases in winter. As for CALL all REMO grid boxes are too high and for HL too low (Fig. 3.2.4), the annual cycle can not be caused by the altitude correction. This annual cycle is in agreement with studies of Christensen et al. (1997), Noguer et al. (1998) and Vidale et al. (2003). They analysed different RCMs with a resolution of about 50 km over the whole of Europe compared to gridded data and showed similar results over the Alps. However, they did not distinguish between low and high elevations.

The warm bias in CALL and HL in summer is small compared to the summer biases in the other subregions and can therefore be attributed to the overall warm summer bias of REMO. In winter the cold biases in subregions CALL and HL are also quite small. For HL a potential explanation might by the slightly too low simulated cloud cover, which agrees with the result of Scheifinger (2006) showing that REMO underestimates precipitation at high elevations. This might cause too strong outgoing radiation and therefore lower temperatures. In CALL the negative winter bias might be caused by the fact that REMO does not resolve the valleys with their low elevations, which might lead to a less effective mixing of the lower atmosphere by valley winds than in the real world as suggested by Bromwich et al. (2005).

However, the REMO bias shows a quite consistent picture over the whole area when compared to both station datasets after the application of the varying lapse rate, with positive values in summer and small or negative values in winter. The comparison between the REMO bias compared to HISTALP and the bias compared to ZMmonthly suggests that the temperature of ZMmonthly is in general

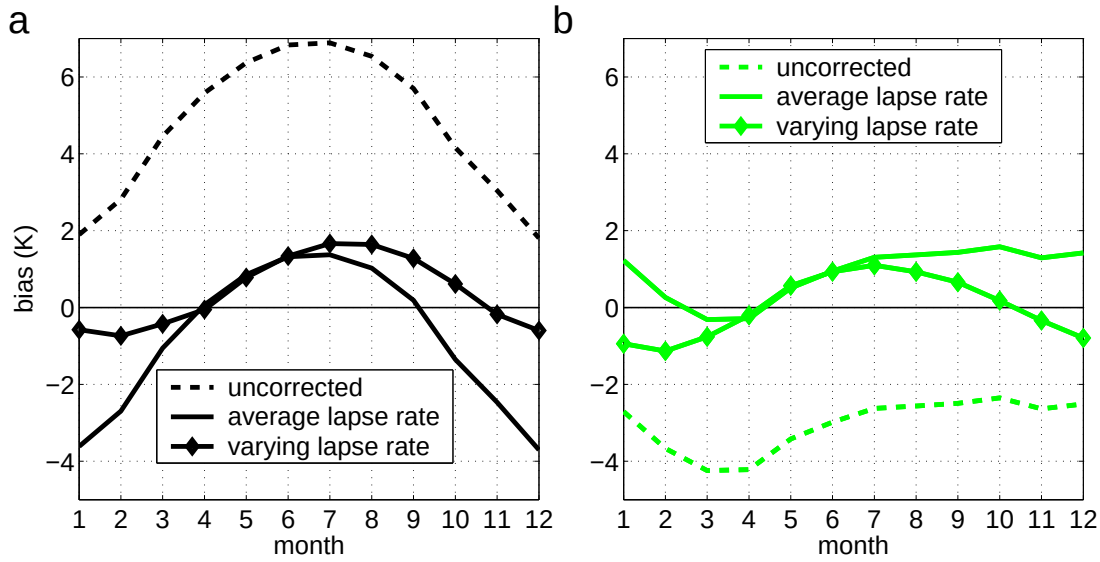

Figure 3.2.7: Annual cycles of biases between REMO and HISTALP calculated without altitude correction (dashed), with the constant lapse rate (solid) and with the varying lapse rate (diamonds) for subregions High Level (a) and Central Alpine Low Level (b).

higher than the temperature of HISTALP. As for both datasets the stations have nearly the same altitude averaged over the subregions, this difference might be due to the quality differences between the two datasets.

To better demonstrate the influence of the lapse rates on the bias, the resulting REMO biases are presented for HL in Fig. 3.2.7a and for CALL in Fig. 3.2.7b. In addition to the biases calculated with the constant and the varying lapse rates the biases calculated without any altitude correction are displayed. In subregion HL the uncorrected REMO bias is much too warm during the whole year with largest positive bias in summer of nearly 7 K. This bias is mainly caused by the too low elevation of the corresponding grid boxes. They are about 260 to 1620 m too low (Fig. 3.2.4). The altitude correction with the constant lapse rate mainly reduces the bias but does not change the annual cycle. However, the application of the monthly varying lapse rate calculated from the station data minimizes the bias throughout the whole year compared to the uncorrected bias. In subregion CALL the REMO grid boxes are too high (270 to 970 m, Fig. 3.2.4) leading to a negative uncorrected bias (Fig. 3.2.7b). Both applied lapse rates improve the bias, but the monthly varying lapse rate leads to a generally slightly lower bias.

For ERA the modified lapse rate has the largest impact on bias in subregions HL, CALL and West (Fig. 3.2.5c and d). For HL the newly calculated bias

is larger in March and from July to September and smaller from November to January. This is quite similar to the bias difference of REMO in this subregion due to the fact that the REMO and ERA biases based on the constant lapse rate have very similar annual cycles, and both REMO and ERA grid boxes are too low compared to the elevation of the stations (Fig. 3.2.4). In subregion CALL the modification of the lapse rate leads to a worsening when using the HISTALP dataset and to an improvement when using ZMmonthly. This is caused by on average too low grid boxes compared to HISTALP and on average too high grid boxes compared to ZMmonthly leading to different averaged biases. In subregion West the application of the monthly varying lapse rate improves the ERA bias for HISTALP as well as for ZMmonthly. For both REMO and ERA improvements can only be found from July to March because from April to June the new lapse rate differs only very little from the prior constant lapse rate of $0.65\,\mathrm{K}/100\,\mathrm{m}$.

As was expected the largest differences between the biases calculated with the different lapse rates occur in winter when the difference between the old and the new lapse rate is largest, and in subregions where the elevation difference between the stations and the corresponding grid boxes is largest. The application of a monthly varying lapse rate calculated from station data leads in general to a reduction in the model bias. This is expected as the varying lapse rate is more realistic. This lapse rate is supposed to be adequte for the application over the GAR because a mean lapse rate calculated from more than seven station pairs covering a larger area would probably not drastically change the mean lapse rate as the existing station pairs already represent different locations and elevation differences without showing a dependency on the lapse rate.

To give an impression of the spatial distribution of the bias calculated with the varying lapse rate, in Fig. 3.2.8 and 3.2.9 the bias between REMO and HISTALP and ERA and HISTALP, respectively, is presented for each month and each station. Significant (α=0.05) biases between HISTALP and REMO or ERA temperature calculated for each station and each month with a t-test testing for the difference in means of two samples are marked by a black circle. As already mentioned in the previous section, the regionalisation, meaning the averaging over the subregions, does not lead to a loss of information. For REMO the relatively low biases in winter and the warm biases in summer with largest values in the East of the GAR are visible. For ERA the less consistent bias with high positive values in winter in the south and in summer in the north is evident.

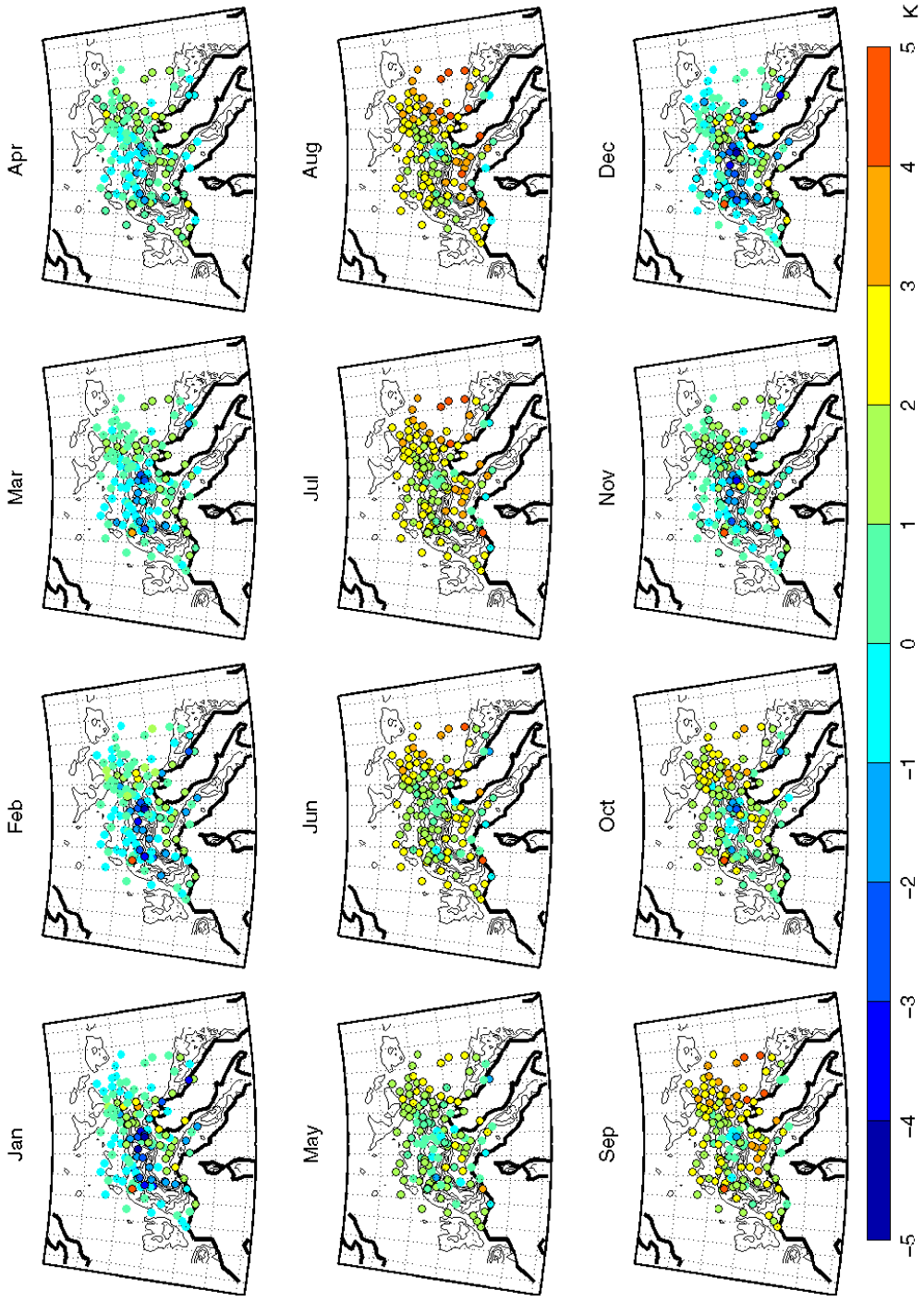

Figure 3.2.8: Biases in Kelvin between REMO and HISTALP calculated with varying lapse rate. Significant values (α=0.05) with black circle. Contour lines in the background represent orography used in REMO with an interval of 500 m.

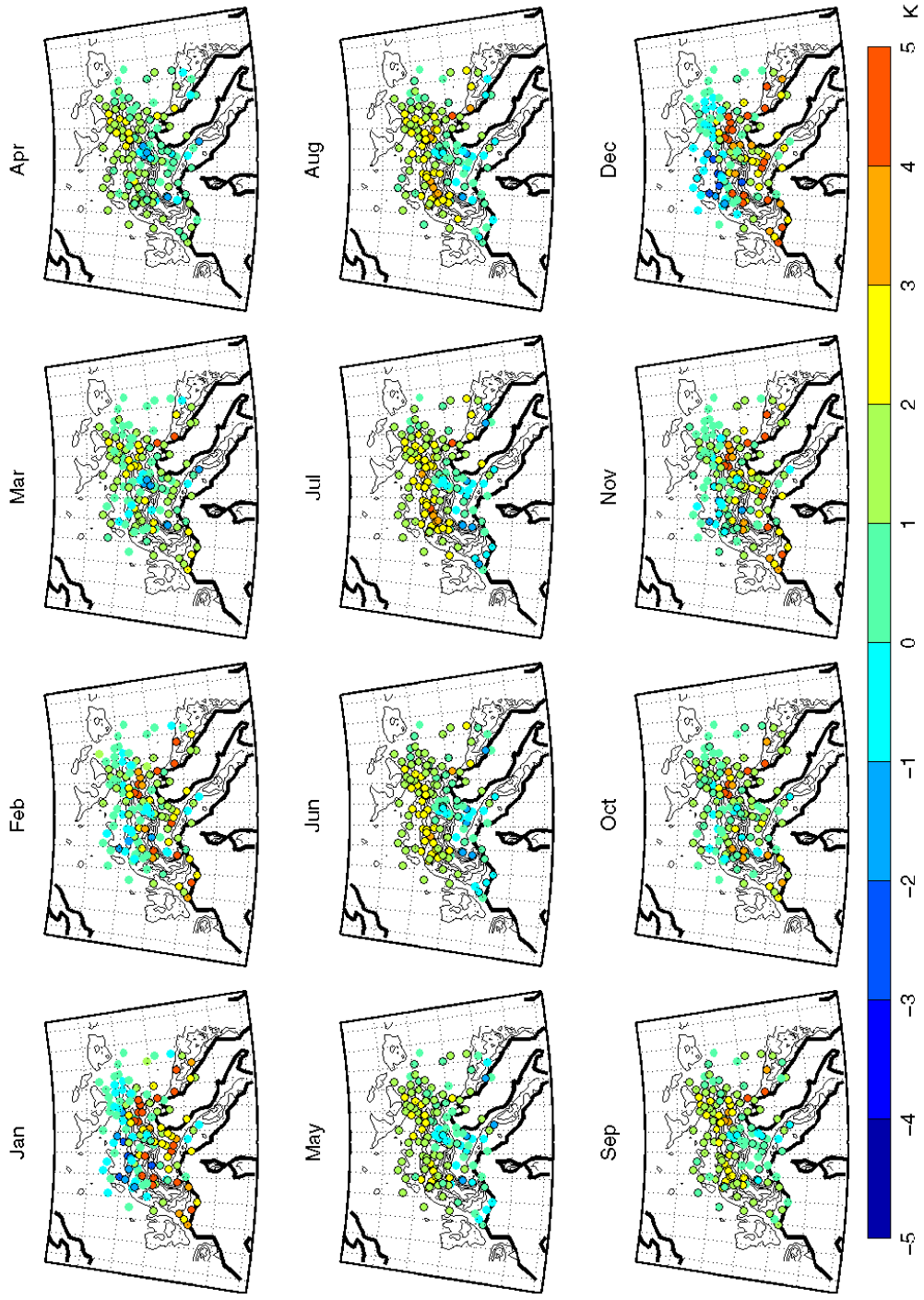

Figure 3.2.9: Biases in Kelvin between ERA and HISTALP calculated with varying lapse rate. Significant values (α=0.05) with black circle. Contour lines in the background represent orography used in REMO with an interval of 500 m.

3.2.2 A comparison of the skill determined from grid box and station data

The problems arising when comparing model grid box data to station data especially over complex orography like the Alps has already been outlined in section 3.1.1. To test whether the validation results depend on the type of data that the simulations are compared with, i.e. grid box or station data, the REMO simulation has also been compared to the gridded temperature dataset CRU TS 2.0 of the Climatic Research Unit (CRU, Mitchell et al. 2004) in addition to the comparison with the HISTALP stations. The gridded CRU dataset has a resolution of 0.5° and is described in section 2.2. As for the station data, correlation, bias and rmse are calculated over the period 1958 to 1998 for each month and each grid box separately. The degree of similarity between these results and those from station data discussed in the previous sections indicates then the potential level of the grid box versus station problem.

The correlation pattern between REMO and the CRU data is very similar to the correlation pattern between REMO and the station data for all months. As an example the correlation and bias patterns for February and August are presented in Fig. 3.2.10 showing the results of the comparison with the CRU data on the 1/6° grid in the background and the results of the comparison with HISTALP by the dots in the foreground. The bias is calculated with the monthly varying lapse rate. The pattern of the bias between REMO and the CRU data is quite similar to the one of the bias between REMO and the station data. This is for example visible for the warm summer bias over south-eastern Europe and the Po Plain and the generally small bias in winter. Largest differences occur in the Dolomite Alps in northern Italy where REMO simulates temperature clearly too warm in comparison to CRU during the whole year, whereas in comparison to the station data in this region the bias is quite small. This means that in this area the gridded CRU temperatures are colder than the HISTALP station data. One explanation for this discrepancy relates to the selection of stations used in the construction of the CRU data, i.e. if large number of mountain compared to valley stations are included this leads to a lower temperature in the grid box. However, the elevation of the stations is included in the interpolation and influences the calculation of temperature, but the inclusion of elevation in the construction of the CRU dataset might be inadequate in areas of complex orography. Another explanation could be that the HISTALP stations in the Dolomite Alps which are part of subregion

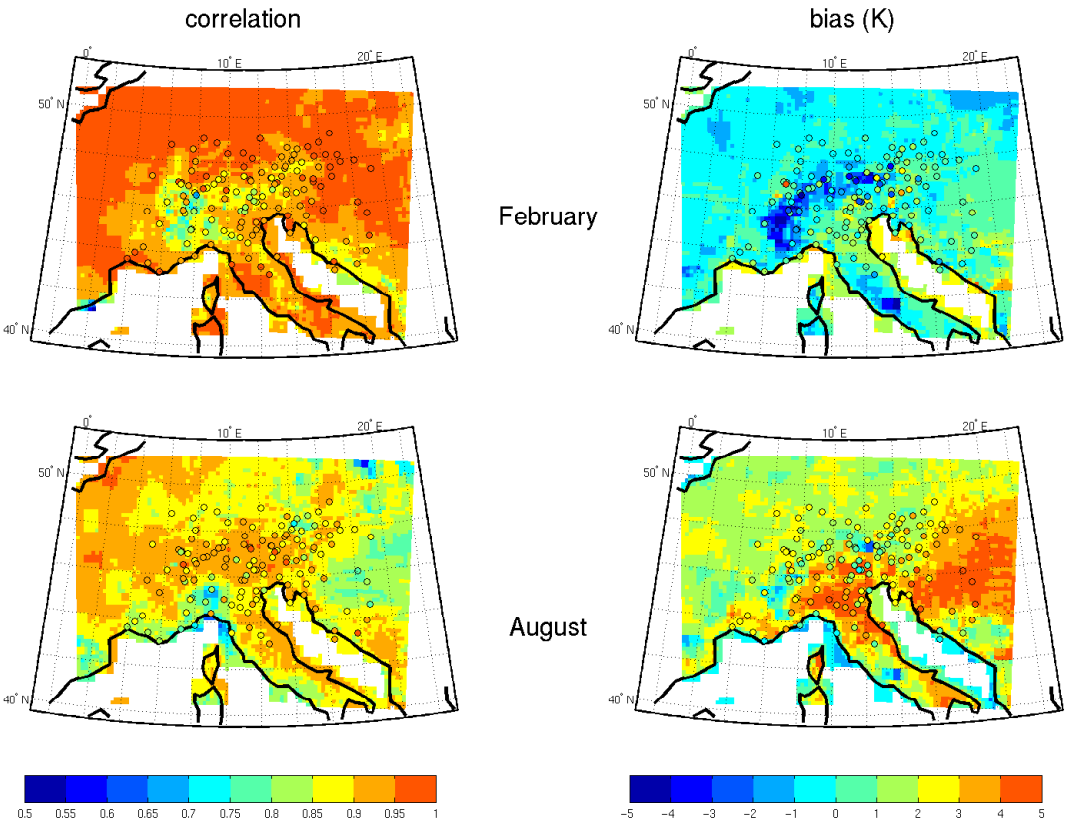

Figure 3.2.10: Temperature correlation patterns (left) and bias patterns (right) for February (top) and August (bottom) between REMO and the gridded CRU data on the 1/6° grid in the background and between REMO and the HISTALP station data on the dots in the foreground. The bias is calculated with the monthly varying lapse rate.

CALL are not representative for this area. The reason for this difference is not clear. The application of the constant lapse rate also shows similar patterns for the bias between REMO and CRU and the bias between REMO and the stations (not shown).

Nevertheless, the comparison grid box/grid box versus grid box/station shows that both comparisons have very similar results. Some larger differences occur in the inner Alpine regions with the most complex orography. Here, the biases should be interpreted with caution.

3.2.3 Added value of REMO compared to ERA

The comparison of the performance of REMO and ERA has so far been separated into correlation and bias. The comparison to HISTALP showed that ERA has

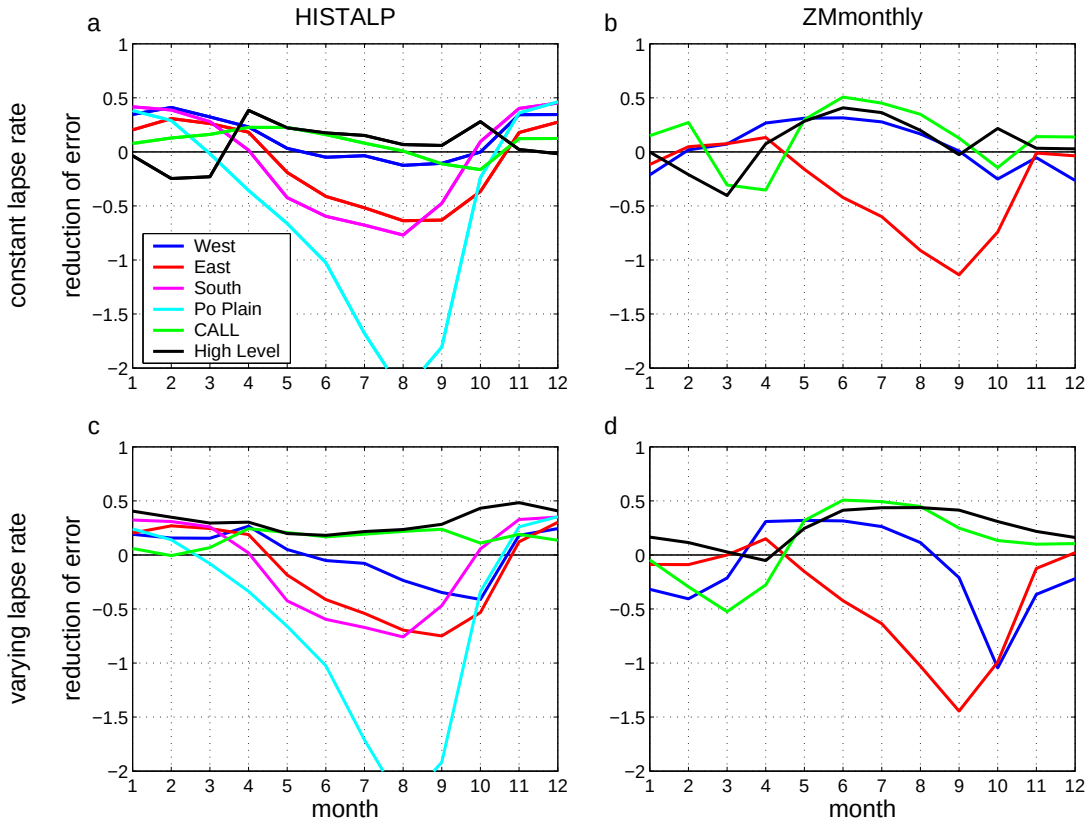

Figure 3.2.11: Annual cycles of the reduction of error of temperature calculated with the constant lapse rate for HISTALP (a) and ZMmonthly (b) and the reduction of error of temperature calculated with the varying lapse rate for HISTALP (c) and ZMmonthly (d) averaged over the subregions.

slightly higher correlations than REMO during the whole year, whereas the bias differences between ERA and REMO vary strongly during the year. Therefore, one cannot conclude whether ERA or REMO has overall a lower bias. To combine the different results derived from the correlation comparison and the bias comparison, in other words, to analyse directly whether the higher resolution of REMO leads to an added value compared to ERA, and to determine a magnitude of improvement of REMO, the reduction of error is calculated and shown in Fig. 3.2.11. The reduction of error is a measure of the skill of the regional model relative to the driving global reanalysis and is calculated by the following equation:

$$RE = 1 - \frac{rmse_{REMO}}{rmse_{ERA}} \tag{3.1}$$

The root mean squared error (rmse) combines the effects of correlation and bias.

The reduction of error ranges from $-\infty$ to $+1$. Positive values indicate the magnitude of improvement of REMO compared to ERA and zero denotes the same performance for REMO and ERA. Negative values indicate that the agreement of REMO with station data is worse than for ERA. However, the negative values do not specify the magnitude of worsening and are therefore not comparable to the positive values.

The analysis based on the HISTALP dataset using the constant lapse rate shows an improvement of REMO compared to ERA in winter and early spring for subregions West, East, South, Po Plain and CALL (Fig. 3.2.11a). For subregion CALL this improvement ranges even from November to August. In subregion HL, REMO shows no improvement in winter but from April to November. The performance of REMO compared to ERA is mainly influenced by the bias as the differences for correlation are very small (Fig. 3.2.1a) and the reduction of error resembles strongly the difference between the REMO and ERA biases (not shown). This is most visible for subregions Po Plain, South and East in summer, where the performance of REMO compared to ERA is worst.

Compared to the results based on HISTALP the results based on the ZMmonthly dataset using the constant lapse rate (Fig. 3.2.11b) show some differences in the performance of REMO. For subregion CALL negative values instead of positive values occur in spring and summer values are more positive. For subregion West the annual cycle is nearly opposite to the one based on HISTALP. These differences can be explained by the differences between HISTALP and ZMmonthly bias in these regions (Fig. 3.2.1c and d). Robust features in the performance of REMO compared to ERA are the annual cycle for subregion HL and the better performance of REMO in subregion CALL in summer and winter.

The reduction of error calculated with the monthly varying lapse rate differs slightly from the one calculated with the constant lapse rate. For HISTALP the differences are very small for subregions West, East, South and Po Plain, but for CALL and HL the reduction of error calculated with the varying lapse rate is now positive throughout the whole year (Fig. 3.2.11c). This is mainly caused by the smaller REMO bias compared to the ERA bias is these regions (Fig. 3.2.5). The largest positive values of reduction of error for REMO are found for subregion HL during the whole year. Therefore, the higher resolution of the REMO simulation compared to the ERA reanalysis adds value especially in regions with most complex orography. For ZMmonthly the newly calculated

reduction of error shows quite similar annual cycles to those calculated with the constant lapse rate but also improvements mainly for subregions CALL and HL (Fig. 3.2.11d). The differences between the reduction of error calculated with the different lapse rates are largest in CALL and HL, which is due to the largest elevation differences between the station and the corresponding grid box leading to a larger influence of different lapse rates.

As mentioned in section 2.1, only temperature from stations whose elevation difference to the ERA orography is smaller than 300 m is assimilated in the ERA40 Reanalysis. Therefore, by comparing REMO and ERA only to those stations with a larger elevation difference, an independent validation and added value analysis is possible. Even though the HISTALP dataset is large leading to a number of potential independent stations, only 60 out of 131 stations are selected and through the averaging over the six subregion, only one station remains in subregion South. In Table 3.2.2 the number of remaining stations and the original number of stations are presented for each subregion.

Region	West	East	South	Po Plain	CALL	HL
original	32	38	18	14	17	12
independent	21	11	1	5	10	12

Table 3.2.2: The original number of stations for each subregion and the number of stations independent from the ERA40 reanalysis.

The reduction of error calculated only with the independent stations not assimilated into ERA and the monthly varying lapse rate is presented in Fig. 3.2.12. Compared to Fig. 3.2.11c, where all HISTALP stations are included, the reduction of error does not change drastically, except for subregion South. However, as only one single independent station represents subregion South, the results of this subregion should not be interpreted. The other noticeable differences are that in subregions West and Po Plain the reduction of error becomes negative in winter, that in Po Plain it becomes less negative in summer and that in subregion CALL it becomes more positive in summer. In subregion HL nothing changed, because all 12 corresponding stations were not included in the assimilation.

It was expected that REMO does not show a clear overall added value using the whole HISTALP dataset because some of the stations used for the comparison are assimilated in ERA leading to a better knowledge of temperature for

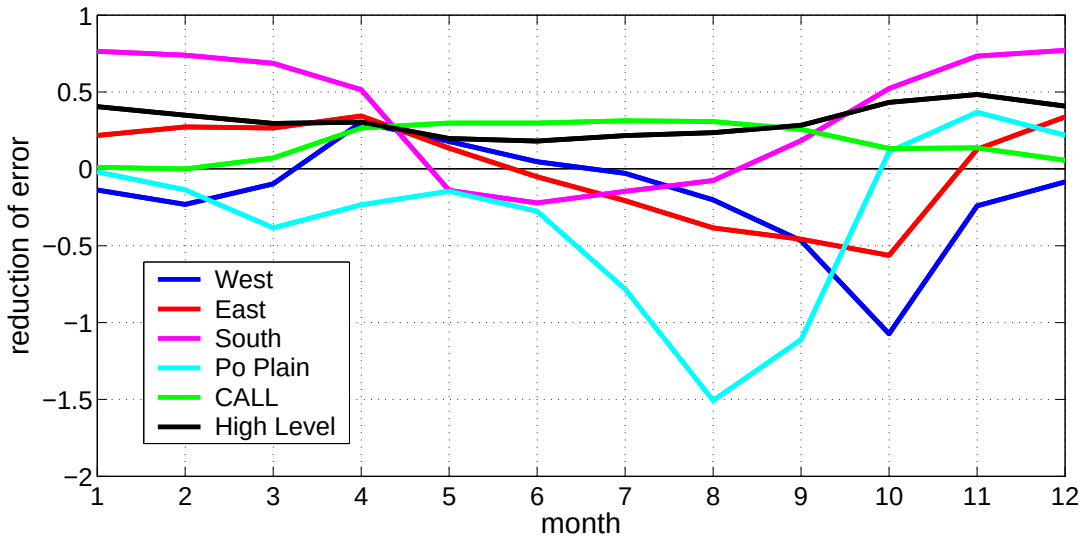

Figure 3.2.12: Annual cycle of the reduction of error of temperature calculated with the HISTALP stations independent from the ERA40 reanalysis and with the monthly varying lapse rate averaged over the subregions.

ERA. However, this analysis shows that the exclusion of station data used for the temperature assimilation does not have a large influence on the added value of REMO compared to ERA. This is caused by the fact that the stations excluded from the assimilation are highly correlated to the assimilated stations nearby (not shown), as temperature does not change drastically in horizontal directions, meaning that spatially small-scale variability is low, and differ mainly because of the different elevation captured by the temperature lapse rate. Due to the horizontal homogenity of temperature, ERA has also knowledge of the temperature of the stations which are not assimilated. Thus, as the small-scale variability is low and REMO is supposed to add value to ERA on small spatial scales, it is obviously difficult for REMO to show an improvement compared to ERA. The horizontal homogenity was analysed by correlating one representative station of each subregion with all other stations for each month (not shown). In summer the correlations mainly range from 0.5 to nearly 1 meaning that temperature homogenity is most pronounced. In winter more inhomogenities occur indicated by lower correlations, which is most obvious for subregions CALL and High Level, potentially due to local inversions.

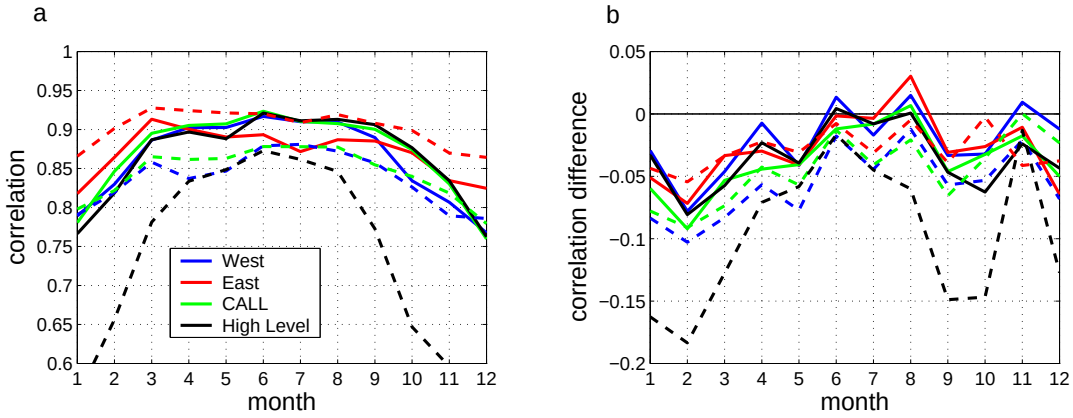

Figure 3.2.13: Annual cycles of the daily temperature correlation (a) between ZMdaily and both REMO (solid) and ERA (dashed) and the correlation difference between ZMdaily and ZMmonthly (b) for REMO (solid) and ERA (dashed) averaged over the subregions.

3.2.4 The skill of REMO and ERA compared to daily station data

One may expect more added value in the performance of the high-resolution regional model compared to a coarser resolution on a daily timescale because spatially small-scale phenomena, which take place on small temporal scales, are simulated better with a higher resolution. On a monthly timescale the influence of these phenomena may disappear during averaging. Therefore, the correlation, bias and reduction of error were also calculated from daily data.

The comparison between REMO and ERA and the daily dataset ZMdaily only partly supports the hypothesis of better representation on daily timescales. Correlation, bias and rmse were calculated for each month based on daily data. As expected the correlations between the simulations and ZMdaily are lower than the correlations on a monthly basis for all subregions and both REMO and ERA (Fig. 3.2.13) because it is easier for REMO and ERA to simulate the month to month variability than the daily variations. As for the comparison to ZMmonthly, REMO has slightly higher correlations than ERA in all subregions except East, indicating that smaller scale variability features are better simulated. This feature is most pronounced for the high level stations in winter, where the ERA correlations are lowered drastically compared to the correlations with ZMmonthly. This might be caused by the fact that the altitude difference between the high level stations and the corresponding ERA grid boxes is largest. Therefore, differences

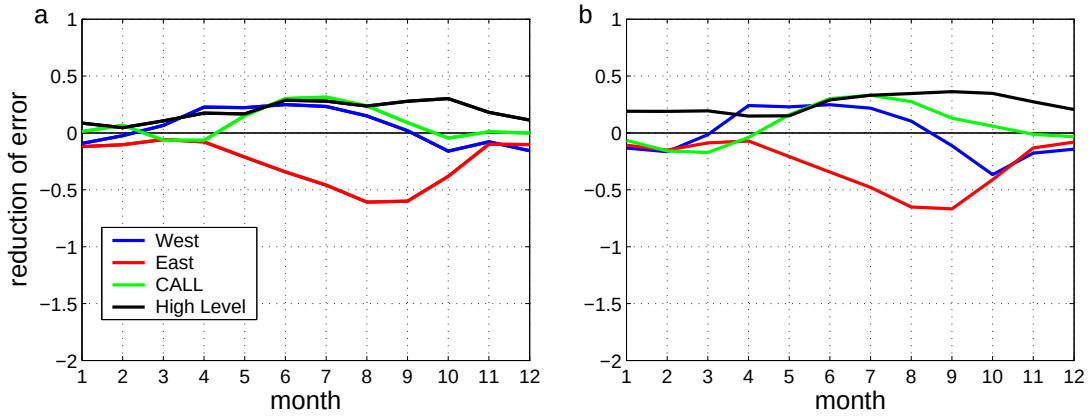

Figure 3.2.14: Annual cycles of the daily reduction of error of temperature based on ZMdaily calculated with the average lapse rate (a) and calculated with the varying lapse rate (b) averaged over the subregions.

in snow fall as well as snow cover occur leading to different temperature variability which is enhanced on the daily timescale. By definition the daily bias averaged over each month is the same as the monthly bias and was discussed in section 3.2.1.2 and 3.2.1.3. The reduction of error calculated with the constant lapse rate (Fig. 3.2.14a) shows as a measure of added value very similar results as for ZMmonthly. However, for subregion HL, REMO performs better than ERA during the whole year due to the very low correlation of ERA. Therefore, for the high elevation stations REMO has a definite added value compared to ERA on the daily timescale, which is higher than that on the monthly timescale, except for summer where it is slightly lower. The reduction of error calculated with the monthly varying lapse rate shows nearly the same results with slightly larger values than calculated with the constant lapse rate for HL during the whole year (Fig. 3.2.14b).

3.3 Conclusions

The temperature performance of a reanalysis-driven hindcast, with spectral nudging applied, compared to homogenised station data has been investigated for the period 1958 to 1998 with a 1/6° resolution version of the regional model REMO. The model domain covers the whole of Europe but the analysis has been focussed on the Greater Alpine Region (GAR). The driving ERA40 reanalysis, which has a resolution of 1.125°, has also been compared to the station data. For REMO

and ERA, correlation, bias and rmse have been calculated on monthly and daily timescales, and the skill of REMO and ERA has been compared to assess the added value of REMO compared to ERA. The results have been summarised over the six subregions West (west and north-west of the Alps), East (north-east and east of the Alps), South (around the Adriatic Sea), Po Plain, Central Alpine Low Level (inner Alpine stations below 1500 m), and High Level (above 1500 m) shown in Fig. 3.1.1.

In most earlier studies RCM simulations were not validated against station data but against gridded data such as the widely used products of the Climatic Research Unit (e.g. Noguer et al. 1998, Giorgi et al. 2003, Vidale et al. 2003). A temperature validation of statistically downscaled GCM output and RCMs against station data has been performed by Kyselý (2002), Moberg and Jones (2004) and Bromwich et al. (2005). As stated earlier, while a comparison of simulations and gridded observations assesses the skill of the model when it is used for estimating area means, a comparison with station data shows how well local values can be estimated. As discussed in section 3.1.1 both approaches are meaningful. Similarly to Moberg and Jones (2004), the present analysis shows in some inner Alpine regions large differences between the validation against gridded and against station data. These differences can either be due to unrealistic estimates for area means in complex terrain given by the gridded temperatures or due to station data that are not representative for the area mean over a grid cell. In the first case the differences would be an artefact of a technical problem, whereas they would reflect a real effect in the second case. However, it is beyond the scope of this thesis to determine to what content these two reasons influence the results. In regions with a less complex orography the comparison with grid box data or with station data leads to very similar results.

The calculated correlations against the station data are very similar for REMO and ERA and show that both represent the temporal variability of temperatures at the stations quite well on monthly and daily timescales. However, the biases in some regions and seasons reach large values and differ strongly between REMO and ERA. In summer REMO shows a pronounced warm bias in south-eastern Europe and the Po Plain which is mainly due to too dry conditions in the model. The comparison with other studies about the summer drying in south-eastern Europe indicates shortcomings in the parameterisation, which is derived from GCMs but not optimised for RCMs (Christensen et al. 1997, Hagemann et al.

2001, van den Hurk et al. 2005). A large negative bias in winter has been found for the high elevation stations and is caused by the constant altitude correction. An altitude correction is needed for comparing absolute temperatures at the stations with those at model grid boxes at different altitudes. As a constant lapse rate is not realistic a monthly varying lapse rate calculated from the station data has been applied and the large negative bias disappears but slightly increases the late summer bias.

The application of different lapse rates to simulated temperature showed that the choice of the lapse rate strongly influences the bias in moutainous areas, where elevation differences between stations and grid boxes are largest. Especially in these ares, it is important to use a more realistic and therefore monthly varying lapse rate because otherwise, in the comparison to station data with a large elevation difference biases would be induced due to the wrong altitude correction. However, as in reality the lapse rate varies from day to day and even from day to night, a time-dependent lapse rate could improve the bias even more.

To address the question of whether REMO has added value to ERA the reduction of error has been calculated for different regions and for each month of the year. The reduction of error is dominated by the differences in the REMO and ERA bias, as the differences in the correlations are negligible. In different subregions and different seasons the reduction of error varies strongly and thus it is not possible to make a general statement about the performance of REMO compared to ERA with respect to GAR temperatures. However, concerning the high elevation stations REMO does add value compared to ERA throughout the whole year on monthly and particularly on daily timescales, which is mainly due to the smaller bias. For the inner Alpine low elevation stations the added value of REMO can be found nearly during the whole year depending on the selection of station data compared with. The added value in this subregion might be due to less stations assimilated in ERA, and a lower horizontal homogenity of temperature of these stations leading to a stronger influence of the better resolved orography in REMO. The performance of REMO is worse than that of ERA in the Po Plain in summer even though the high resolution of REMO reproduces the orographic details of this region quite well, and the plain is not even represented in the ERA orography due to the coarse resolution (Fig. 2.1.2). An explanation for the low performance might be the frequent occurrence of convective instabilities in this region in summer as mentioned in section 1.1, which may not be

captured by REMO but whose effect on temperature is included in ERA through the assimilation of temperature observations. In some other cases the reduction of error varies substantially between the stations in a given region, which then makes it difficult to assess the value added through REMO.

This study quite clearly detects a better representation of temperature by the high-resolution REMO hindcast than by the ERA40 reanalysis in inner Alpine regions with the most complex orography. However, in regions surrounding the mountain range with less complex terrain a clear added value of the higher resolution is missing. A main reason for the lack of clear added value in these regions may be the fact that temperature observations are assimilated in the reanalysis but not in the regional model and that temperature shows in these regions a low variability on small spatial scales. It should be noted that the REMO domain in the present simulation is quite large, and thus the reanalysis-based temperature information that reaches the GAR from the boundaries through advection is limited. A lack of added value of a high-resolution hindcast compared to a driving simulation with coarser resolution has also been found recently in studies for other regions (Roads et al. 2003, Duffy et al. 2006, Seth et al. 2007). Besides our study there are only a few others that have analysed the added value in hindcasts with regional climate models relative to the driving, coarser resolution reanalysis (Roads et al. 2003, Sotillo et al. 2005, Feser 2006). Roads et al. (2003) analysed precipitation over the whole of South America and showed that only the ensemble mean of all RCMs adds value to the reanalysis. They attribute this to parameterisations that are not optimised for the regional models. The work of Sotillo et al. (2005) on sea level pressure, 2 m temperature and 10 m wind speed in the Mediterranean showed an improvement of the regional simulation mainly for 10 m wind speed and extreme values of temperature. They compared REMO with a resolution of 0.5° and the driving NCEP/NCAR reanalysis to 15 Atlantic and Mediterranean offshore buoy stations and 20 Spanish inland stations. For temperature the added value is larger inland demonstrating the influence of the better resolved orography, which is in agreement with the present study. Feser (2006) performed a spatial scale dependent analysis of REMO with a resolution of 0.5° compared to the driving NCEP/NCAR reanalysis over the whole of Europe for sea level pressure and 2 m temperature. She separated the fields into large (larger than 700 km) and medium spatial scales (about 250 to 550 km) and calculated pattern correlations over the whole domain between REMO and DWD analy-

ses and between the reanalysis and DWD analyses. As was expected (Laprise 2003), for temperature a clear added value of the regional simulation was found only on medium spatial scales. However, when focussing on the Alps the added value is less clear on medium spatial scales, especially in summer. However, a more detailed comparison to the present study is not possible due to the coarser resolution and the more general analysis over the whole of Europe.

The similar performance of the regional hindcast and of the driving reanalysis in less complex terrain, despite the fact that observations are assimilated in the reanalysis but not in the regional model, and the better performance of the regional hindcast in regions with complex orography found in this study, show the considerable skill of the regional model. However, improvements of RCMs appear to be required to fully exploit their higher resolution and provide hindcasts that are consistently better than the reanalyses. It turns out in the present analysis that parameterisations adapted to and optimised for RCMs would improve their performance, which has already been suggested by Roads et al. (2003) and Seth et al. (2007).

Chapter 4

Analysis of the North Atlantic Oscillation influence on Alpine temperatures using a dense station dataset and a high-resolution simulation

It is shown in the previous chapter that the high-resolution regional climate model REMO adds value to the simulation of 2 m temperature in the GAR, at least in the areas of most complex orography, compared to the ERA40 reanalysis with a much coarser resolution. This analysis concentrated solely on the simulation of temperature. In the present chapter it is analysed whether the higher resolution adds also value to the temperature response to large-scale atmospheric circulation. One large-scale phenomenon with a strong influence on European climate is the North Atlantic Oscillation (NAO). Therefore, the influence of the NAO on temperature in the GAR is analysed in this study. A quite similar phenomenon is the Arctic Oscillation (Thompson and Wallace 1998) with a zonal structure over the whole Northern Hemisphere, which in contrast to the NAO does not concentrate on the Atlantic sector (Ambaum et al. 2001). As the present study concentrates on the GAR and nearly all previous studies about the influence of the large-scale circulation on climate in the GAR used the NAO, that is what is also used here.

In this study the structure of the NAO pattern over Europe and its impact on

temperature in the Alps is analysed in detail based on a dense station dataset and on the high-resolution simulation described in section 2.1. Before interpreting the NAO signal from the regional model, this signal is validated against the NAO signal from the station data. This chapter is organised as follows: In section 4.1 the NAO and its influence on climate are discussed. The NAO index and station data used in this chapter are described in section 4.2. The NAO pattern is presented in section 4.3.1 followed by the linear (section 4.3.2) and nonlinear (section 4.3.3) NAO temperature signal based on both station and model data. Section 4.4 concludes this chapter.

4.1 North Atlantic Oscillation and its influence on European and Alpine climate

The NAO is a dominant pattern of atmospheric circulation variablity in the Northern Hemisphere, which was first described as a temperature see-saw between Greenland and Denmark about 230 years ago (van Loon and Rogers 1978) and which was denoted the NAO in the early 1930s by Walker and Bliss (1932). This circulation variability is a change in the intensity of the Icelandic Low and the Azores High. It is most pronounced in winter and affects climate in Europe as well as in North America (e.g. Hurrell 1995, Hurrell and van Loon 1997, Wanner et al. 2001). In the positive phase of the NAO both pressure systems are intensified leading to a stronger than normal pressure difference, which enhances the westerly winds across the North Atlantic and leads to a more northerly track of cyclones. Thus, in winter relatively warm and moist air is transported to middle and northern Europe, whereas in southern Europe it is drier than normal due to the missing cyclones, which are located more to the north. In the negative phase the pressure difference between the Icelandic Low and the Azores High is weaker than normal leading to weaker westerly winds with a more southerly cyclone track. This causes wet conditions in the Mediterranean region and dry and cold conditions in middle and northern Europe.

The influence of the NAO on climate has been analysed in many studies during the last 20 to 30 years. Besides the analysis of the influence on the whole Northern Hemispheric climate (Hurrell 1995, Hurrell and van Loon 1997, Marshall et al. 2001, Hurrell and Dickson 2004), also the influence on European climate has been analysed based on gridded climatologies (Pozo-Vázquez et al. 2001, Slonosky et

al. 2001b), station data (Slonosky et al. 2001a, Haylock and Goodess 2004), RCMs (Bojariu and Giorgi 2005) and GCMs (Fil and Dubus 2005). Over Europe the precipitation and temperature responses have a dipole pattern with a node more or less located over the Alps. These results over Europe are based on gridded data not finer resolved than 0.5° and station data not closer to each other than about 1°. Therefore, small-scale responses are not fully captured, especially over ares of complex orography like the Alps.

Under average winter climate conditions the westerly jet stream is situated over the North Atlantic and the Alps are located southeast in the right exit zone of this jet (Wanner et al. 1997). In the exit zone, where the isohypses fan out and the pressure gradient weakens, the air particles have a too high velocity compared to the gradient, and the Coriolis force is therefore larger than the pressure gradient force leading to an ageostrophic mass transport from low to high pressure (Warnecke 1991). This causes in the right exit zone at upper levels a convergence of mass, which causes subsidence and an increase of sea level pressure. In the positive phase of the NAO, when the jet is strengthened (e.g. Hurrell 1995) and warm maritime air is transported farther towards the European inland, subsidence of warm air and sea level pressure increase are intensified in the right exit zone, where the Alps are located, which leads to higher temperatures due to adiabatic warming and suppresses the formation of clouds and precipitation (Wanner et al. 1997). In the negative phase of the NAO the weaker-than-normal westerly winds are located on a more southerly track causing a lower-than-normal sea level pressure over the Alps and the Mediterranean. This leads to lower temperatures and more precipitation (Wanner et al. 1997).

These climatic responses to the NAO in winter have been confirmed by a number of studies over the Alps (Beniston et al. 1994, Jungo and Beniston 2001, Quadrelli et al. 2001, Beniston and Jungo 2002, Schmidli et al. 2002, Casty et al. 2005, Scherrer and Appenzeller 2006, Efthymiadis et al. 2007). The rise in mean sea level pressure (MSLP) over the Alps during the positive phase of the NAO has been found by analysing the pressure data at Zurich in Switzerland (Beniston et al. 1994). They found MSLP to be highly correlated with the NAO and to show frequently occuring and extended periods of blocking high events in the Alps during the 1980s, when the NAO was in a more positive phase. A strong correlation between the high pressure weather type and the NAO in the Alps in winter is also documented for the period 1945 to 1994 (Stefanicki et al. 1998).

Beniston and Jungo (2002) analysed the responses to the NAO of different variables at two sites in Switzerland representing high and low elevations. They found for periods where the NAO is in the positive phase, higher pressure and a shift of both minimum and maximum temperature distribution to a warmer climate with less extreme cold conditions and a longer duration of milder temperatures. At high elevations the diurnal warming is enhanced due to a clear reduction in moisture and therefore less clouds and above-avarage sunshine. At low elevations the clear reduction in moisture was found to be absent as in this layer more moisture is available leading to stratus or fog and therefore less warming. This elevational dependency of the warming due to the NAO was also found in other studies (Beniston and Rebetz 1996, Giorgi et al. 1997, Jungo and Beniston 2001, Efthymiadis et al. 2007).

By analysing the influence of the NAO on precipitation Quadrelli et al. (2001) found drier-than-normal conditions in the whole Alpine region during the positive phase of the NAO with the largest influence south-east of the Alps, which is in agreement with Efthymiadis et al. (2007). Schmidli et al. (2002) identified for nearly the same period significant negative correlations between precipitation and the NAO only south of the Alps and very small and partly positive correlations over the rest of the Alps. As a variable affected by both temperature and precipitation, Scherrer and Appenzeller (2006) analysed snow cover and its response to the NAO. In the positive phase snow cover is small, which fits with the reduced precipitation and increased temperature. Additionally, they found a separation between high and low elevations which is highly correlated to the NAO. All these studies investigating the influence of the NAO on Alpine climate are limited to the 20th century. For longer timescales Casty et al. (2005) analysed the influence from 1659 to 2000 based on recontructed temperature and precipitation on a 0.5° grid. They found that the influence was not stable over time and not always significant.

The studies concentrating on the spatial pattern of the NAO influence on European climate use either too few station data or too coarse gridded datasets to resolve fine-scale structures. Most of the studies concentrating on Alpine climate presented above do not analyse the small-scale structures of the pattern of the NAO signal, but rather the NAO influence on a few single stations, which are considered representative for high and low elevations (Beniston et al. 1994, Jungo and Beniston 2001, Beniston and Jungo 2002), or they analyse the relation to the

principal components of fields of different variables over the whole GAR or over subregions (Quadrelli et al. 2001, Scherrer and Appenzeller 2006, Efthymiadis et al. 2007). The study by Schmidli et al. (2002) is the only one that presents the NAO signal in a spatial pattern. They correlated a gridded reconstruction of precipitation over the GAR with a resolution of 25 km with a station based NAO index. Such an analysis does not exist for temperature due to the lack of high-resolution gridded datasets and dense homogenised station datasets until now. Therefore, the recently published dense high-quality HISTALP monthly mean temperature dataset (Auer et al. 2007) consisting of 131 stations over the whole GAR is an adequate dataset to allow for the first time an analysis of the spatial pattern of the NAO temperature signal in this region. The dataset is described in detail in section 2.2. As a high-resolution gridded dataset is still lacking, a high-resolution regional climate simulation in hindcast mode driven by a global reanalysis is used as an alternative to analyse the NAO temperature signal over the entire region covering areas where no station data are available. Therefore, the regional model yields spatial information which is absent in a station dataset. The first time a regional climate simulation was used to analyse the fine-scale NAO signal was in a study by Bojariu and Giorgi (2005). They performed a regional climate simulation over Europe with a resolution of 50 km and concentrated on the NAO influence on precipitation over Scandinavia, the Iberian Peninsula and the Balkan/Alpine region and on the influence on precipitation and temperature over the Carpathian mountains, where orography modulates the NAO signal. To analyse how the orographically induced NAO signal is influenced by the large-scale forcing the results from the regional model can be compared to the NAO signal from the driving global model or reanalysis, in this case ERA. The use of regional climate models in this context is also important for assessing the regional influence of the NAO on climate under various future climate change scenarios. Several studies show, that in a climate with increasing CO_2 concentrations the NAO moves to a more positive phase (e.g. Cubasch et al. 2001, Gillett et al. 2003, Meehl et al. 2007). This leads to changes in the response of regional climate, which can be assesed by RCMs.

4.2 NAO index and station data

The intensity of the NAO is described by the NAO index (NAOI), which is either defined as the first principal component of mean sea level pressure over the North Atlantic and surrounding land masses (20° to 80° North and 110° West to 70° East) or as the normalised pressure difference between a station on the Azores, Gibraltar or Lisbon and one on Iceland (Osborn et al. 1999). The NAOI used in this study is calculated by the Climatic Research Unit from Gibraltar and south-western Iceland (Jones et al. 1997). As mentioned in section 4.1 the influence of the NAO on European climate is largest in winter. Therefore, this study concentrates on means over December, January and February. As the REMO simulation ranges from 1958-1998, the winter means are calculated from 1958/59 to 1997/98. The winter mean NAOI used in this study is presented in Fig. 4.2.1.

For the analysis of the observed temperature a combination of the two station datasets presented in section 2.2 is used to obtain a station dataset as spatially dense as possible. The high-quality HISTALP monthly mean temperature dataset is included completely (131 stations), whereas from the second station dataset ZMmonthly, only those stations are included which do not exist in HISTALP. This leads to 36 additional Swiss and Austrian stations, meaning a total number of 167 stations covering the GAR. As the quality of HISTALP and ZMmonthly is different, the mixture of both datasets might lead to problems in the interpretation of the results. However, a station dataset as dense as possible is desired for this analysis and the gain in information due to the larger dataset outweighs the difficulties due to the mixture of the datasets. The coverage of this new station dataset is presented in Fig. 4.2.2 with a division into low and high (above 1500 m above mean sea level) elevation stations. The station data are averaged over winter from 1958/59 to 1997/98.

4.3 Results

4.3.1 NAO pattern over Europe

The winter mean NAO pattern over the period 1958 to 1998 over Europe is shown in Fig. 4.3.1. It is displayed as the linear regression coefficients between the NAO index and the ERA MSLP. The centers of action are located to the west off the

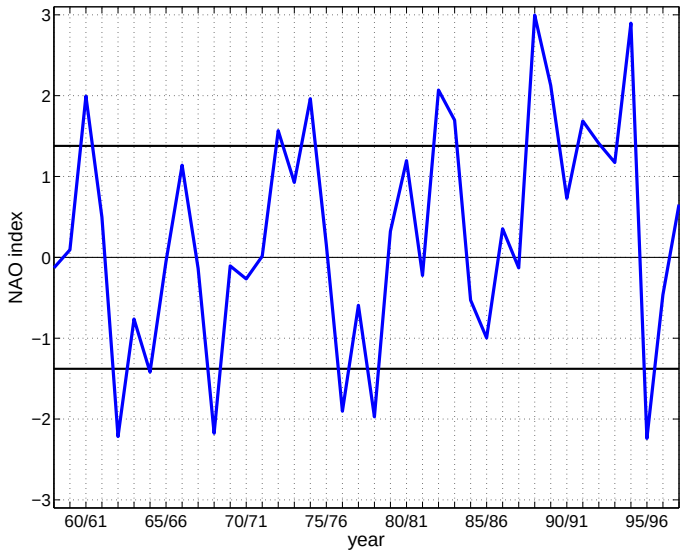

Figure 4.2.1: Winter (DJF) mean of the North Atlantic Oscillation index from 1958/59 to 1997/98 (Jones et al. 1997). Thick black lines indicate ± 1 standard deviation calculated over the this period.

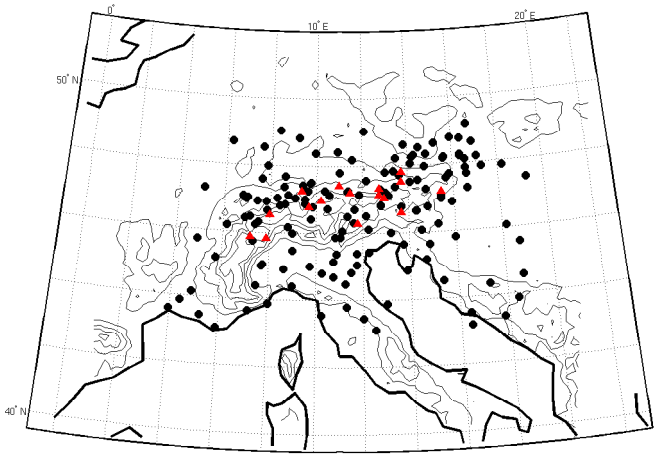

Figure 4.2.2: Stations in the GAR from the HISTALP dataset and those from the ZMmonthly dataset not included in HISTALP divided into low (black dots) and high elevations (red triangles). Contour lines in the background represent orography used in REMO with an interval of 500 m.

north-western coast of the Iberian Penisula and near Iceland, which is in agreement with Hurrell (1995). In the positive phase pressure is higher than normal over central and southern Europe and lower than normal over northern Europe leading to a stronger north-south pressure gradient and therefore to stronger winds, especially over the northwest Atlantic, with a more westerly component. Over the Alps pressure is increased and winds have a more north-westerly com-

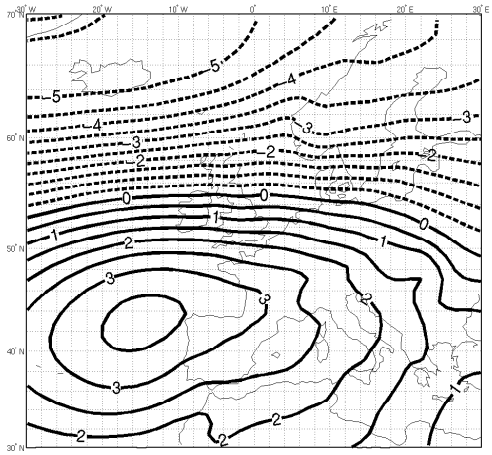

Figure 4.3.1: Linear regression coefficients between the NAOI and winter mean sea level pressure from the ERA40 reanalysis. Units in hPa per unit deviation of the NAOI.

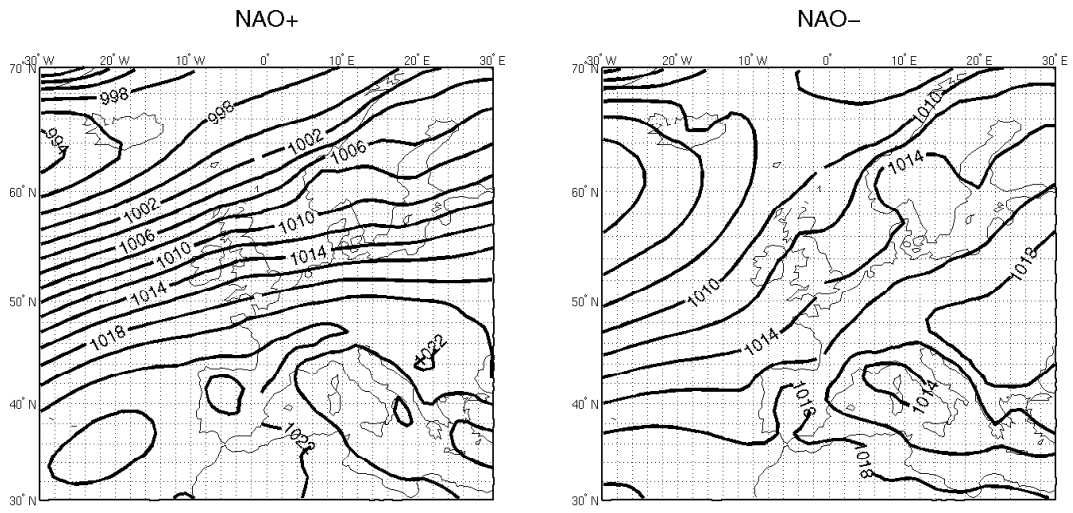

Figure 4.3.2: Winter mean sea level pressure in hPa from the ERA40 reanalysis during the positive (left) and the negative (right) phase of the NAO based on winter mean sea level pressure and regression coefficients shown in Fig. 4.3.1.

ponent compared to the winter mean over the whole period. The corresponding MSLP pattern is presented in Fig. 4.3.2 (left) and is derived from the NAO pattern in Fig. 4.3.1 by adding the regression coefficients to the winter mean MSLP. It shows a strong pressure gradient over the north-west Atlantic and an extensive area of higher than normal pressure from the Azores to the Alps.

In the negative phase pressure is increased over northern Europe und decreased over central and southern Europe. Therefore, the pressure gradient is weakened, which causes weaker winds over the whole area. The pressure over the Alps is

decreased and winds have a more south-easterly component. The MSLP pattern in the negative phase of the NAO is shown in Fig. 4.3.2 (right) indicating a very weak pressure gradient over the whole area. The Alps are influenced by the low pressure over the Gulf of Genoa.

4.3.2 The linear NAO-temperature signal

To analyse the linear temperature signal, linear regression and correlation are calculated between the detrended NAOI and both observed and simulated detrended temperature for the period 1958 to 1998. Linear regression describes how temperature is numerically related to the NAOI meaning it finds the line that best predicts temperature from NAOI. However, the regression coefficient does not indicate how strongly the data spread around this line. This is indicated by the correlation coefficient ranging from -1 to $+1$. Thus, correlation quantifies how well temperature and the NAOI vary together.

4.3.2.1 Linear signal based on station data

The relationship between the NAOI and observed temperature at the 167 stations divided into low and high elevations is presented in Fig. 4.3.3 and Fig. 4.3.4. The change in observed winter temperature corresponding to a positive change of one standard deviation of the NAOI shows a strong south to north gradient with smallest values around 0.2 K around the Adriatic coast and largest and significant (α=0.05) values of 1.3 K in the north-east of the GAR (Fig. 4.3.3). The corresponding correlation shows a very similar pattern with values ranging from 0.1 along the Adriatic coast to 0.7 in the north-east of the GAR (Fig. 4.3.4). This south to north gradient shows that the influence of the NAO on Alpine temperature increases from south to north, which is in agreement with the European-wide temperature response to the NAO (e.g. Hurrell and van Loon 1997).

Efthymiadis et al. (2007) also found this gradient with small values in the south-east and large values in the north-east of the GAR in winter by analysing the temperature variance explained by a station based NAOI and an NAO corresponding Empirical Orthogonal Function (EOF) for different regions in the GAR based on the HISTALP temperature dataset. However, as the region with the largest influence of the NAO on winter temperature they detected the region containing high elevation stations. This elevational dependency is absent in the present study in both regression and correlation coefficients although both stud-

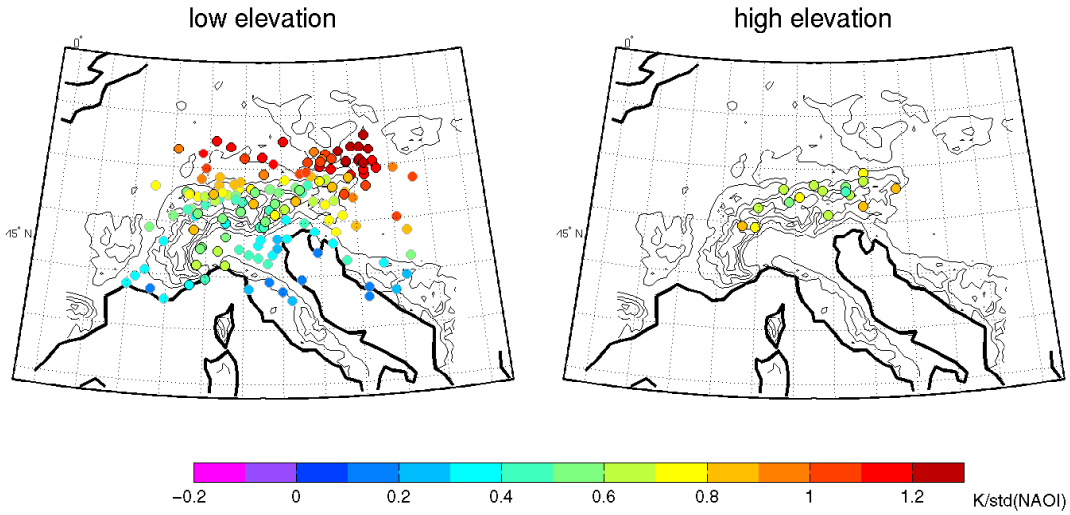

Figure 4.3.3: Linear regression coefficients between the NAOI and winter mean temperature at low (left) and high (right) elevation stations. Stations with significant (α=0.05) regression coefficients have a black circle. Units in K per unit deviation of the NAOI. Contour lines in the background represent orography used in REMO with an interval of 500 m.

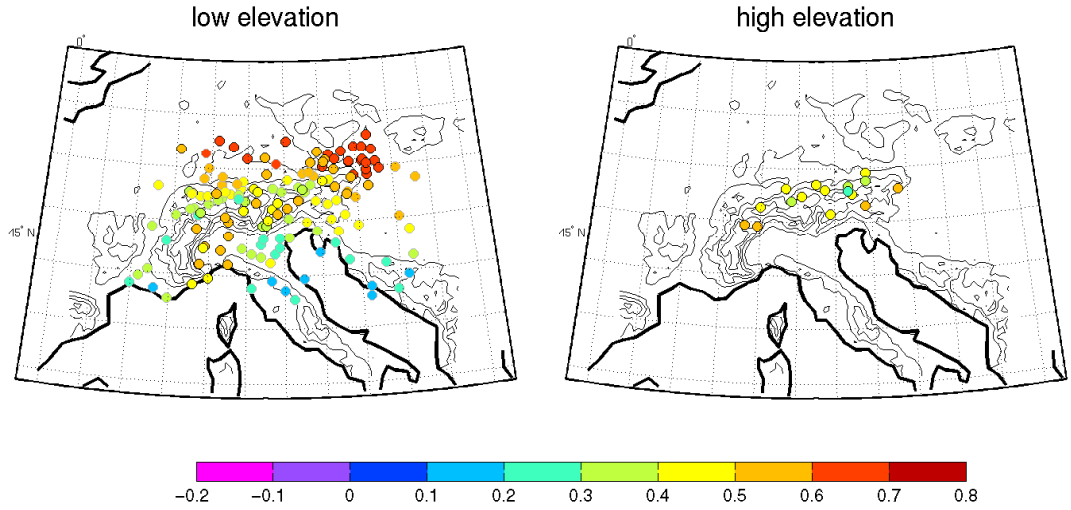

Figure 4.3.4: Same as 4.3.3 but for correlation coefficients.

ies use the HISTALP temperature dataset to analyse the elevational dependency of the NAO signal. However, Efthymiadis et al. (2007) did not use the raw data but representative temperature time series for each subregion based on an EOF analysis, and they analysed the influence of the NAO on these time series for the last 100 to 150 years, whereas the present thesis uses the raw data and concentrates on the period 1958 to 1998. As mentioned in section 4.1 studies by

Beniston and Rebetz (1996), Giorgi et al. (1997) and Beniston and Jungo (2002) also show an altitudinal dependency using several Swiss station data. This dependency was explained in Beniston and Jungo (1996) by the connection of the high elevation stations to the free atmosphere and therefore to the large-scale circulation influenced by the NAO, whereas lower elevations are more subject to local influences. In the aforementioned studies minimum and maximum temperatures were analysed concentrating on years with a strongly positive or a strongly negative NAO index, which is an important difference to the present study analysing the influence of the NAO on winter mean temperature with linear regression and correlation. Therefore, a nonlinear analysis follows in section 4.3.3.

Besides the overall south to north gradient the correlation pattern (Fig. 4.3.4 left) shows in the small area of the inner Alps an opposite gradient from north to south. Values range from about 0.3 along the northern side of the main Alpine ridge to about 0.5 along the southern side, which is also visible for the high elevation stations (Fig. 4.3.4 right). The higher values reach into the area bounded by Milan, the French Alps and the Gulf of Genoa. The inner Alpine north to south gradient is also visible for regression (Fig. 4.3.3) but is less clear except for the high elevation stations. This feature was not detected by earlier studies potentailly because their station datasets had a too sparse coverage and the gridded datasets had too low a resolution to capture this small-scale pattern. Potential explanations for this feature are discussed in the next section.

4.3.2.2 Linear signal based on reanalysis and model data

The influence of the NAO on temperature from the ERA40 reanalysis in the GAR is presented in Fig. 4.3.5 for regression (left) and correlation (right) and shows for both a south to north gradient. For regression the values range from $-0.5\,\mathrm{K}$ per unit standard deviation of the NAOI in the south-eastern grid boxes over southern Italy and Albania to $1.4\,\mathrm{K}$ in the north-eastern grid boxes of the domain. The correlation coefficients range from -0.4 in the south-eastern grid boxes to 0.7 in the north-western grid boxes over north-western France. Some regional indications are found in the correlation pattern on the southern slope of the Alps, which are represented in the ERA orography as one large ridge due to the coarse resolution as already mentioned in section 2.1. In this area the influence of the NAO is slightly stronger than in the surrounding grid boxes, especially compared to the grid boxes to the west, south and east. The overall

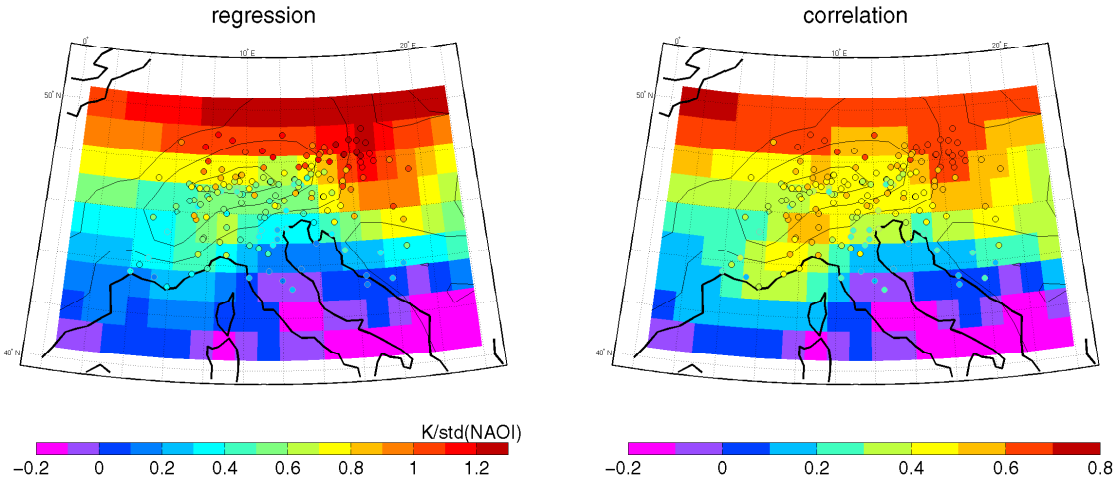

Figure 4.3.5: Linear regression coefficients (left) and correlation coefficients (right) between the NAOI and winter mean temperature from the ERA40 reanalysis. The dots in the foreground show the linear regression/correlation coefficients with station temperature as in Fig. 4.3.3 and Fig. 4.3.4. Units of regression coefficients in K per unit deviation of the NAOI. Contour lines in the background represent orography used in ERA with an interval of 400 m.

south to north gradient and the slightly stronger influence of the NAO on the southern slope of the Alps are in agreement with the results based on the station data. However, due to the coarse resolution of the reanalysis data it is not possible to detect more regional details.

Before analysing the NAO temperature signal based on temperature simulated by REMO, it is compared to the signal based on observed temperature. This additional validation of the model is necessary to correctly interpret its NAO temperature signal. The differences between the signals based on the observations and on REMO are presented in Fig. 4.3.6 for regression and in Fig. 4.3.7 for correlation. The values are generally quite small with negative values north and positive values south of the Alps. As in general REMO does capture the south to north gradient of the NAO influence on temperature (Fig. 4.3.8), this bias pattern indicates that REMO does not fully capture the strength of the gradient. This is the case for both regression and correlation. However, the differences are not significant (α=0.05) so that the influence on temperature simulated by REMO can be considered as additional valuable information in regions where no station data are available.

The NAO temperature signal based on temperature simulated by the high-

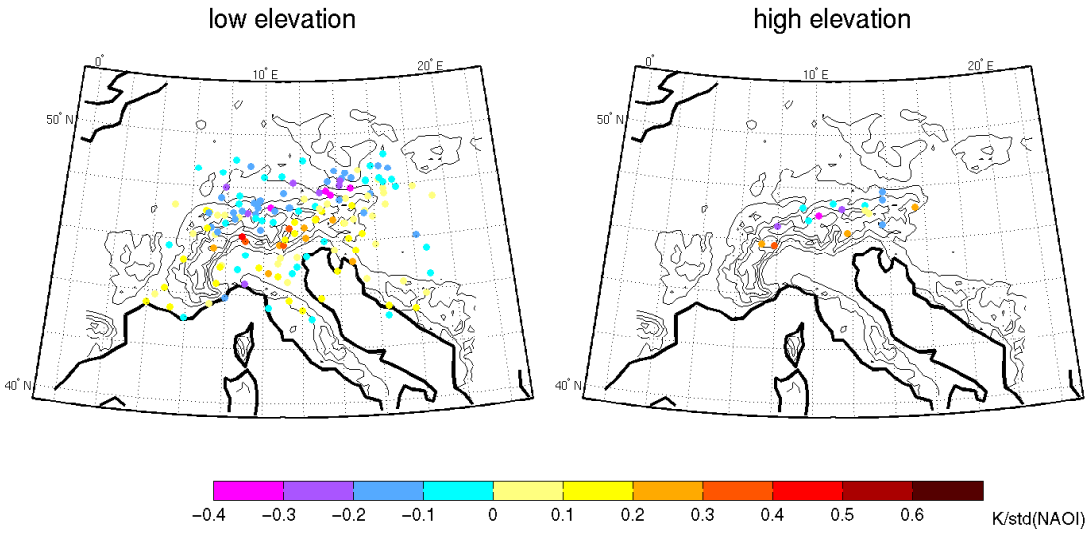

Figure 4.3.6: Difference between linear regression coefficients between the NAOI and REMO temperature and linear regression coefficients between the NAOI and station temperature at low (left) and high (right) elevation stations. Positive (negative) values indicate larger (smaller) regression coefficients for REMO. Units in K per unit deviation of the NAOI. Contour lines in the background represent orography used in REMO with an interval of 500 m.

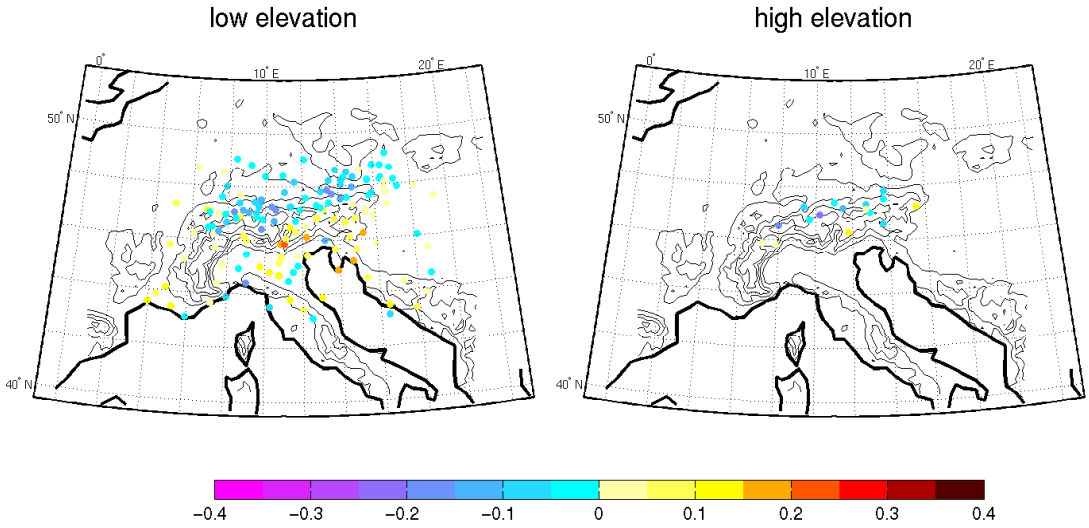

Figure 4.3.7: Same as 4.3.6 but for correlation coefficients.

resolution regional model presented in Fig. 4.3.8 shows much more regional details than the signal based on ERA temperature due to the much higher resolution. The overall pattern with smallest and negative values of -0.2 K per unit standard deviation of the NAOI for regression and of -0.3 for correlation in the south and largest values of 1.7 K in the north for regression and of 0.7 in the north-west for

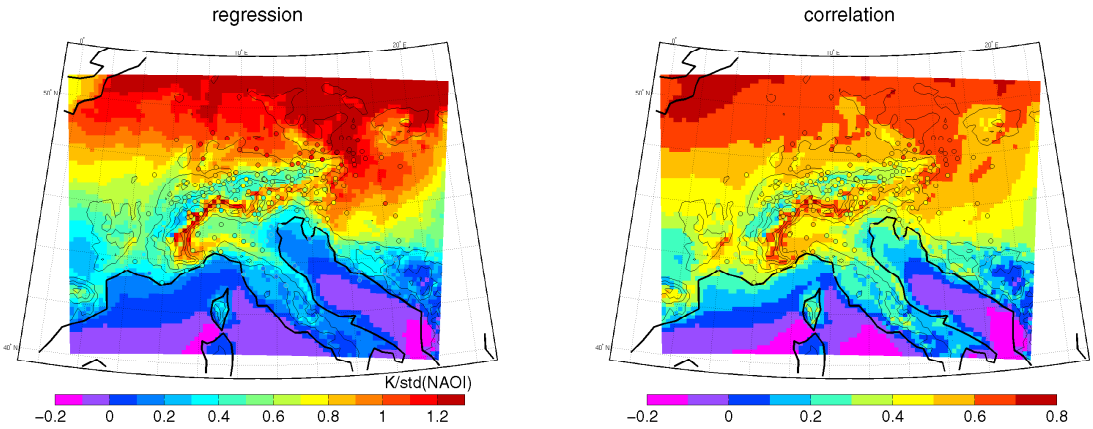

Figure 4.3.8: Linear regression coefficients (left) and correlation coefficients (right) between the NAOI and winter mean temperature from the high-resolution REMO simulation. The dots in the foreground show the linear regression/correlation coefficients with station temperature as in Fig. 4.3.3 and Fig. 4.3.4. Units of regression coefficients in K per unit deviation of the NAOI. Contour lines in the background represent orography used in REMO with an interval of 500 m.

correlation is also visible for REMO temperature.

The small-scale pattern in the inner Alps with the north to south gradient opposite to the overall gradient, which was described in the previous section, is also evident for REMO. This gradient is clearly visible for regression as well as for correlation and is more pronounced than for the station data. However, the differences between REMO and the station data are not significant as mentioned earlier. By including the orography of REMO in Fig. 4.3.8 it is possible to clearly identify that the smaller values are restricted to the northern slopes and larger values to the southern slopes of the Alps with the ridge separating them. This pattern can be found along the whole Alpine chain. In the positive (negative) phase of the NAO this pattern indicates an only slightly higher (lower) than normal temperature on the northern slopes and a considerably higher (lower) than normal temperature on the southern slopes.

A mechanism which can cause different temperature anomalies on the slopes of a mountain chain is the föhn, which is a dynamic-thermodynamic process with a warm and dry downslope wind in the lee of a mountain chain (Barry 1992, Steinacker 2006). Föhn is caused by a forced rise of air against a mountain chain leading to the formation of clouds and precipitation on the windward slope. The rising air cools at the saturated adiabatic lapse rate of 0.5 to 0.8 K/100 m

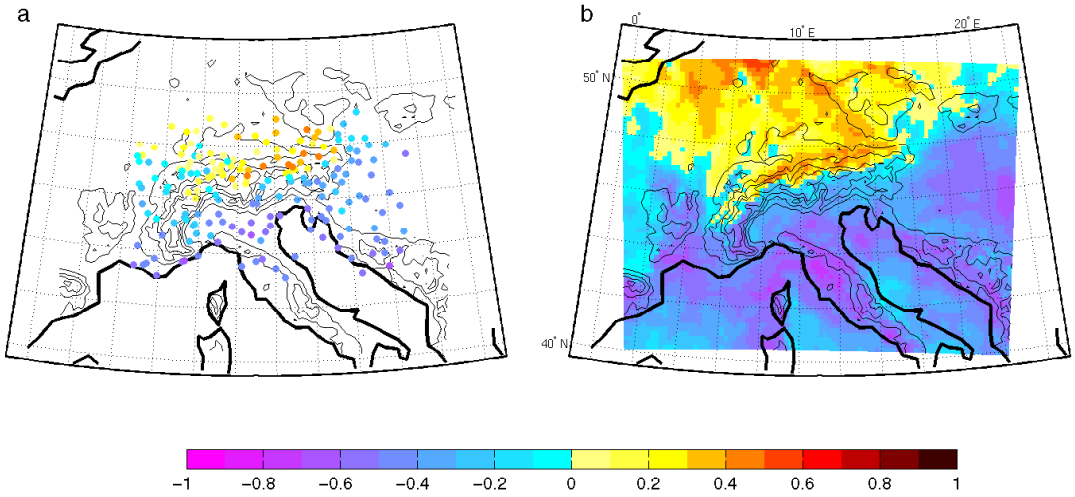

Figure 4.3.9: Correlation coefficients between the NAOI and winter mean precipitation from station data (a) and from the high-resolution REMO simulation (b). Contour lines in the background represent orography used in REMO with an interval of 500 m.

above the cloud base, where latent heat is released by condensation, and the precipitation leads to a reduction in moisture content of the air. On the lee slope the drier air descends and warms at the dry adiabatic lapse rate of 0.98 K/100 m. The different lapse rates, which are caused by the different moisture content, lead to lower temperatures at the windward slopes than at the lee slopes at the same heights. As the present study concentrates on winter means of temperature it should be noted that in areas, where föhn often occurs as e.g. in Altdorf in Switzerland on 11 days in winter (Schmitt 1930), it affects saisonal mean temperatures noticeable in the difference to seasonal mean temperature of areas, where föhn is rare (Malberg 1997).

To determine whether föhn can be an explanation for the small-scale inner Alpine structures in the temperature response to the NAO, the precipitation response is also analysed. The correlation coefficients between the NAO index and precipitation are presented in Fig. 4.3.9 for station data and for REMO. The station data are part of the HISTALP monthly mean precipitation dataset (Auer et al. 2005, Auer et al. 2007) containing 192 stations in the GAR. Both the station data and REMO show the same pattern with positive values north of the Alps and negative values south of the Alps. This indicates in the positive phase of the NAO an increase in precipitation in the north and a decrease in the south. In the negative phase it is the other way around. These results resemble those

from Schmidli et al. (2002) who used reconstructed precipitation data on a 25 km grid based on spatially dense observations from a short period (Frei and Schär 1998) and sparse observations from a long period.

As discussed in section 4.3.1 in the positive phase of the NAO winds are stronger and have a more north-westerly component over the Alps. The air coming from the Atlantic is moist and is flowing towards the Alps, where it is forced to rise. This leads to more precipitation on the windward slope as found in the station data and REMO. On the lee side of the Alps the drier air decends and warms, which is supported by the station data as well as by REMO showing less precipitation and considerably higher temperatures. A warming observed on the lee side of a mountain chain caused by stronger winds and therefore a stronger föhn effect is also described in some recent studies over the Antarctic Peninsula (Marshall et al. 2006, Orr et al. 2007, van Lipzig et al. 2007). In the negative phase of the NAO winds over the Alps have a more south-easterly component meaning the air comes from the Mediterranean and contains a lot of moisture. This leads to a north föhn with more precipitation in the south and less precipitation and higher temperatures in the north as shown by the station data and REMO. A further investigation of the correlation between NAO and föhn, which was not analysed with such detailed datasets until now, is beyond the scope of this thesis. However, the additional analysis of the precipitation response supports the hypothesis that the small-scale temperature response to the NAO might be caused by the föhn effect.

4.3.3 The nonlinear NAO-temperature signal

In section 4.3.2 the linear relationship between temperature and the NAO in winter is described. To answer the question, whether the response of temperature is different for strong positive and strong negative NAO events, the nonlinearity is analysed in this section. Strong NAO events are defined by the NAO index exceeding ± 1 standard deviation, which is indicated in Fig. 4.2.1 showing the winter mean NAO index from 1958/59 to 1997/98. This results in ten strong positive NAOI winters in this period and six strong negative NAOI winters. Based on these years the mean temperature anomaly patterns for strong positive NAO years and strong negative NAO years called composites are calculated from the station data, the ERA40 reanalysis and the REMO high-resolution simulation. The anomalies are deviations from the mean winter temperature of the whole

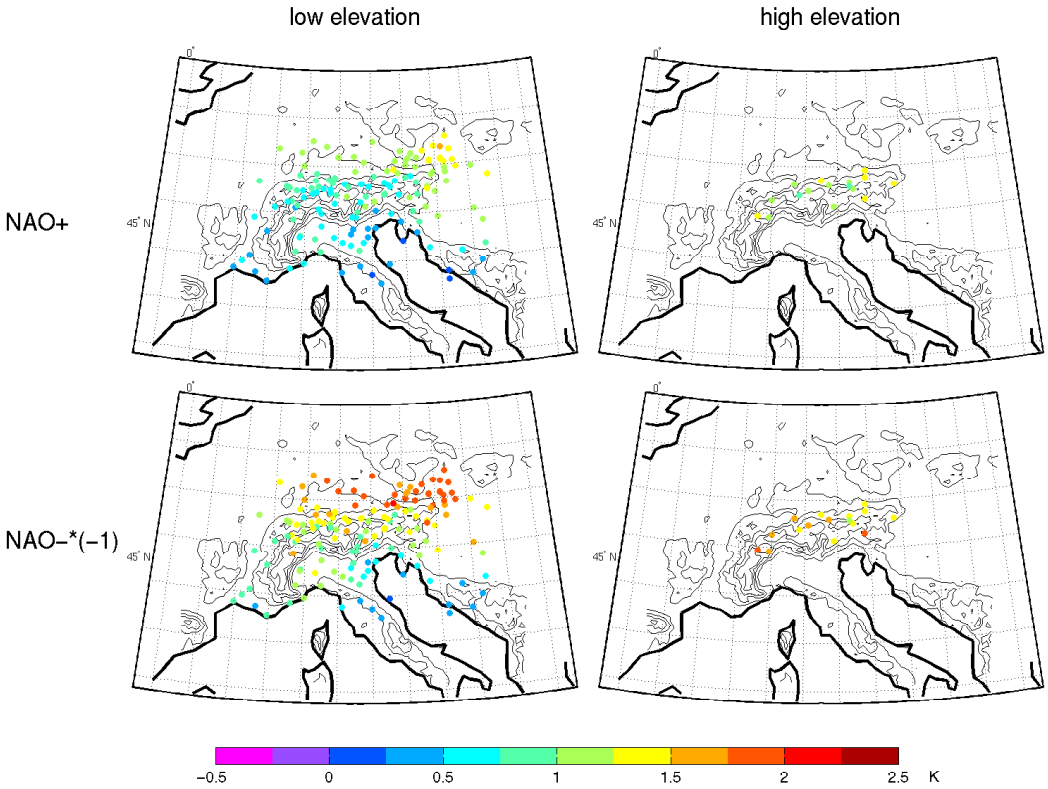

Figure 4.3.10: Temperature composites based on station data for low (left) and high (right) elevation stations for years, where the NAOI exceeds +1 standard deviation (NAO+, top) and −1 standard deviation (NAO−, bottom). The composites for NAO− are muliplied by −1 for a better comparison. Units in K. Contour lines in the background represent orography used in REMO with an interval of 500 m.

period 1958/59 to 1997/98. These composites are discussed in the next sections.

4.3.3.1 Nonlinear signal based on station data

In Fig. 4.3.10 the temperature composites calculated from the station data are shown separated for low and high elevations. The temperature pattern calculated for strong negative NAO years (NAO−) are multiplied by −1 to better compare the values to those for strong positive NAO years (NAO+). If the values and patterns are similar the temperature response to the NAO is a linear phenomenon. Indeed the patterns are quite similar with a south to north gradient but for negative NAO years the temperature anomalies in the north are larger than 1.5 K whereas for positive NAO years the anomalies exceed this value at only one station. The stronger influence of the NAO on temperature during NAO−

years is observable for both low and high elevation stations. This nonlinearity of the NAO temperature signal has already been suggested by Pozo-Vázquez et al. (2001). They calculated temperature composites over the whole of Europe for moderate and strong positive and negative NAO years based on temperature data from CRU for the period 1852-1997.

The composites in Fig. 4.3.10 show that the temperature anomalies are for both NAO+ and NAO− slightly larger for high elevation stations than for low elevation stations in the inner Alps, which is in agreement with Beniston and Rebetz (1996), Giorgi et al. (1997) and Beniston and Jungo (2002) analysing NAO+ and NAO− years. This elevational dependency was absent in the linear NAO temperature signal.

As described earlier a small-scale pattern in the inner Alps with a north to south gradient opposite to the overall gradient was found in the linear signal. In the nonlinear signal this pattern is less clear. For both NAO+ and NAO− only some single inner Alpine low and high elevation stations south of the main ridge show larger values compared to the surrounding stations.

4.3.3.2 Nonlinear signal based on reanalysis and model data

In Fig. 4.3.11 the temperature anomalies from the ERA40 reanalysis and the REMO high-resolution simulation for NAO+ and NAO− years are presented. For ERA a south to north gradient is visible as for the linear NAO temperature signal. However, this gradient is stronger for NAO−, which is in agreement with the temperature composites based on the station data. The only visible regional detail for both NAO+ and NAO− is a slightly stronger impact of the NAO on temperature in some grid boxes south-west of the peak in the orography of ERA as in the linear signal.

Before analysing the nonlinear NAO temperature signal simulated by REMO it is compared to the signal from the station data (Fig. 4.3.12). The differences are small and rarely exceed $\pm 0.8\,\mathrm{K}$ for both NAO+ and NAO−. Largest negative differences can be found for the high elevation stations north of the main ridge. Largest positive differences occur along the southern slope meaning that REMO simulates a slightly too large temperature anomaly in this area. These areas with the largest differences to the station data stand out on the REMO temperature composites (Fig. 4.3.11 right). These composites also show an overall south to north gradient in agreement with ERA and the station data, but in

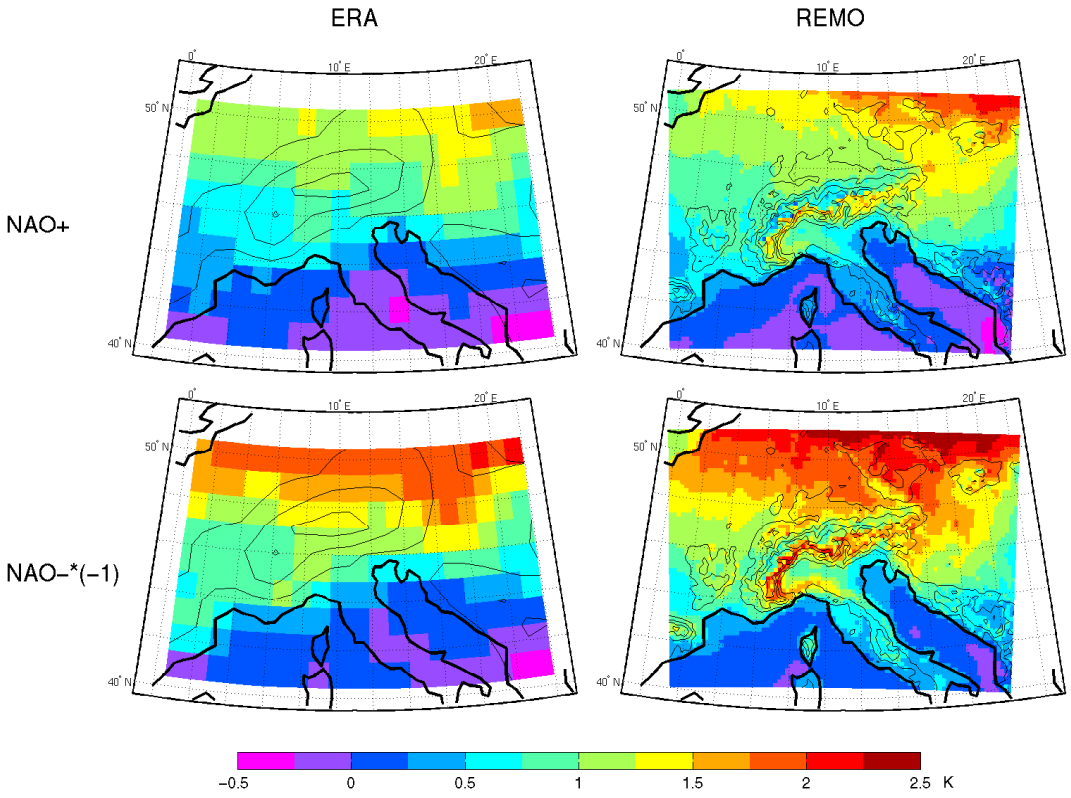

Figure 4.3.11: Temperature composites based on the ERA40 reanalysis (left) and REMO (right) for years, where the NAOI exceeds +1 standard deviation (NAO+, top) and where it exceeds −1 standard deviation (NAO−, bottom). The composites for NAO− are muliplied by −1 for a better comparison. Units in K. Contour lines in the background represent orography used in ERA (REMO) with an interval of 400 m (500 m).

the inner Alpine area this gradient is reversed with a small temperature response to the north and a large response to the south. This reversed gradient is more pronounced for NAO− than for NAO+ and was also found in the linear NAO temperature signal. However, this small-scale feature seems to be overestimated by REMO as it is less pronounced for the station data, which is in contrast to the linear signal, where REMO and the station data agree very well in the whole GAR.

For a better understanding of this small-scale feature also precipitation composites are analysed for station data and for REMO (Fig. 4.3.13). For both the station data and REMO the nonlinearity with a stronger influence during NAO− as found for temperature is also visible for precipitation. However, the nonlinearity is less pronounced for precipitation, which indicates that precipitation might

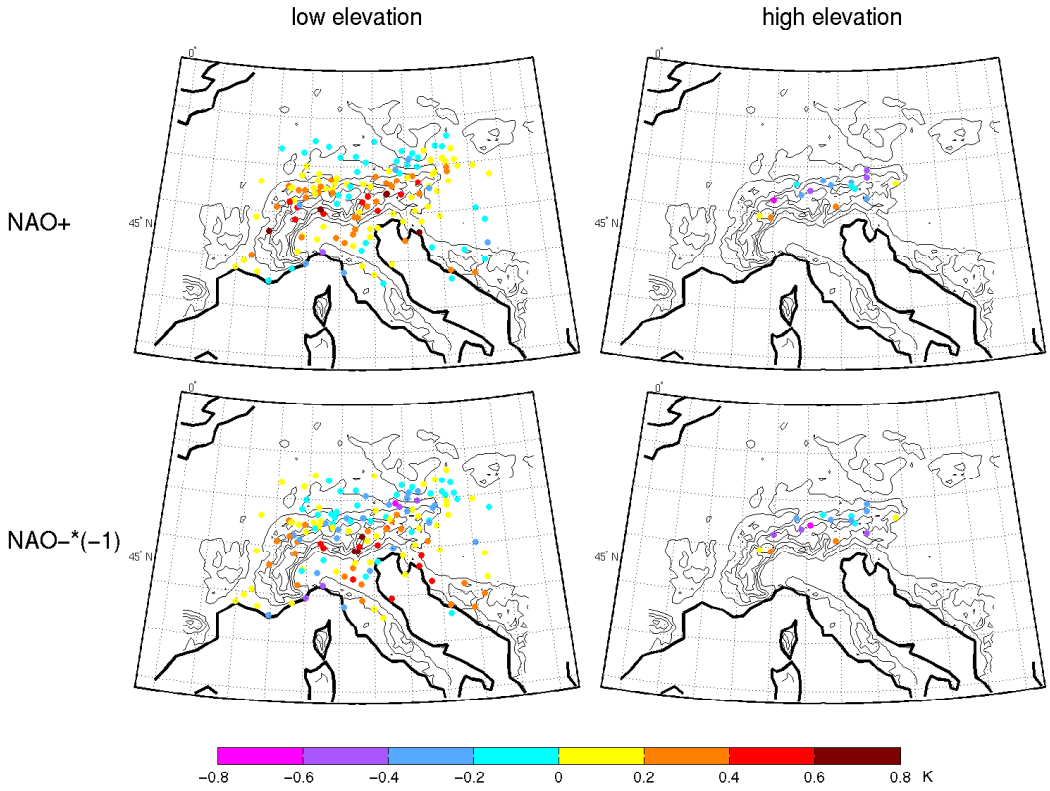

Figure 4.3.12: Difference between temperature composites based on the station data and based on REMO for low (left) and high (right) elevation stations for years, where the NAOI exceeds +1 standard deviation (NAO+, top) and where it exceeds −1 standard deviation (NAO−, bottom). Units in K. Contour lines in the background represent orography used in REMO with an interval of 500 m.

have a slightly stronger impact on temperature during NAO− than NAO+.

4.4 Conclusions

In this chapter the spatial pattern of the influence of the NAO on Alpine temperature has been analysed with different datasets. As the Greater Alpine Region has a very complex orography, a high-quality and dense station dataset is needed to analyse the spatial pattern in detail. This dataset is provided by a combination of the HISTALP monthly mean temperature dataset (Auer et al. 2007) and the ZMmonthly dataset described in section 2.2. To obtain information about the influence of the NAO also in areas where no station data are available a high-resolution gridded dataset is required. As such a dataset does not exist for temperature over the GAR the high-resolution regional climate simulation performed

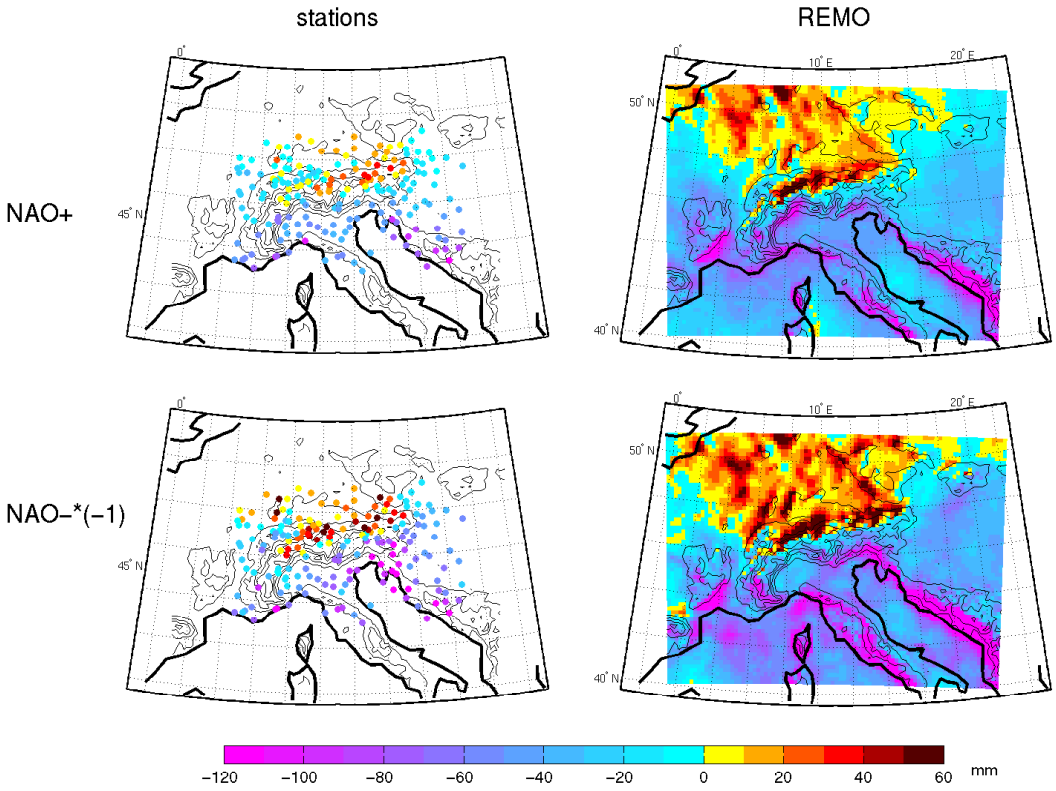

Figure 4.3.13: Precipitation composites based on the HISTALP station data (left) and REMO (right) for years, where the NAOI exceeds +1 standard deviation (NAO+, top) and where it exceeds −1 standard deviation (NAO−, bottom). The composites for NAO− are muliplied by −1 for a better comparison. Units in mm. Contour lines in the background represent orography used in REMO with an interval of 500 m.

with REMO is used. This simulation has been performed in hindcast mode and has been forced with the global ERA40 reanalysis as outlined in section 2.1. It is therefore an alternative to a high-resolution reanalysis as discussed in section 1.3. Based on the station dataset, the high-resolution simulation and the global reanalysis, the influence of the NAO has been investigated using linear regression and correlation to analyse the linear NAO temperature signal. Composites of NAO+ and NAO− have been used to analyse the nonlinear temperature signal. As the NAO has its largest influence on European climate during winter, only the winter means of the period 1958/59 to 1997/98 have been studied.

Based on the station data it has been shown that the influence of the NAO on temperature in the GAR is quite small in the south and increases to the north, which agrees with earlier studies (e.g. Hurrell and van Loon 1997, Efthymiadis

et al. 2007). This gradient has been found for both the linear and the nonlinear signals. The analysis of temperature composites shows that the NAO temperature signal is not linear. During years with a strongly negative NAO index the impact on temperature is larger than during positive NAO years, especially more to the north.

Due to the densly located stations it has been possible to detect a small-scale feature, which is most pronounced for correlation but also visible for linear regression and the composites of NAO+ and NAO−. This feature shows a north to south gradient of the NAO influence opposite to the gradient over the whole region. It is limited to the inner Alps and includes the high elevation stations. A potential explanation for this small-scale pattern is the föhn effect of warm and moist air forced to flow over the Alps. The spatial pattern of the NAO influence on precipitation supports this hypothesis.

As the station data are separated into low and high elevation stations, an investigation of the elevational dependency of the NAO temperature signal has been possible. Some previous studies exist describing an increasing influence of the NAO on winter temperature with elevation in the Alps by analysing the temperature response to strongly positive and strongly negative NAO years (Beniston and Rebetz 1996, Giorgi et al. 1997, Beniston and Jungo 2002). Efthymiadis et al. (2007) found this elevational dependency with a linear analysis of the HISTALP temperature data transformed into timeseries representing subregions. In the present study the linear analysis with the raw HISTALP data does not show an elevational dependency suggesting a strong influence of the kind of data used for the analysis. However, in the nonlinear analysis an increasing influence of the NAO with elevation is visible. Together with the studies by Beniston and Rebetz (1996), Giorgi et al. (1997) and Beniston and Jungo (2002) this leads to the conclusion that the elevational dependency is only visible for extreme NAO+ and NAO− years.

The NAO influence on Alpine temperature simulated by the high-resolution regional model has first been compared to the signal from the station data to analyse the credibility of the simulated pattern and to validate the NAO temperature signal in the regional model. It has been shown that for both the linear and the nonlinear signal the difference between the station and the model based signal is quite small and not significant, with largest values in the inner Alps. The simulated signal shows in the inner Alps the same pattern as the station based signal

described in the previous paragraph but it is much more pronounced, especially in the nonlinear signal, which leads to the conclusion that REMO overestimates this inner Alpine pattern. This overestimation is most obvious for the composites but also visible for regression and correlation.

This inner Alpine pattern of temperature response to the NAO in combination with the precipitation response can be explained by the föhn effect, which largly depends on the shape of the orography. As the orography of the regional model is smoothed compared to the real orography, the föhn effect might have different proportions leading to the slight overestimation of the temperature response simulated by the regional model. As stated by Steinacker (2006) a model resolution of about 1 km is necessary to show all details and local features of the föhn caused by the orography. Therefore, in the present simulation with a resolution of 1/6° it is only possible to simulate the concept of föhn (or the föhn effect) as a flow over a mountain range with different lapse rates on the windward and on the leeward side of the mountain affecting temperature.

The comparison of the simulated climate response to the station-based response shows that the high-resolution regional model REMO is able to correctly simulate the influence of the NAO as an example of large-scale circulation variability on temperature in a region with complex orography. This validation is also needed for the usage of regional models in climate change simulations analysing the regional influence of the NAO, which is thought to increase in future (e.g. Cubasch et al. 2001, Gillett et al. 2003, Meehl et al. 2007), which might lead to changes in the temperature response. The information about the NAO temperature signal based on station data is limited to single locations, but by applying the high-resolution model, information about the signal is added in areas where no station data are available. Compared to the temperature response from the ERA40 reanalysis the REMO simulation driven by ERA is able to show much more regional detail due to the much higher resolution.

Chapter 5

Summary and concluding remarks

Within the present study a high-resolution regional climate simulation has been analysed and validated for means and variability of Alpine temperature for the period 1958 to 1998. The simulation has been performed with the regional model REMO with a resolution of 1/6° in hindcast mode driven by the ERA40 reanalysis with a resolution of 1.125°. The model domain covers the whole of Europe but the focus of this study is on the Greater Alpine Region (GAR) with its complex orography.

Different questions have been addressed in this thesis. After the validation of the simulation showing its performance, it has been analysed whether the application of a high-resolution simulation in hindcast mode adds value to the driving reanalysis with a much coarser resolution. Furthermore, the ability of the model to simulate small-scale responses to large-scale circulation variability has been investigated.

The high resolution of the simulation and the recent availability of a dense station dataset (Auer et al. 2007) provides the opportunity to validate the model against station data in the orographically complex area of the GAR and to summarise the results over quite small subregions. Such a detailed validation in complex orography has been possible for the first time. Due to the partly large elevation differences between the stations and the corresponding grid boxes, this validation demonstrates the importance of the application of an adequate temperature lapse rate. This study advises to apply a monthly varying lapse rate instead of a constant lapse rate in areas with such a complex orography to reduce

biases caused by elevation differences.

The validation of REMO reveals a positive summer bias, which is most pronounced in south-eastern Europe, where it is due to the drying-out of the soil. This so called summer drying problem known for many years can be found in many RCMs and is caused by shortcomings in the parameterisation (e.g. Noguer et al. 1998, Hagemann et al. 2001, Vidale et al. 2003, Räisänen et al. 2004, Jacob et al. 2007). However, it is still not fully understand and therefore still an issue in many recent analyses (Christensen et al. 2007). In the inner Alps winter temperature is underestimated, which is in agreement with Christensen et al. (1997), Noguer et al. (1998) and Vidale et al. (2003). For the low elevations the negative winter bias can be explained by the poor representation of valleys in the model and therefore the missing ability to simulate the effective mixing of the lower atmosphere by valley winds as suggested by Bromwich et al. (2005). Concerning the high elevations the study by Kotlarski (2007) showed that the implementation of a glacier parameterisation scheme in REMO actually increases the existing negative winter bias compared to a simulation with standard REMO reflecting general shortcomings of REMO in the Alps, which he suggests are probably related to the spatial distribution of precipitation.

By comparing the performance of a regional model in hindcast mode with the performance of a global reanalysis for present climate, it is assessed whether the higher resolution of the hindcast leads to a more realistic reconstruction of present climate. In this study it turns out that the much higher resolution of the regional model clearly adds value to the temperature performance of the reanalysis in regions with the most complex orography. This is the case for monthly mean values and even more pronounced for daily mean values. As in these inner Alpine regions less stations are assimilated into the reanalysis and temperature is horizontally less homogenous, the better representation of orography in the regional model plays a more important role in the temperature performance. Therefore, in orographically complex regions a high resolution is necessary to realistically simulate climate, either in a hindcast to serve as a gridded reconstruction or in dynamically downscaled future climate change scenarios. In regions where temperature is horizontally more homogenous, i.e. where the variability of small spatial scales is low, it is difficult for REMO to add value to the reanalysis, as added value is supposed on small spatial scales (Feser 2005), which are included in the reanalysis through the assimilation of stations. A comparison of the added

value in the GAR to previous studies is not possible as the present study is the first analysing the added value in an area of complex orography in such detail. However, the study by Feser (2006) shows a tendency to an added value in the Alps in winter.

The analysis of the temperature response to the NAO in the Alps based on station data, REMO, and ERA provides two main conclusions. First, REMO is able to reproduce the temperature response pattern over the GAR found in the station data. Second, REMO adds information to the response patterns of ERA and the station data. Compared to ERA, the REMO temperature response pattern shows much more spatial detail due to the much higher resolution. Compared to the spatially dense station data already showing a quite detailed response pattern, REMO adds information in areas where no station data are available. Thus, REMO helps identifying a small-scale pattern that is less obvious in the station data. This pattern is located over the inner Alps showing a reversed gradient in the temperature response, which can be explained by the föhn effect and is described in this study for the first time.

The validation of high-resolution hindcasts can be performed for mean climate and variability. Such a validation provides more information about the RCM than the validation of a regional simulation for present climate driven by a GCM, which can only be performed for climatologies. Therefore, the validation of a hindcast serves as a reference for the validation of simulations for present climate performed with GCM boundary conditions. These GCM-driven regional simulations for present climate are control simulations for future climate change scenarios driven by the same GCM. Thus, before simulating future climate change, the validation of RCMs forced with perfect boundary conditions should be performed (Giorgi et al. 2001). Concerning the added value analysis, it is difficult to transfer the results of a reanalysis-driven hindcast to a downscaled future climate change simulation performed with the same RCM. Due to the assimilation of observations the reanalysis provides fields close to reality. This leads to a tougher added value analysis than that performed with a GCM-driven regional simulation for present climate. The latter analysis delivers an added value, that can be expected to be similar to an added value for a downscaled future climate change simulation. The added value from a reanalysis-driven hindcast might serve as a lower limit of the added value of the same RCM driven by a GCM simulation for future climate.

Also the analysis of the influence of the NAO on temperature in the GAR

provides information, which is relevant for future climate change applications. As stated in Randall et al. (2007) the capability of a GCM to realistically simulate the NAO pattern is important, because this pattern and that of the Arctic Oscillation resemble the simulated response pattern to greenhouse gas forcing, which strongly influences temperature. Therefore, the realistic simulation of the NAO temperature response is also important, which is the case for many GCMs (Randall et al. 2007). Additionally, the NAO is thought to move to a more positive phase in future (e.g. Cubasch et al. 2001, Gillett et al. 2003, Meehl et al. 2007), which might change the response of regional climate. Therefore, RCMs are needed to analyse the influence of the NAO on regional scales. As demonstrated here, strong temperature responses are found on regional scales, which can therefore also be expected in downscaled future climate change scenarios and would be absent in the GCM simulations.

List of Abbreviations

ALP-IMP	Multi-centennial climate variability in the Alps based on Instrumental data, Model simulations and Proxy Data
CALL	Central Alpine Low Level
CRU	Climatic Research Unit
DJF	December, January, February
DWD	German Weather Service (Deutscher Wetterdienst)
ECMWF	European Centre for Medium-Range Weather Forecasts
EM	Europa Modell
EOF	Empirical Orthogonal Function
ERA	ECMWF reanalysis
GAR	Greater Alpine Region
GCM	General Circulation Model
HISTALP	Historical Instrumental climatological Surface Time series of the greater ALPine region
HL	High Level
JJA	June, July, August
MPI	Max Planck Institute for Meteorology, Hamburg
MSLP	Mean Sea Level Pressure
NAO	North Atlantic Oscillation

NAOI	NAO index
NARR	North American Regional Reanalysis
NCEP/NCAR	National Centers for Environmental Prediction/National Center for Atmospheric Research
RCM	Regional Climate Model
REMO	REgional MOdell
rmse	root mean squared error
ZAMG	Central Institute for Meteorology and Geodynamics, Austria
ZMdaily/ZMmonthly	daily/monthly mean temperature dataset consisting of Austrian and Swiss stations

List of Figures

References

Ambaum MHP, Hoskins BJ, Stephenson DB (2001) Arctic Oscillation or North Atlantic Oscillation? J Clim 14: 3495-3507

Auer I, Böhm R, Jurković A, Orlik A, Potzmann R, Schöner W, Ungersböck M, Brunetti M, Nanni T, Maugeri M, Briffa K, Jones P, Efthymiadis D, Mestre O, Moisselin J-M, Begert M, Brazdil R, Bochnicek O, Cegnar T, Gajić-Capka M, Zaninović K, Majstorović Z, Szalai S, Szentimrey T, Mercalli L (2005) A new instrumental precipitation dataset for the Greater Alpine Region for the period 1800-2002. Int J Climatol 25: 139-166, DOI 10.1002/joc.1135

Auer I, Böhm R, Jurković A, Lipa W, Orlik A, Potzmann R, Schöner W, Ungersböck M, Matulla C, Briffa K, Jones P, Efthymiadis D, Brunetti M, Nanni T, Maugeri M, Mercalli L, Mestre O, Moisselin J-M, Begert M, Müller-Westermeier G, Kveton V, Bochnicek O, Stastny P, Lapin M, Szalai S, Szentimrey T, Cegnar T, Dolinar M, Gajić-Capka M, Zaninović K, Majstorović Z, Nieplova E (2007) HISTALP - historical instrumental climatological surface time series of the Greater Alpine Region. Int J Climatol 27: 17-46, DOI 10.1002/joc.1377

Barry RG (1978) H.B. de Saussure: the first mountain meteorologist. Bull Am Met Soc 59: 702-705

Barry RG (1992) Mountain weather and climate, 2nd edition. Routledge, London, 402 pp

Beniston M, Rebetz M, Giorgi F, Marinucci MR (1994) An analysis of regional climate change in Switzerland. Theor Appl Climatol 49: 135-159

Beniston M, Rebetz M (1996) Regional behavior of minimum temperatures in Switzerland for the period 1979-1993. Theor Appl Climatol 53: 231-243

Beniston M, Jungo P (2002) Shifts in the distribution of pressure, temperature and moisture and changes in the typical weather patterns in the Alpine region in

response to the behavior of the North Atlantic Oscillation. Theor Appl Climatol 71: 29-42

Bergant K, Belda M, Halenka T (2007) Systematic errors in the simulation of European climate (1961-2000) with RegCM3 driven by NCEP/NCAR renanlysis. Int J Climatol 27: 455-472, DOI 10.1002/joc.1413

Böhm R, Auer I, Brunetti M, Maugeri M, Nanni T, Schöner W (2001) Regional temperature variability in the European Alps: 1760-1998 from homogenized instrumental time series. Int J Climatol 21: 1779-1801

Bojariu R, Giorgi F (2005) The North Atlantic Oscillation signal in a regional climate simulation for the European region. Tellus 57A: 641-653

Bromwich D, Bai L, Bjarnason GG (2005) High-resolution regional climate simulations over Iceland using Polar MM5. Mon Weather Rev 133: 3527-3547

Brunetti M, Nanni T, Maugeri M, Auer I, Böhm R, Schöner W (2006) Precipitation variability and changes in the Greater Alpine Region over the 1800-2003 period. J Geophys Res 111: D11107

Büntgen U, Esper J, Frank DC, Nicolussi K, Schmidhalter M (2005) A 1052-year tree-ring proxy of Alpine summer temperatures. Clim Dyn 25: 141-153, DOI 10.1007/s00382-005-0028-1

Cantú V (1977) The climate of Italy. In: Wallén CC (eds) World survey of climatology volume 6: Climates of Central and Southern Europe. Elsevier Scientific Publishing Company, Amsterdam, The Netherlands, pp 127-183

Casty C, Wanner H, Luterbacher J, Esper J, Böhm R (2005) Temperature and precipitation variability in the European Alps since 1500. Int J Climatol 25: 1855-1880, DOI 10.1002/joc.1216

Christensen JH, Machenhauer B, Jones RG, Schär C, Ruti PM, Castro M, Visconti G (1997) Validation of present-day regional climate simulations over Europe: LAM simulations with observed boundary conditions. Clim Dyn 13: 489-506

Christensen JH, Hewiston B, Busuioc A, Chen A, Gao X, Held I, Jones R, Kolli RK, Kwon W-T, Laprise R, Magaña Rueda V, Mearns L, Menéndez CG, Räisänen J, Rinke A, Sarr A, Whetton P (2007) Regional climate projections. In: Solomon S, Qin D, Manning M, Chen Z, Marquis M, Averyt KB, Tignor M, Miller HL (eds) Climate change 2007: The physical science basis. Contribution of working group

I to the fourth assessment report of the Intergovernmental Panel on Climate Change. Cambridge University Press, Cambridge, United Kingdom and New York, NY, USA, pp 847-940

Cox R, Bauer BL, Smith T (1998) A mesoscale model intercomparison. Bull Americ Met Soc 79: 265-283

Cubasch U, Meehl GA, Boer GJ, Stouffer RJ, Dix M, Noda A, Senior CA, Raper S, Yap KS (2001) Projections od future climate change. In: Houghton JT, Ding Y, Griggs DJ, Noguer M, van der Linden PJ, Dai X, Maskell K, Johnson CA (eds) Climate change 2001: The scientific basis. Contribution of working group I to the third assessment report of the Intergovernmental Panel on Climate Change. Cambridge University Press, Cambridge, pp 525-582

Denis B, Laprise R, Caya D, Côté J (2002) Downscaling ability of one-way nested regional climate models: the Big-Brother Experiment, Clim Dyn 18: 627-646, DOI 10.1007/s00382-001-0201-0

Duffy PB, Arritt RW, Coquard J, Gutowski W, Han J, Iorio J, Kim J, Leung L-R, Roads J, Zeledon E (2006) Simulations of present and future climates in the Western United States with four nested regional climate models. J Clim 19: 873-895

ECMWF: `http://www.ecmwf.int/about/special_projects/saenz_mesoscale_meteor_reanalysis/index.html`, last accessed on 6 November 2007

Efthymiadis D, Jones PD, Briffa KR, Auer I, Böhm R, Schöner W, Frei C, Schmidli J (2006) Construction of a 10-min-gridded precipitation dataset for the Greater Alpine Region for 1800-2003. J Geophys Res 111: D01105, DOI 10.1029/2005JD006120

Efthymiadis D, Jones PD, Briffa KR, Böhm R, Maugeri M (2007) Influence of large-scale atmospheric circulation on climate variability in the Greater Alpine Region of Europe. J Geophys Res 112: D12104, DOI 10.1029/2006JD008021

Feser F (2005) Spatial scale separation in regional climate modelling. GKSS Research Centre, Report No. 2005/9, 112pp

Feser F (2006) Enhanced detectability of added value in limited-area model results separated into different spatial scales. Mon Weather Rev 134: 2180-2190

Feser F, von Storch H (2005) A spatial two-dimensional discrete filter for limited-area-model evaluation purposes. Mon Weather Rev 133: 1774-1786

Fil C, Dubus L (2005) Winter climate regimes over the North Atlantic and European region in ERA40 reanalysis and DEMETER seasonal hindcasts. Tellus 57A: 290-307

Frei C, Schär C (1998) A precipitation climatology for the Alps from high-resolution rain-gauge observations. Int J Climatol 18: 873-900

Frei C, Christensen JH, Déqué M, Jacob D, Jones RG, Vidale PL (2003) Daily precipitation statistics in regional climate models: Evaluation and intercomparison for the European Alps. J Geophys Res 108: 4124, DOI 10.1029/2002JD002287

Gibson JK, Kållberg P, Uppala S, Nomura A, Hernandez A, Serrano E (1997) ERA description. ECMWF ERA-15 Project Series 1: 71pp.

Gillett NP, Allen MR, Williams KD (2003) Modelling the atmospheric response to doubled CO_2 and depleted stratospheric ozone using a stratosphere-resolving coupled GCM, Q J R Meteorol Soc 129: 947-966

Giorgi F, Hurrell JW, Marinucci MR (1997) Elevation dependency of the surface climate change signal: a model study. J Clim 10: 288-296

Giorgi F, Hewitson B, Christensen J, Hulme M, von Storch H, Whetton P, Jones R, Mearns L, Fu C (2001) Regional climate information - evaluation and projections. In: Houghton JT, Ding Y, Griggs DJ, Noguer M, van der Linden PJ, Dai X, Maskell K, Johnson CA (eds) Climate change 2001: The scientific basis. Contribution of working group I to the third assessment report of the Intergovernmental Panel on Climate Change. Cambridge University Press, Cambridge, pp 583-638

Giorgi F, Francisco R, Pal J (2003) Effects of a subgrid-scale topography and land use scheme on the simulation of surface climate and hydrology. Part 1: effects of temperature and water vapor disaggregation. J Hydrometeorol 4: 317-333

Hagemann S, Botzet M, Machenhauer B (2001) The summer drying problem over south-eastern Europe: sensitivity of the limited area model HIRHAM4 to improvements in physical parameterization and resolution. Phys Chem Earth (B) 26: 391-396

Hagemann S, Machenhauer B, Christensen OB, Déqué M, Jacob D, Jones R, Vidale

PL (2002) Intercomparison of water and energy budgets simulated by regional climate models applied over Europe. Max Planck Institute, Report No. 338, 45pp

Haylock MR, Goodess CM (2004) Interannual variability of European extreme winter rainfall and links with mean large-scale circulation. Int J Climatol 24: 759-776, DOI 10.1002/joc.1033

Hurrell JW (1995) Decadal trends in the North Atlantic Oscillation: regional temperatures and precipitation. Science 269: 676-679

Hurrell JW, van Loon H (1997) Decadal variations in climate associated with the North Atlantic Oscillation. Clim Change 36, 301-326

Hurrell JW, Dickson RR (2004) Climate variability over the North Atlantic. In Marine Ecosystems and Climate Variation - the North Atlantic by Stenseth NC, Ottersen G, Hurrell JW, Belgrano A, Eds. Oxford University Press, pp 15-31

IPY: `http://classic.ipy.org/development/eoi/details.php?id=113`, last accessed 6 November 2007

Jacob D, Podzun R (1997) Sensitivity studies with the regional climate model REMO. Meteorol Atmos Phys 63: 119-129

Jacob D, Bärring L, Christiansen OB, Christiansen JH, de Castro M, Déqué M, Giorgi F, Hagemann S, Hirschi M, Jones R, Kjellström E, Lenderink G, Rockel B, Sánchez E, Schär C, Seneviratne SI, Somot S, van Ulden A, van den Hurk B (2007) An inter-comparison of regional climate models for Europe: model performance in present-day climate. Clim Change 81: 31-52, DOI 10.1007/s10584-006-9213-4

Jacobson MZ (2005) Fundamentals of atmospheric modeling. Cambridge University Press, 828 pp

Jones PD, Jonsson T, Wheeler D (1997) Extention to the North Atlantic Oscillation using early instrumental pressure observations from Gibraltar and south-west Iceland. Int J Climatol 17: 1433-1450

Jungo P, Beniston M (2001) Changes in the anomalies of extreme temperature anomalies in the 20th century at Swiss climatological stations located at different latitudes and altitudes. Theor Appl Climatol 69: 1-12

Kalnay E, Kanamitsu M, Kistler R, Collins W, Deaven D, Gandin L, Iredell M, Saha S, White G, Woollen J, Zhu Y, Chelliah M, Ebisuzaki W, Higgins W, Janowiak

J, Mo KC, Ropelewski C, Wang J, Leetmaa A, Reynolds R, Jenne R, Joseph D (1996) The NCEP/NCAR 40-year renalysis project. Bull Am Met Soc 77: 437-471

Kotlarski S, Block A, Böhm U, Jacob D, Keuler K, Knoche R, Rechid D, Walter A (2005) Regional climate model simulations as input for hydrological applications: evaluation of uncertainties. Adv Geosci 5, 119-125

Kotlarski S (2007) A subgrid glacier parameterisation for use in regional climate modelling. Max Planck Institute, Reports on Earth System Science, Report No. 42, 180pp

Kyselý J (2002) Comparison of extremes in GCM-simulated, downscaled and observed central-European temperature series. Clim Res 20: 211-222

Laprise R (2003) Resolved scales and nonlinear interactions in limited-area models. J Atmos Sci 60: 768-779

Machenhauer B, Windelband M, Botzet M, Christensen JH, Déqué M, Jones RG, Ruti PM, Visconti G (1998) Validation and analysis of regional present-day climate and climate change simulations over Europe. Max Planck Institut für Meteorologie, Report No. 275

Majewski D, Schrodin P (1994) Short description of the Europa-Modell (EM) and Deutschland-Modell (DM) of the Deutscher Wetterdienst (DWD). Quarterly Bulletin (April):1-31

Malberg H (1997) Meteorologie und Klimatologie - Eine Einführung. Springer, Berlin, 354pp

Marshall GJ, Orr A, van Lipzig NPM, King JC (2006) The impact of changing Southern Hemisphere Annular Mode on Antarctic Peninsula summer temperatures. J Clim 19: 5388-5404

Marshall J, Kushnir Y, Battisti D, Chang P, Czaja A, Dickson R, Hurrell J, McCartney M, Saravanan R, Visbeck M (2001) North Atlantic climate variability: phenomena, impacts and mechanisms. Int J Climatol 21: 1863-1898, DOI 10.1002/joc.693

Meehl GA, Stocker TF, Collins WD, Friedlingstein P, Gaye AT, Gregory JM, Kitoh A, Knutti R, Murphy JM, Noda A, Raper SCB, Watterson IG, Weaver AJ, Zhao Z-C (2007) Global climate projections. In: Solomon S, Qin D, Manning M, Chen

Z, Marquis M, Averyt KB, Tignor M, Miller HL (eds) Climate change 2007: The physical science basis. Contribution of working group I to the fourth assessment report of the Intergovernmental Panel on Climate Change. Cambridge University Press, Cambridge, United Kingdom and New York, NY, USA, pp 747-845

Mesinger F, DiMego G, Kalnay E, Mitchell K, Shafran PC, Ebisuzaki W, Jović D, Woollen J, Rogers E, Berbery EH, Ek MB, Fan Y, Grumbine R, Higgins W, Li H, Lin Y, Manikin G, Parrish D, Shi W (2006) North American regional reanalysis. Bull Americ Meteo Soc 87: 343-360

Mitchell TD, Carter TR, Jones PD, Hulme M, New M (2004) A comprehensive set of high-resolution grids of monthly climate for Europe and the globe: the observed record (1901-2000) and 16 scenarios (2001-2100). Tyndall Working Paper 55, Tyndall Centre, UEA, Norwich, UK

Mitchell TD, Jones PD (2005) An improved method of constructing a database of monthly climate observations and associated high-resolution grids. Int J Climatol 25: 693-712

Moberg A, Jones PD (2004) Regional climate model simulations of daily maximum and minimum near-surface temperatures across Europe compared with observed station data 1961-1990. Clim Dyn 23: 695-715, DOI 10.1007/s00382-004-0464-3

New M, Hulme M, Jones PD (1999) Representing twentieth-century space-time climate variability. Part 1: Development of a 1961-90 mean monthly terrestrial climatology. J Clim 12: 829-856

New M, Hulme M, Jones PD (2000) Representing twentieth-century space-time climate variability. Part 2: Development of 1901-96 monthly grids of terrestrial surface climate. J Clim 13: 2217-2238

Noguer M, Jones R, Murphy J (1998) Sources of systematic errors in the climatology of a regional climate model over Europe. Clim Dyn 14: 691-712

Orr A, Marshall GJ, Hunt JCR, Sommeria J, Wang C-G, van Lipzig NPM, Cresswell D (2007) Characteristics of summer airflow over the Antarctic Peninsula in response to recent strengthening of westerly circumpolar winds. J Atmos Sci, in press

Osborn TJ, Hulme M (1997) Development of a relationship between station and grid-box rainday frequencies for climate model evaluation. J Clim 10: 1885-1908

Osborn TJ, Briffa KR, Tett SFB, Jones PD, Trigo RM (1999) Evaluation of the North

Atlantic Oscillation as simulated by a coupled climate model. Clim Dyn 15: 685-702

Pozo-Vázquez D, Esteban-Parra MJ, Rodrigo FS, Castro-Díez Y (2001) A study of NAO variability and its possible non-linear influences on European surface temperature. Clim Dyn 17: 701-715

Quadrelli R, Lazzeri M, Cacciamani C, Tibaldi S (2001) Observed winter Alpine precipitation variability and links with large-scale circulation patterns. Clim Res 17: 275-284

Räisänen J, Hansen U, Ullerstig A, Döscher R, Graham LP, Jones C, Meier HEM, Samuelsson P, Willén U (2004) European climate in the late twenty-first century: regional simulations with two driving global models and two forcing scenarios. Clim Dyn 22: 13-31, DOI 10.1007/s00382-003-0365-x

Randall DA, Wood RA, Bony S, Colman R, Fichefet T, Fyfe J, Kattsov V, Pitman A, Shukla J, Srinivasan J, Stouffer RJ, Sumi A, Taylor KE (2007) Climate models and their evaluation. In: Solomon S, Qin D, Manning M, Chen Z, Marquis M, Averyt KB, Tignor M, Miller HL (eds) Climate change 2007: The physical science basis. Contribution of working group I to the fourth assessment report of the intergovernmental panel on climate change. Cambridge University Press, Cambridge, United Kingdom and New York, NY, USA, pp 589-662

Roads J, Chen S, Cocke S, Druyan L, Fulakeza M, LaRow T, Lonergan P, Qian J-H, Zebiak S (2003) International Research Institute/Applied Research Centers (IRI/ARCs) regional model intercomparison over South America. J Geophys Res 108: D14, 4425, DOI 10.1029/2002JD003201

Roeckner E, Arpe K, Bengtsson L, Christoph M, Claussen M, Dümenil L, Esch M, Giorgetta M, Schlese U, Schulzweida U (1996) The atmospheric general circulation model ECHAM4: model description and simulation of present-day climate. Max Planck Institut für Meteorologie, Report No. 218

Rolland C (2003) Spatial and seasonal variations of air temperature lapse rates in Alpine regions. J Clim 16: 1032-1046

Scheifinger H (2006) Climatological evaluation of the REMO (regional model) precipitation simulation 1971-1999. Internal ALP-IMP project report

Scherrer SC, Appenzeller C (2006) Swiss Alpine snow pack variability: major patterns and links to local cimate and large-scale flow. Clim Res 32: 187-199

Schlünzen KH, Katzfey JJ (2003) Relevance of sub-grid-scale land-use effects for mesoscale models. Tellus 55A: 232-246

Schmidli J, Schmutz C, Frei C, Wanner H, Schär C (2002) Mesoscale precipitation variability in the region of the European Alps during the 20th century. Int J Climatol 22: 1049-1074, DOI 10.1002/joc.769

Schmitt W (1930) Föhnerscheinungen und Föhngebiete. Wiss Veröff dt u österr Alpenvereins, Innsbruck

Schöner W, Auer I, Böhm R, Thaler S (2003) Qualitätskontrolle und statistische Eigenschaften ausgewählter Klimaparameter auf Tageswertbasis im Hinblick auf Extremwertanalysen. StartClim-Startprojekt Klimaschutz: Erste Analysen extremer Wetterereignisse und ihrer Auswirkungen in Österreich. Endbericht Projekt 1: 1-39

Schüepp M, Schirmer H (1977) Climates of Central Europe. In: Wallén CC (eds) World survey of climatology volume 6: Climates of Central and Southern Europe. Elsevier Scientific Publishing Company, Amsterdam, The Netherlands, pp 3-73

Seth A, Rauscher SA, Camargo SJ, Qian J-H, Pal JS (2007) RegCM3 regional climatologies for South America using reanalysis and ECHAM global model driving fields. Clim Dyn 28: 461-480, DOI 10.1007/s00382-006-0191-z

Simmons AJ, Jones PD, da Costa Bechtold V, Beljaars ACM, Kållberg PW, Saarinen S, Uppala SM, Viterbo P, Wedi N (2004) Comparison of trends and low-frequency variability in CRU, ERA-40, and NCEP/NCAR analyses of surface air temperature. J Geophys Res 109: D24115, DOI 10.1029/2004JD005306

Slonosky VC, Jones PD, Davies TD (2001a) Atmospheric circulation and surface temperature in Europe from the 18th century to 1995. Int J Climatol 21: 63-75

Slonosky VC, Yiou P (2001b) The North Atlantic Oscillation and its relationship with near surface temperature. Geophys Res Lett 28: 807-810

Sotillo MG, Ratsimandresy AW, Carretero JC, Bentamy A, Valero F, González-Rouco F (2005) A high-resolution 44-year atmospheric hindcast for the Mediterranean Basin: contribution to the regional improvement of global reanalysis. Clim Dyn 25: 219-236, DOI 10.1007/s00328-005-0030-7

Sotillo MG, Martín ML, Valero F, Luna MY (2006) Validation of a homogeneous 41-year (1961-2001) winter precipitation hindcast dataset over the Iberian Peninsula:

assessment of the regional improvement of global reanalysis. Clim Dyn 27: 627-645, DOI 10.1007/s00382-006-0155-3

Stefanicki G, Talkner P, Weber RO (1998) Frequency changes of weather types in the Alpine region since 1945. Theor Appl Climatol 60: 47-61

Steinacker R (2006) Alpiner Föhn - eine neue Strophe zu einem alten Lied. promet 32: 3-10

Thompson DWJ, Wallace JM (1998) The Arctic Oscillation signature in the wintertime geopotential height and temperature fields. Geophys Res Lett 25: 1297-1300

Uppala SM, Kållberg PW, Simmons AJ, Andrae U, da Costa Bechtold V, Fiorino M, Gison JK, Haseler J, Hernandez A, Kelly GA, Li X, Onogi K, Saarinen S, Sokka N, Allan RP, Andersson E, Arpe K, Balmaseda MA, Beljaars ACM, van de Berg L, Bidlot J, Bormann N, Caires S, Chevallier F, Dethof A, Dragosavac M, Fisher M, Fuentes M, Hagemann S, Hólm E, Hoskins BJ, Isaksen L, Janssen PAEM, Jenne R, McNally AP, Mahfouf J-F, Moscrette J-J, Rayner NA, Saunders RW, Simon P, Sterl A, Trenberth KE, Untch A, Vasiljevic D, Viterbo P, Woollen J (2005) The ERA-40 reanalysis. Q J R Meteorol Soc 131: 2961-3012

van den Hurk B, Hirschi M, Schär C, Lenderink G, van Meijgaard E, van Ulden A, Rockel B, Hagemann S, Graham P, Kjellström E, Jones R (2005) Soil control on runoff response to climate change in regional climate model simulations. J Clim 18: 3536-3551

van Lipzig NPM, Marshall GJ, Orr A, King J (2007) The relationship between the Southern Hemisphere Annular Mode and Antarctic Peninsula summer temperatures: Analysis of a high-resolution model climatology. J Clim, in press

van Loon H, Rogers JC (1978) The seesaw in winter temperatures between Greenland and northern Europe. Part 1: General descriptions. Mon Weather Rev 106: 296-310

Vidale PL, Lüthi D, Frei C, Seneviratne SI, Schär C (2003) Predictability and uncertainty in a regional climate model. J Geophys Res 108: D18, 4586, DOI 10.1029/2002JD002810

von Storch H, Langenberg H, Feser F (2000) A spectral nudging technique for dynamical downscaling purposes. Mon Weather Rev 128: 3664-3673

Walker GT, Bliss EW (1932) World Weather V. Mem Roy Met Soc 4: 53-84

Wang Y, Leung LR, McGregor JL, Lee D-K, Wang W-C, Ding Y, Kimura F (2004) Regional climate modeling: progress, challenges, and prospects. J Meteorol Soc Japan 82: 1599-1628

Wanner H, Rickli R, Salvisberg E, Schmutz C, Schüepp M (1997) Global climate change and variability and its influence on Alpine climate - concepts and observations. Theor Appl Climatol 58: 221-243

Wanner H, Brönnimann S, Casty C, Gyalistras D, Luterbacher J, Schmutz C, Stephenson DB, Xoplaki E (2001) North Atlantic Oscillation - concepts and studies. Survey Geophys 22: 321-328

Warnecke G (1991) Meteorologie und Umwelt. Berlin, Springer, 342 pp.

Weisse R, Feser F (2003) Evaluation of a method to reduce uncertainty in wind hindcasts performed with regional atmosphere models. Coastal Engineering 48: 211-225

Wikipedia, the free encyclopedia: `http://en.wikipedia.org/wiki/Image:Alpenrelief_01.jpg`, extracted on 18 July 2007

Zemp M, Paul F, Hoelzle M, Salzmann N, Haeberli W (2007) Glacier fluctuations in the European Alps 1850-2000: an overview and spatio-temporal analysis of available data. In: Orlove, B., Wiegandt, E. and B. Luckman (eds.): The darkening peaks: Glacial retreat in scientific and social context. University of California Press, in press

Acknowledgements

First of all, I would like to thank Prof. Dr. Hans von Storch for giving me the opportunity to accomplish this thesis at the Institute for Coastal Research at the GKSS Research Centre Geesthacht and for the appraisal of this work. Furthermore, I am grateful to Prof. Dr. K. Heinke Schlünzen for examining this dissertation.

I would like to express my gratitude to my day-to-day advisors Dr. Julie M. Jones and Dr. Martin Widmann for numerous fruitful scientific discussions strengthening my work and for their support even from England.

I am grateful to Dr. Beate Geyer for performing the REMO simulation and for her assistance with the postprocessing and with any questions concerning the simulation. I am also thankful to Dr. Frauke Feser for her help with REMO and discussions on regional models.

This work has been realised within the EU framework 5 project ALP-IMP and I wish to thank all partners of the ALP-IMP project for an interesting, interdisciplinary and detailed view on Alpine climate. Especially Reinhard Böhm, Wolfgang Schöner, Nadine Salzmann, Martin Hoelzle, Fabio Monti and Michele Brunetti are acknowledged for providing station data and for their assistance with these data.

I would also like to thank Dr. Nikolaus Groll, Dr. Elke Meyer, Dr. Sebastian Wagner, Ivonne Anders and all other colleagues for valuable discussions, not always concerning this work. Concerning the computer support I am grateful to Dr. Jens Meywerk. I also thank Beate Gardeike for her help with my posters and figures and Ilona Liesner for her help with the administration.

My parents always supported me in every way and I am deeply grateful to them. Special thanks go to Alex, Maren and Mel for their close friendship despite the long distance.